9-2-2012

International Conference on Electrical & Electronics Engineering

Prof.Srikanta Patnaik Mentor
IRNet India, patnaik_srikanta@yahoo.co.in

Proceedings of International Conference on

Electrical & Electronics Engineering

(ICEEE-2012)
2nd September, 2012
BANGALORE, India

Interscience Research Network (IRNet)
Bhubaneswar, India

Editorial

Electrical engineering is a field of engineering that generally deals with the study and application of electricity, electronics and electromagnetism. The field first became an identifiable occupation in the late nineteenth century after commercialization of the electric telegraph and electrical power supply. It now covers a range of subtopics including power, electronics, control systems, signal processing and telecommunications.

Electrical engineering may include electronic engineering. Where a distinction is made, usually outside of the United States, electrical engineering is considered to deal with the problems associated with large-scale electrical systems such as power transmission and motor control, whereas electronic engineering deals with the study of small-scale electronic systems including computers and integrated circuits.[1] Alternatively, electrical engineers are usually concerned with using electricity to transmit energy, while electronic engineers are concerned with using electricity to process information. More recently, the distinction has become blurred by the growth of power electronics.

Electronics is a subfield within the wider electrical engineering academic subject. An academic degree with a major in electronics engineering can be acquired from some universities, while other universities use electrical engineering as the subject. The term electrical engineer is still used in the academic world to include electronic engineers. However, some people think the term 'electrical engineer' should be reserved for those having specialized in power and heavy current or high voltage engineering, while others believe that power is just one subset of electrical engineering (and indeed the term 'power engineering' is used in that industry) as well as 'electrical distribution engineering'. Again, in recent years there has been a growth of new separate-entry degree courses such as 'information engineering', 'systems engineering' and 'communication systems engineering', often followed by academic departments of similar name, which are typically not considered as subfields of electronics engineering but of electrical engineering.

Beginning in the 1980s, the term computer engineer was often used to refer to a subfield of electronic or information engineers. However, Computer Engineering is now considered a subset of Electronics Engineering and computer science and the term is now becoming archaic.

Electronic engineering as a profession sprang from technological improvements in the telegraph industry in the late 19th century and the radio and the telephone industries in the early 20th century. People were attracted to radio by the technical fascination it inspired, first in receiving and then in transmitting. Many who went into broadcasting in the 1920s were only 'amateurs' in the period before World War

Fundamental to the discipline are the sciences of physics and mathematics as these help to obtain both a qualitative and quantitative description of how such systems will work. Today most engineering work involves the use of computers and it is commonplace to use computer-aided design and simulation software programs when designing electronic systems. Although most electronic engineers will understand basic circuit theory, the theories employed by engineers generally depend upon the work they do.

Editor-in-Chief

Dr. Srikanta Patnaik

Chairman, I.I.M.T., Bhubaneswar

Intersceince Campus,

At/Po.: Kantabada, Via-Janla, Dist-Khurda

Bhubaneswar, Pin:752054. Orissa, INDIA.

Simulation of Space Vector PWM Control Algorithm for 3 Level Diode Clamped Inverter

[1]Naveen.G & [2]Eranna,

[1&2]Department of Electrical & Electronics Engineering,
Dr. Ambedkar Institute of Technology, Bangalore.

Abstract— In this paper, an effective space vector pulse width modulation (SVPWM) method for multi-level inverter fed induction motor is presented. In multilevel inverters due to the large number of space vectors and redundant switching states, a simple and general space vector PWM algorithm is proposed. Based on this algorithm, the location of the reference voltage vector can be easily determined and the calculation of dwell times becomes very simple. More importantly, the proposed algorithm is general and can be directly applied to the multilevel inverter of any voltage levels. In addition, the speed of an induction motor is controlled by using three level diode clamped multilevel inverter. The simulation results reveals that the proposed circuit effectively controls the motor speed and enhances the drive performance through reduction in Switching losses and Total Harmonic Distortion (THD).

Keywords*— Multilevel inverter; Space vector PWM; Dwelling times; Diode clamped inverter; switching states.*

I. INTRODUCTION

The research on the multilevel inverter has been receiving wide attention mainly due to its capability of high voltage operation without switching devices connected in series. In addition, with the increase of voltage levels, the inverter output contains less harmonics and will eventually approach a desired sinusoidal waveform [1]. Therefore, the multilevel inverters have been selected as a preferred power converter topology for high voltage and high power applications [2], [3].

Among all the switching algorithms proposed in the literature for multilevel converters [1]-[6], space vector modulation (SVM) seems most promising since it offers a great flexibility in optimizing switching pattern design and it is also well suited for digital implementation. Traditionally, three phase voltage is transformed reference voltage vector, the angle and amplitude of reference voltage vector is used to calculate the duration-time of voltage vector. But, as the level is increasing, the control algorithm becomes more and more complex [7].

In this paper, a general space vector algorithm is proposed, which has the following features:

- The algorithm is very simple and effective. The location of the reference voltage vector and the dwell times of the space vectors can be calculated very easily;
- The generated PWM pattern contains minimal voltage harmonic content; and
- The proposed algorithm is general and can be used in any high-level multilevel inverters.

The proposed methods are verified by simulation and experimental results and discussed in detail in following parts.

II. REFERENCE VECTOR LOCATION AND DWELL TIME CALCULAION

A typical 3-level Diode Clamped Inverter is shown in Fig.1, and the corresponding space voltage vector diagram is illustrated in Fig. 2, in which the vectors for the 3, 5, 7 and 9-level inverters are also illustrated. For the 3-level inverter, there are 9 small triangles and the vertex of each triangle represents a space vector, which is defined by

$$Vs = Va.e^{j0} + Vb.e^{j2\pi/3} + Vc\, e^{j4\pi/3} \quad (1)$$

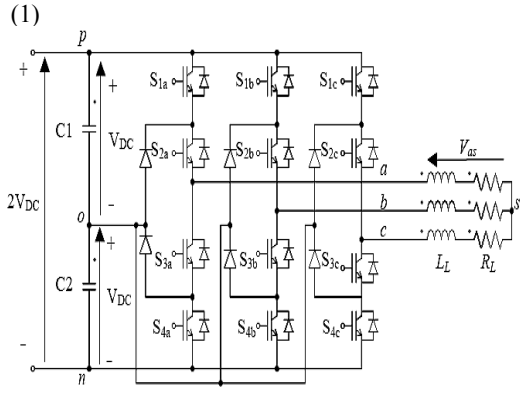

Fig. 1. Configuration of 3 –level Diode Clamped Inverter

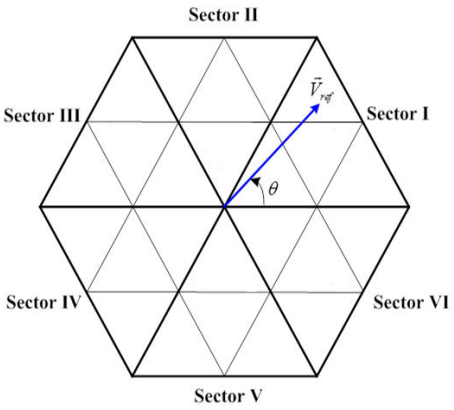

Figure 2. Voltage vectors of 3 - level voltage source inverters

where *Va , Vb* and *Vc* are the phase voltages of the inverter. The vectors can be divided into six major triangular sectors (I to VI), and the details of sector I is given in Fig. 3. The coordinates of each vector in the commonly used Cartesian coordinate system, *Vx* and *Vy*, can be calculated by

$$V_x = V_a - (V_b + V_c)/2$$

$$V_Y = \sqrt{3} (V_b - V_c)/2 \quad (2)$$

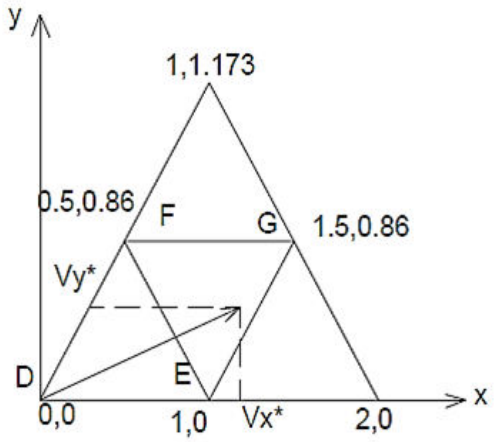

Figure 3. Space vectors in the Cartesian coordinate system (sector I)

The co-ordinates of all the space vectors, assuming a unity dc supply voltage (i.e., V_{dc} = 1 per unit), can be shown in the figure as well. To reduce the voltage harmonic distortion, the reference voltage V^* can be synthesized by the three nearest vectors. With V^* lying in triangle Δ EFG, the reference voltage can be approximated by vectors $V_E = 1 + j\ 0$, $V_F = 0.5 + j\ 0.86$ and $V_G = 1.5 + j\ 0.86$.

There are in general two problems with the use of Cartesian coordinates:

a) It is quite tedious to determine which triangle the end point of the reference vector falls into; and

b) The equations for the calculation of dwell times usually change with the triangle that V^* is in. In other words, each triangle has its own equations for the dwell time calculation.

To solve the above-mentioned problems, the Cartesian coordinate system can be transformed to a 60° coordinate system (shown in Fig. 4) by

$$V_\alpha = V \cos\theta - V \sin\theta/\sqrt{3} \quad (3)$$

$$V_\beta = 2\ V \sin\theta/\sqrt{3}$$

where V_α and V_β are the co-ordinates of a space vector V^* in the 60° co-ordinate system, and *V* and θ are its amplitude (length) and phase angle, respectively. The benefits of such a transformation will be demonstrated in the following sections

A. Fast Determination of Reference Vector

Assume that the reference vector V^* in Fig. 4 lies in triangle Δ *EFG* . To determine the location of the reference vector, the co-ordinates of the space vector V_D, $V_{D\alpha} = \text{int}(V_\alpha^*)$ and $V_{D\beta} = \text{int}(V_\beta^*)$, will be used, where int( ) is a lower rounded integer function, for example, int(4,6) = 4. The co-ordinates of V_D indicate the reference vector must lie in one of the two triangles, Δ DEF and Δ EFG. Based on V_D, the coordinates of space vectors V_E, V_F and V_G can be calculated by

$$(V_{E\alpha} , V_{E\beta}) = (V_{D\alpha} + 1, V_{D\beta})$$

$$(V_{F\alpha} , V_{F\beta}) = (V_{D\alpha} , V_{D\beta} + 1) \quad (4)$$

$$(V_{G\alpha} , V_{G\beta}) = (V_{D\alpha} + 1 , V_{D\beta} + 1)$$

respectively. To further determine whether the reference vector is in Δ DEF or Δ EFG, the following criterion can be used:

$$V^* \in \Delta \text{ DEF} \quad \text{If } (V_\alpha^* + V_\beta^*) \le (V_{E\alpha} + V_{E\beta})$$

$$V^* \in \Delta \text{ EFG} \quad \text{If } (V_\alpha^* + V_\beta^*) > (V_{E\alpha} + V_{E\beta}) \quad (5)$$

The above algorithm provides a very simple means to determine the location of the reference vector quickly and accurately.

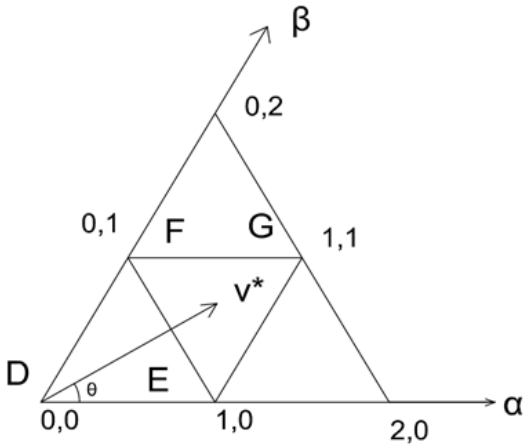

Figure 4. Space vectors in the 60º coordinate system (sectorI).

B.Dwell Time Calculation

With the reference vector in Δ EFG, the following two equations can be established according to the commonly used volt-second balancing principle:

$$V_F T_F + V_E T_E + V_G T_G = V^* T_S$$

$$T_F + T_E + T_G = T_S \qquad (6)$$

where T_F,T_E and T_G are the dwell times of the vectors V_F , V_E and V_G , respectively. Decomposing (6) into α and β - axis components yields

$$V_{F\alpha} T_F + V_{E\alpha} T_E + V_{G\alpha} T_G = V\alpha^* T_S$$

$$V_{F\beta} T_F + V_{E\beta} T_E + V_{G\beta} T_G = V_\beta^* T_S \qquad (7)$$

Substituting (4) into (7), the dwell times can be calculated by

$$T_E = (V_{D\beta} + 1 - V_\beta^*) T_S$$

$$T_F = (V_{D\alpha} + 1 - V_\alpha^*) T_S \qquad (8)$$

$$T_G = T_S - T_E - T_F$$

Similarly, with the reference vector lying in Δ DEF, the dwell times of the space vectors, V_F , V_E and V_D, are given by

$$T_E = (V_\alpha^* - V_{D\alpha}) T_S$$

$$T_F = (V_\beta^* - V_{D\beta}) T_S \qquad (9)$$

$$T_G = T_S - T_E - T_F$$

Assuming that V^* and θ of the reference vector in Fig. 5 are 1.2 and 20°, the dwell times can be calculated by

a. $V_\alpha^* = 0.89$, and $V_\beta^* = 0.47$
b. $V_{D\alpha} = \text{int}(0.89) = 0$, $V_{D\beta} = \text{int}(0.47) = 0$
c. V^* is in Δ EFG since $(V_\alpha^* + V_\beta^*) > (V_{D\alpha}+V_{D\beta}+1)$
d. $T_E = (0 + 1 - 0.47)T_S = 0.53T_S$,
$T_F = (0 + 1 - 0.89)T_S = 0.11T_S$, and
$T_G = (1 - T_E - T_F)T_S = 0.36\ T_S$.

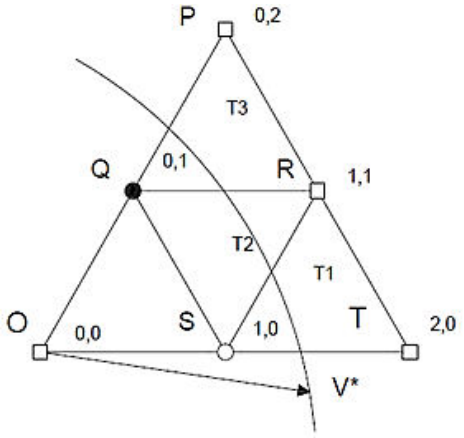

□ mean switching state for even vectors

O large switching state for odd vectors

● small switching state for odd vectors

Figure 5. Graphical representation of the proposed LSA method

The above example demonstrates how simple it is to determine the triangle that reference voltage falls in and to calculate the dwell times. More importantly, the algorithm has another two features:

a) It is a general algorithm, which can be used for inverters with any number of voltage levels; and

b) There are only two sets of equations for dwell time calculation. Compared with the Cartesian coordinate system where there are many sets of different equations for the calculation of the dwell time, the proposed algorithm is much simpler and easier for digital implementation.

III. GENERAL RELATIONSHIP BETWEEN SPACE VECTORS AND SWITCHING STATES

In the multilevel inverters, a space voltage vector could be represented by more than one switching state. For instance, space vector (1,0) in Fig. 4 has two switching states composed of [0,−1,−1] and [1,0,0], both of which produce an output voltage with the same magnitude and phase angle. With the increase in the voltage levels, there exist more redundant switching states. It is desirable

to find a general expression which describes the relationship between space vectors and their corresponding switching states for any multilevel inverters.

Space vectors in the 60° coordinate system shown in Fig. 4 can be generally expressed by (α , β), where α = 1, 2, …, 2*m*, and β = 1, 2, …, 2*m*. The number *m* is defined by

$$m = (n - 1) / 2 \quad (10)$$

where *n* is the number of phase voltage levels of the inverter, which is always an odd number for multilevel inverters.

The relationship between a space vector (α ,β) and its switching states [V_a, V_b, V_c] is obtained by a detailed study on all the possible states in a multilevel inverter. The results are given by

$$V_a = -m, -m+1, -m+2, \ldots, m$$

$$V_b = V_a - \alpha \quad (11)$$

$$V_c = V_a - \alpha - \beta$$

TABLE I. SWITCHING STATES IN SECTOR I OF A 3 - LEVEL SPACE VECTOR DIAGRAM

V_a	V_b	V_c
-1	-1-α	-1- α-β
0	0-α	0- α-β
1	1-α	1-α-β

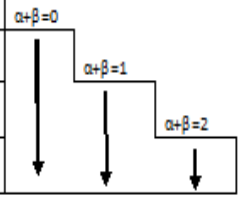

TABLE II. RELATIONSHIP BETWEEN SWITCHING STATES IN VARIOUS SECTORS

Sector	Phase A, B and C			Example:V(1, 0)
I	Va	Vb	Vc	[0, -1, -1], [1, 0, 0]
II	-Vb	-Vc	-Va	[1, 1, 0], [0, 0, -1]
III	Vc	Va	Vb	[-1, 0, -1], [0, 1, 0]
IV	-Va	-Vb	-Vc	[0, 1, 1], [-1, 0, 0]
V	Vb	Vc	Va	[-1, -1, 0], [0, 0, 1]
VI	-Vc	-Va	-Vb	[1, 0, 1], [0, -1, 0]

For a given space vector (α,β), the number of switching states n_{sw} can be obtained by

$$n_{sw} = n - (\alpha + \beta) .$$

Eqs. (10) and (11) are the general expressions, which can be used for any multilevel Alternatively, for a given space vector (α, β), all of its switching state can be calculated by

$$[\ V_a \quad V_b \quad V_c\ ]$$

$$[\ \alpha+\beta-m,\ \ \beta-m\ \ -m\ ]$$

$$[\ \alpha+\beta-m+1,\ \ \beta-m+1,\ \ -m+1\ ]$$

$$[\ \alpha+\beta-m+2,\ \ \beta-m+2,\ \ -m+2\ ] \quad (12)$$

……

$$[\ m,\ \ m-\alpha,\ \ m-\alpha-\beta\ ]$$

The switching states in other sectors (II to VI) can be obtained from Table I and the details are given in Table II.

IV. SELECTION OF SWITCHING STATES

In the multilevel inverter, the redundant switching states increase with the voltage level. For example, the 5, 7, and 9-level inverters have the redundant states of 4, 6 and 8, respectively for zero voltage vector. In the diode clamped multilevel inverters, the redundant switching states can be utilized to balance the voltage of capacitors in the dc link. The cascaded H-bridge inverter inherently does not have this problem. In this paper, the redundancy is employed to minimize the voltage harmonic distortion.

A. Definition of Mean, Small and Large Switching States

Any space vectors (α, β) in Fig. 4 can be classified into the following two categories:

Category 1: even vector – the sum of its coordinates, α + β , is an even number; and

Category 2: odd vector – the sum of its coordinates is an odd number.

It is interesting to note that the difference between the coordinates, α − β, of an even vector is always an even number while for an odd vector, the difference between α and β is always an odd number. Based on (12), the mean switching state of a space vector can be calculated by

$$V_{a\_mean} = \{(\alpha+\beta-m)+m\} / 2 = (\alpha+\beta) / 2$$
$$V_{b\_mean} = \{(\beta-m)+(m-\alpha)\} / 2 = (\beta-\alpha) / 2 \quad (13)$$
$$V_{c\_mean} = \{(-m)+(m-\alpha-\beta)\} / 2 = -(\alpha+\beta) / 2$$

Which can be rewritten [(α + β) / 2, (β – α) / 2, – (α + β) / 2].

For an even vector, each component of its mean switching state is an integer, and the state is implementable. For instance, space vector (1,1) in Fig. 4 has only one state: [1,0,−1. Its mean state is [1,0,−1], which can be realized by the inverter with output voltages of $Va = 1$, $Vb = 0$, and $Vc = -1$. However, for an odd vector where $\alpha + \beta$ and $\alpha - \beta$ is an odd number, its mean state cannot be implemented since the inverter cannot produce half-level voltages. In this case, a small or large switching state can be used:

small state $[(\alpha + \beta - 1)/2, (\beta - \alpha - 1)/2, (-\alpha - \beta - 1)/2]$ and

large state $[(\alpha + \beta + 1)/2, (\beta - \alpha + 1)/2, (-\alpha - \beta + 1)/2]$.

To minimize the voltage harmonic distortion, the arrangement of switching states are as follows:

a) for those triangles having one even vector, select one mean switching state, one small state and one large state; and

b) for the other triangles with two even vectors, select two mean states and one small or one large state alternatively when the reference vector moves along.

B. Switching Sequence Design

The switching sequence design has to meet a number of requirements such as

a) minimization of number of switchings per sampling period,

b) one voltage level change per commutation of switching devices, and

c) adoption of the LSA method.

For example, when the reference vector lies in triangles T1, T2, T3 and T4 in Fig. 5, switching sequence and inverter output waveforms are given in Fig.7, where D, E, F and G are the vertexes (space vectors) of these triangles. The number in each column represents the switching states of a given space vector.

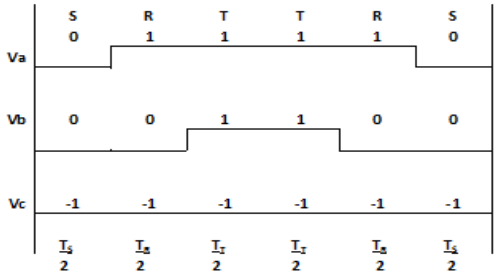

(a) V^* lying in T1

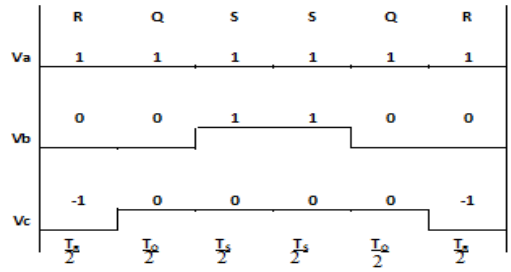

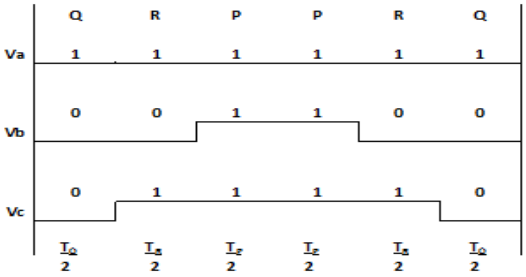

c) V^* lying in T3

Figure 7. Switching sequence and inverter output waveforms generated by the LSA method with the referece vector lying in triangles T1, T2, T3 and T4.

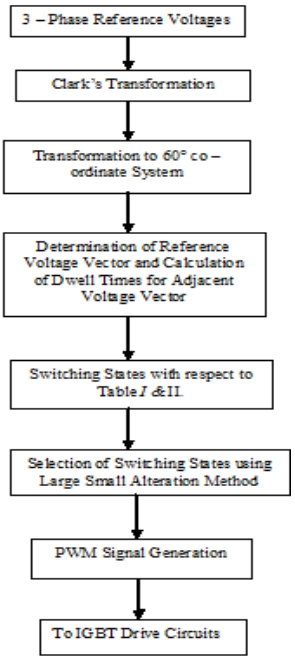

Figure 8: flowchart of the proposed SVPWM Algorithm

SIMULATION OF SPACE VECTOR PWM CONTROL ALGORITHM FOR 3 LEVEL DIODE CLAMPED INVERTER USING MATLAB/SIMULINK SOFTWARE

The design procedure is as follows:

(b) V^* lying in T2

- The inverter consists of 3 IGBT arms which forms a 3 level diode clamped inverter.
- The input is a DC voltage source.
- The gate pulses to the inverter is given by the space vector modulation block.

- The timing signals, timing generation and the timing calculations, the sequence of switching devices are designed and are given by the space vector modulation block.
- The simulation is carried out using matlab.
- The motor speed and the torque has been controlled which enhances the drive performance through reduction in Switching losses and Total Harmonic Distortion (THD).
-

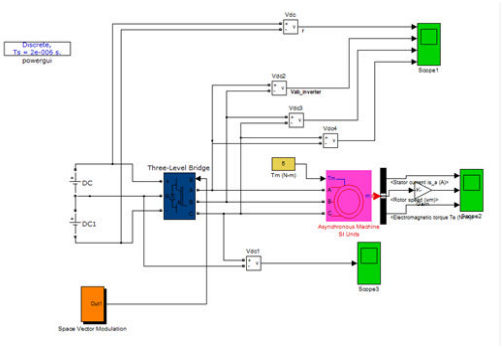

Figure 8: Simulation Model of a 3 level diode clamped inverter

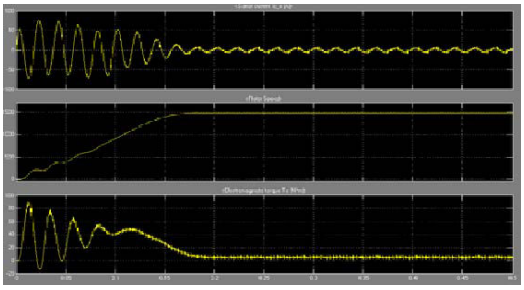

Figure 9: Response of stator current, rotor speed and torque in SVPWM

FFT Window: 4 of 50 cycles of selected signal

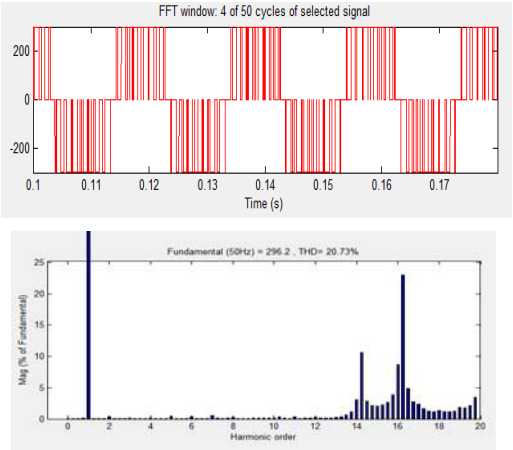

IV. CONCLUSION

A simple and general space vector PWM algorithm has been proposed in this paper. To facilitate the design and digital implementation of the space vector algorithm, all the space vectors are transformed from the commonly used Cartesian coordinate system to a 60° coordinate system. The proposed algorithm substantially simplifies the calculation of space vectors and their corresponding dwell times. Based on the proposed algorithm, a new switching pattern, referred to as Large-Small Alternation (LSA), for the 3 level diode clamped multilevel inverters has been developed. The LSA algorithm features easy implementation and more importantly, minimum harmonic content in the inverter output voltage. The most important aspect of the proposed algorithms lies in their generality. These algorithms are verified through computer simulations.

REFERENCES.

[1] L. Yiqiao, and C.O. Nwankpa, "A new type of STATCOM based on cascading voltage source inverters with phase-shifted unipolar SPWM," IEEE Trans. on Industry Applications, Vol.35, No.5, 1999, pp1118-1123.

[2] L. Li, C. Dariusz, and Y. Liu, "Multilevel space vector PWM technique based on phase-shift harmonic suppression," Applied Power Electronics Conference and Exposition(APEC), Vol.1, 2000, pp535-541.

[3] M.L. Tolbert, and F.Z. Peng, "Multilevel Converters for Large Electric Drives," IEEE Trans. On Industry Applications, Vol.35, No.1, 1999, pp36-44

[4] D.W. Kang, Y.H. Lee, B.S. Suh, C.H. Choi, and D.S. Hyun, "Acarrierwave-based SVPWM using phase-voltage redundancies for multilevel H-bridge inverter," International Conference on Industrial Electronics, Control, and Instrumentation(IECON), Vol.1, 1999, pp324-329.

[5] B.S. Suh, and D.S. Hyun, "A New N-Level High Voltage Inversion System," IEEE Trans. On Industrial Electronics, Vol.44, No.1, 1997, pp107-115.

[6] D.G. Holmes, and P.M. Brendan, "Opportunities for harmonic cancellation with carrier based PWM for two level and multilevel cascaded inverters," IEEE Trans. on Industry Applications, Vol.37, No.2,2001, pp574-582.

[7] S. Busquets-Monge, J. Bordonau, D. Boroyevich, and S. Somavilla, —The Nearest Three Virtual Space Vector PWM—A Modulation for the Comprehensive Neutral-Point Balancing in the Three-Level NPC Inverter, IEEE Power Electronics Letters, Vol.2, No.1, pp 11-15, March 2004.

◈◈◈

Anti-jamming Techniques using Cognitive Radio Networks

Suthikshn Kumar

Dept of EE, Defence Institute of Advanced Technology(DIAT),
Girinagar, Pune 411025

Abstract- Cognitive Radios perform spectrum sensing, channel hopping and hence are ideal for detecting and overcoming jamming techniques. Cognitive Radios can be used to detect the available spectrum and transmit information even in the presence of jamming. Cognitive Radio Network(CRN) is a distributed network of cognitive Radios. Thus in military scenerios, in the presence of heavy jamming, CRNs can share information and intelligently take counter jamming measures to transmit information securely and efficiently.

Key Words: *Cognitive Radios, Cognitive Radio Networks, Jamming, Anti-jamming, DSSS, FHSS, Multi-armed Bandit, Markov Decision Process.*

1. INTRODUCTION

Jamming is a Denial of Service(DoS) attack on wireless communication networks. It prevents the genuine users from communicating. While jamming, an attacker usually transmits RF signals interfering with the actual communication. Jamming is easier to carry out but is very hard to defend from. Robust Anti-jamming techniques are very much essential for secure military and civilian communication.

There are several techniques proposed which help to mitigate the effects of jamming[1]. The techniques based on Cognitive Radio Networks (CRNs) have received increased attention recently[3, 9, 20, 21]. Cognitive Radios(CRs) continuously sense the spectrum, intelligently identify the unused spectrum. They operate in this spectrum when other radios are not using it. CRs seem to be an elegant solution for spectrum sharing problem. The Dynamic Spectrum Access(DSA) technique ensures that CRNs can be granted access to the licensed spectrum as Secondary Users. This is while ensuring that Primary Users (who are Licensed users) do not observe interference from the CRNs. The CRNs continuously sense the spectrum and vacate the channels whenever they detect any Primary user activity.

A conceptual view of Cognitive Radios and CRNs is presented. This will facilitate the better analysis of the strengths and weaknesses of CRNs. After presenting a discussion on Anti-jamming, we review prominent research in anti-jamming using CRNs. We classify the anti-jamming techniques and comment on the utility of each proposed technique with references.

This paper is structured as follows: In the next section, we provide an overview of Cognitive Radios and CRNs. This is followed by section 3, where we present the Anti-jamming techniques using CRNs. In section 4, we review the results of anti-jamming. Summary and conclusion are presented in Section 5.

2. COGNITIVE RADIOS

Cognitive Radios were initially proposed by Mittola III in his Doctoral Thesis[2]. This thesis dealt with the crossing of personal wireless technology and computational intelligence. A cognitive Radio architecture was proposed which combined agent based control, natural language processing(NLP) and machine learning(ML) technology into Software Defined Radios(SDR) platforms. The Cognition in CRs correspond to intelligent actions such as Observation, Planning, Orienting, Decision making.

Cognitive Radios perform intelligent spectrum sensing and determine unused sprectrum for communication[12]. Cognitive Radio Networks(CRNs) are a distributed network of CR devices and form self-configuring and multi-hop network[11]. Each of the CR devices within CRN has to independently make its decision regarding spectrum sharing. The CR devices in the network can share information about the spectrum usage.

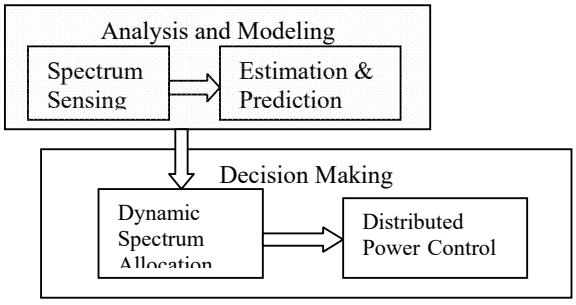

Fig.1 Block Diagram of Cognitive Radio

The functions of Cognitive Radios are manifold[14]:

- Spectrum Sensing, Estimation and Prediction
- Dynamic Spectrum Management and Power Control

The first set of functions can be grouped as Analysis and Modeling functions. The second set of functions are Decision Making functions. These functions require that Cognitive Radios should have intelligence inbuilt into them or they should be capable of learning from examples.

Spectrum sensing is an integral function of Cognitive Radio. This function determines whether a part of spectrum is used or unused or partially used. These are called as Spectrum Holes. White and Gray spectrum holes have all or some unused spectrum available, while black spectrum hole indicates that this part of spectrum is completely utilized. The total sensed power in a particular frequency band is sometimes referred to as Interference Temperature. This is a very useful metric for spectrum sensing[15]. The Cognitive Radio may sense the spectrum reactively or pro-actively. On demand sensing is also known as reactive spectrum sensing whereby the CR will try to determine the spectrum availability when data has to be sent.

The Cognitive Radios need to make quick and accurate decisions on utilizing the spectrum based on the data collected by spectrum sensing. Decision making requires that CRs should have some kind of intelligence built into them. Dynamic Spectrum Allocation (DSA) involves distributing the data traffic into spectrum holes. The users are trying to maximize their benefits by trying to utilize the available spectrum. However, the presence of several users mean that some kind of fairness strategies need to be adapted inorder to ensure fairness. The decision making process resembles game playing with user as a player, strategies as rules of the game. Thus decision making in CRs can utilize the concepts of game theory. Exact Potential Game model has been proposed to be applied for Dynamic Spectrum Allocation[14]. Two algorithms have been studied i.e., Load Balancing algorithm and Genetic Algorithm.

Cognitive Radio Networks(CRNs)

A network of Cognitive Radios which share information on Spectrum sensing and usage co-operatively form CRN. Each CR in CRN is independent in its operation but relies on shared information from the distributed CRs. There is no central entity to synchronize. Game theory is well suited for modeling CRNs.

At different networking protocol layers, variety of game models can be there as follows[11]:

- Physical Layer: Waveform Adaptation Game, Power Control Game and Spectrum Sharing Game
- Medium Access Control(MAC) Layer: Location Awareness Game, Multiple Access Game, Distributed Control Game
- Network Layer Game: Forwarder's Dilemma, Network packet forwarding Game

The CRNs prolong the battery life of the nodes by performing power control. They can co-ordinate the power co-control to minimize the interference. Power control along with the Dynamic Spectrum allocation forms an important task for the CRNs.

3. ANTI-JAMMING USING CRNS

Jamming is a Denial of Service (DoS) attack on wireless networks due to which nodes cannot communicate. Various techniques can be used for jamming[1]. Jamming can be carried out in Phy or MAC layer. An attacker with the knowledge of frequency spectrum being used for communication can set up a transmitter in the same frequency band which emits noise. This will interfere with the genuine RF signals of the wireless networks. Jammers can be classified into following categories:

- Non-stop jammers
  - Constant Jammers
  - Deceptive jammers
- Intermittent jammers
  - Random Jammers
  - Reactive Jammers

RF jammers have many applications such as disabling remote controlled bombs, obstructing radio communication of terrorists/rioters. Commercial RF jammers are available for various end user applications[19]. The main advantage of Intermittent jammers over non-stop jammers is the power conservation. Jamming devices can be battery powered and hence need to conserve their battery power to be effective over a period of time. There are three jamming strategies used :

- Strong jamming
- Light Jamming
- Smart Jamming

The first strategy of strong jamming works towards jamming any transmission. Smart jamming strategy involves jamming the channel sensing and channel switching slots.

Anti-Jamming is concerned with counter measures for successful communication in the presence of jamming attacks. Anti-jamming techniques may involve frequency hopping and coding. For an Anti-jamming technique to be useful it has to be innovative, scalable, resilient, robust and universal.

The current Anti-jamming techniques are based on the a priori knowledge of jammers and nature of interference they may generate. Such techniques are termed Fixed Anti-Jammer Techniques(FATS).

Frequency Hopping Spread Spectrum (FHSS) and Directi Sequence Spread Sprectum(DSSS) have been proposed to as anti-jamming techniques. In these protocols, the hopping sequence or the spreading codes are preshared secretly between the sender and receiver. However these techniques may not be directly applicable to CRNs due to the following reasons[22]:

- Pre-sharing of secrets may not be applicable to Secondary Units as they may not meet before the communication.
- FHSS requires the availability of wide range of frequencies. This spectrum may not be easily available in CRNs.

Anti-Jamming using CRNs: The CRN based Anti-jamming techniques are adaptive based on the sensing of the interfering environment[20]. The characteristics of the interference are sensed and are used in optimizing signal processing and machine learning algorithms which reduce the impact of the interference. The capability of CRN to hop among many channels is an added adavantage towards anti-jamming. However the flexible MAC and Physical layer in the CRN would mean that they are more susceptible for jamming attacks.

There are three main categories of anti-jamming techniques in Wireless networks:

- Network Layer Anti-jamming
- Link Layer Anti-Jamming
- Physical Layer Anti-Jamming

Network Layer Anti-jamming usually involves network coding which prevents such attacks as Snooping and eavesdropping attack. Random Linear coding based schemes provide good anti-jamming capabilities. Channel Hopping is the popular link layer anti-jamming technique. Beam-forming, directional antennas and spread spectrum are Physical layer techniques for anti-jamming.

4. REVIEW RESULTS

Wu et al., have discussed anti-jamming games Multi-channel CRNs[3]. The interaction of secondary users and jammers is analyzed. Based on this analysis, a channel hopping strategy is developed using Markov Decision Process. Two learning schemes have also been presented for Secondary users who have deficient knowledge of the attackers. The major drawback of this technique is that Primary User's traffic statistics details may be unavailable to Secondary Users. The traffic statistics may consist of initial information states and transition probabilities.

Su et al have presented Anti-jamming dynamic multi-channel access in CRNs as a Multiple-Armed Bandit(MAB) problem[9]. A time-slotted system is proposed where each time-slot consists of Sensing and Ack components. The secondary Units optimize their channel access using MAB algorithm. The performance of this technique was evaluated using the following metrics:

- Mean of successful transmissions
- Throughput and channel selection strategy

The results demonstrate that this technique is tolerant to jamming attacks.

Q. Wang et al have presented a formulation of Anti-jamming in Multi channel access in CRNs as Non stochastic Multi-Arm Bandit problem[22]. The secondary sender and receiver adaptively choose their transmitting and receiving channels in respective timeslots to optimize their throughput. The proposed technique tries to ensure that the sender and receiver simultaneously hop to the same channel with high probability. Extensive simulations have been carried to validate the model and ensure that the protocol is highly resistant to jamming attacks. Each of the CR nodes in CRN are modeled as One-arm bandit or slot machine. A set of CRs in CRN thus may be modeled as Multi-arm bandit. The sending and receiving nodes repeatedly generate random numbers which indicate the channel for them to communicate. The transceivers need to keep exploring for most suitable set of channels for transmission. The channels may be blocked by jammers or by the transmission of PU itself. The jammer may keep updating its strategy and thus the transceivers need to keep exploring for available channels. In order to minimize the exploration phase, the transceivers also need to maximize their utilization of the channels previously chosen. This protocol thus tries to balance between exploitation and exploration.

Coding techniques such as Rateless Coding and piecewise coding have been considered to be efficient Anti-jamming techniques[21]. The rateless coding offers low encoding and decoding complexities. The piecewise coding is an effective anti-jamming coding technique. Here K Blocks of L data sequences, the first bits are picked from all the K Blocks and encode them to produce length N codeword. These are transmitted through the N-Subchannels. The piecewise coding scheme is suited for parallel decoding and provides fast response to packet loss. Both the coding schemes have been extensively simulated and performance results demonstrate that they provide reliable transmission with high throughput and small redundancy.

5. SUMMARY AND CONCLUSION

Cognitive Radio(CRs) intelligently sense and utilize the spectrum efficiently. CRNs are prone to jamming attacks and require robust protocols to be designed for ensuring that they are resilient from jamming.

We have reviewed the architecture of CRNs, various issues related to anti-jamming. Three important research works have been reviewed. The Multi-Arm Bandit problem formulation and Markov Decision process models have been utilized by various researchers to propose anti-jamming protocols for CRNs. The MAB formulations are equivalent to single state Markov Decision Process[23].

5. REFERENCES

[1] R. A.Poisel. "Modern Communications Jamming Principles and Techniques", Artech House, 2011.

[2] J. Mitola III, "Cognitive Radio: An Integrated Agent Architecture for Software Defined Radio", PhD Thesis, KTH, Sweden, May 2000.

[3] Y. Wu at al., "Anti-Jamming Games in Multi-Channel Cognitive Radio Networks", IEEE Journal of Selected Areas in Communications, Vol 30, No.1, Jan 2012.

[4] R. Nikjah and N.C. Beaulieu, "On Anti-Jamming in general CDMA Systems Part II: Anti-Jamming Performance of Coded Multi-carrier Frequency Hopping Spread Spectrum Systems", IEEE Trans on Wireless Communication, Vol 7, No 3, March 2008.

[5] S.V. Saboji and C.B. Akki, "Congestion Aware Proactive Vertical Handoff Decision using Coalition Game", International Journal of Soft Computing and Engineering(IJSCE), Vol. 1, Issue 6, Jan 2012, pp 91-97.

[6] Mark Felegyhazi, Jean-Pierre Hubaux, "Game Theory in Wireless Networks: A Tutorial", EPFL Technical report: LCA-REPORT-2006-002, submitted on Feb. 21, 2006;

[7] J. Neel, "How does Game Theory Apply to Radio Resource Management?", PhD Thesis, Virginia Tech Doctoral Program.

[8] Bo Liang, "Power Control and Security Games for Wireless Communication Networks", MS Thesis, University of Nebraska, Dec 2011.

[9] Hai Su, Q. Wang, K. Ren and K. Xing, "Jamming-Resilient Dynamic Spectrum Access for Cognitive Radio Networks", Proc. Of IEEE ICC 2011.

[10] Yan Zhang and Mohsen Guzani, Game Theory for Wireless Communication and Networking, CRC Press.

[11] Saurabh Mehta and K.S. Kwak, "Game Theory and Cognitive Radio Based Wireless Networks", KES-AMSTA 2009, LNAI 5559, pp. 803–812, 2009

[12] S. Ashley, "Cognitive Radios" Scientific American, Feb 2006.

[13] G.Staple and K. Werbach, "End of Spectrum Scarcity", IEEE Spectrum, March 2004.

[14] M.G.A Elnourani, "Cognitive Radio and Game Theory: Overview and Simulation", MS Thesis, Electrical Engineering, Blekinge Inst of Technology, 2008.

[15] T.C. Clancy III, "Dynamic Spectrum Access in Cognitive Radio Networks", PhD Thesis, University of Maryland, College Park, USA, 2006.

[16] J. Neel, J. Reed, R. Gilles, "Game Models for Cognitive Radio Analysis," *SDR Forum Technical Conference 2004*, Phoenix, AZ, Nov. 15-18, 2004.

[17] Y. Xiao and F. Hu(Editors), "Cognitive Radio Networks", CRC Press, 2009.

[18] S. Haykin, "Cognitive Radio: Brain-Empowered Wireless Communication", IEEE Journal of Selected Areas in Communications, Vol. 23, No. 2, Feb 2005, pp 205-220.

[19] RF Jammer Solutions from SESP: http://www.sesp.com/rf-jammers.asp

[20] R. S. Prabhu, E. Valles, P. Dafesh, "Cognitive antijam radio system", in the Proceedings of SDR 2009 Tech. Conference.

[21] G. Yue, H. Wang and M. Madihian, "Design of Anti-jamming coding for Cognitive Radio", Proc of IEEE Globecom 2007.

[22] Qian Wang, Kui Ren, and Peng Ning, "Anti-jamming Communication in Cognitive Radio Networks with Unknown Channel Statistics" Proceedings of IEEE ICNP 2011, Canada.

[23] Wikipedia on Multi-Arm Bandit:

http://en.wikipedia.org/wiki/Multi-armed_bandit

GPS Vehicle Theft Tracking and Identification Control System

[1]C.Deenadayalan & [2]P.S.Prasanth

[1]Department of Electronics and Communication Engineering,
J.N.N Institute of Engineering College, Thiruvallur District, Chennai, Tamilndu-601102, India
[2]Department of Mechanical Engineering,
T.J.S. Engineering College Thiruvallur District, Chennai, Tamilnadu - 601 206, India

Abstract- This project greatly reduces the man power, time and operates efficiently without human interferences. In modern world, many new technologies such as RFID, bio metric recognition, GPS, GSM or mobile communication techniques and so on have been integrated into car security system. At the same time the amount of accident of car still remains high especially lost. In the system the processing system sends the signal to the processing unit. In this project, GPS is used to find the position of the vehicle and GSM used to send the message to the specified person whose number is stored in the micro controlled. At once if the vehicle seems to be theft, the owner has to just send SMS to that vehicle means vehicle will be stop all the door will be locked then theft will be locked in the car.

Index items: *GPS, GSM, SMS, microcontroller, vehicle tracking.*

I. INTRODUCTION

The purpose of the study is investigate the feasibility of vehicle tracking technologies for vehicles as probes two technologies were evaluated. Global positioning system (GPS), Global system for mobile communication (GSM) Vehicle probes information can be complementary to those freeways that have single loops since the single loops are not capable of producing the most accurate GPS location probe vehicle data can also be used for rural freeways or minor urban freeways where no instrumentation is planned. Local streets and arterials are also good candidates for collecting data from probe vehicles.GPS is one of the most promising techniques for vehicle positional accuracy available to data.

Especially with different GPS, a greater accuracy can be achieved by using two ground based satellite receivers one of receiver monitors variation of the GPS signal and communicates them to the other receiver that corrects its positional calculation for a greater accuracy carrier phase GPS is another technique to improve the position accuracy. It can be used for more precise timing measurement since its carrier frequency is much higher than the GPS signal. Another type of GPS is called augmented GPS. This technique is used for the transmission of differential correction and GPS satellite status information for instrument landing in space.

A mobile cellular network converts all the areas where its communication service is available, which implies that the freeway to be monitored is also converted with a series of cells. In particular, in the case of a freeway in rural areas, the mobile cellular network is provided with a group of cells exclusively for the freeway, the shape of which narrower and longer than that of the conventional cells in urban areas. The newly proposed cell based methodology involves all possible reference points that reside on the freeway e.g., the location of existing detectors or variable message signs, the entry and exit points of the freeway and other points based on these, travel times are calculated.

In the earlier systems the car alarms were used where if the intruder but the car the alarm starts sound but the safety is not assumed and then the car once theft can't be assured that we can get back the car. The alarm sound made by the car remains unnoticed and this major cause for the car theft.

II. RELATED STUDIES

The proposed system we introduced a low cost extendable frame work for car security. It consists of 1. Password protection module 2 GPS, 3.GSM, 4 Controllers

2. RFID MODULULE

2.1 RFID Technologies

Radio frequency identification as known as RFID is generic term of technologies that use radio to automatically identify people or object. The acronym reference to small electronic devices that consist of small chip and an antenna the chip typically a capable of carrying 2000 bytes of data or less the RFID provides a unique identifies for that object.

2.1.1 RFID SYSTEM

An RFID system is composed of three main components 1.An antenna or coil.2.A Transceiver (with decoder) and 3.An RFID Tag. The antenna will transmit radio signal to activate the tag so the data could be read or written Data Storage and retrieval purposes are performed using special devices the RFID Tag. The tag is very small and can be placed anywhere on anything.

2.1.2 RFID TAG

RFID Tag is a small object that can be attached to or incorporated into a product. It contains antennas to enable them to receive and transmit radio frequencies to and from transceiver. There are two bases of the RFID Tags passive and active. Passive tags required no internal power source and are commonly used with issues relating to securing. In contrasts, active tag required a power source, and is expensive. In addition, there is another type of tag which is called semi-passive tags except to the addition of a very small battery allowing in having a small amount of constant power

2.1.3 RFID reader

RFID reader is device that is used to interrogate an RFID tag the reader has an antenna that emits radio waves the tag responds by sending back its data. A number of factors can affect the distance at which a tag can be read the frequency used for identification the antenna gain, the orientation and polarization of the reader antenna as well as the placement of the tag on the object to be identified will have an impact on the RFID system read range.

Name	Power source	Transmission mode	Range within	Life
Passive	Scanning	Reflective	3m	Unlimited
Semi-passive	Battery	Reflective	10m	5-10years
Active	Battery	Active	100m	1-5years

Table 2.1 RFID tags classified by the source

2.2 GSM

GSM (Global system for mobile communication) is a digital mobile telephony system that is widely used in Europe and other parts of the world.GSM uses a variation of time division multiple access (TDMA) and is the most widely used of the three digital wireless telephony technologies (TDMA, GSM and CDMA). GSM digitizes and compresses data then sends it down a channel with two other streams of user data each in its own time slot it operates at either the 900MHZ frequency band.

2.3 GPS

GPS (Global positioning system) is a great boon to anyone who has the need to navigate either great or small distances. This wonderful navigation technology was actually first available for government use back in the late 1970s. In the past 10 years it has been made a valuable to the general public in the form of handheld receivers that use this satellite technology provided by the U.S. government.

GPS receiver help us to navigate back to a starting point or other predetermined location without the use of maps or any other equipment.

2.4 PIC micro controller

The controller we are used here is PIC (peripheral interface controller) separate code and data spaces for device other than PIC 16f877A which has a von Neumann architecture instruction most instruction are single cycle exclusions and skips.

2.5 SMS

SMS (short message service) is a service available on most digital mobile phone that permits the sending of short message. Short message also knows as text message or more conoquially SMS, text or even texts between mobile phone, other handheld devices and even landline telephones other uses of text messaging can be for ordering ringtones, wallpaper and entering competitions.

II. IMPLEMENTATION OF PROTOTYPE SYSTEM

The system requirement is divided into hardware and software part. First, the project criteria was examined and outlined in the following paragraph. The remaining paragraphs elaborate the hardware and software.

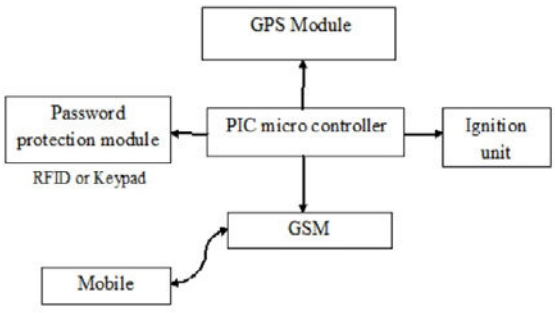

Fig.1 System Architecture

Password protection module is used for security identification of driver. Password protection is connected to the PIC to track the user details by correlating the password and the user details already stored in micro controller which has inbuilt. After the user enters the password in password protection the engine will start.

The processor is connected with the ignition unit, the GSM, the password protection, the end user who will be the owner where his/her mobile number is stored in the data based on the latest technology. After the user enters the password in password protection the motor will be start. If the password is wrong the GPS location is sent to the owner's mobile. If any unauthorized person is trying it drive the car, at that time we can stop the vehicle and lock the entire door.

IV. CONCLUSION

In this project GPS vehicle theft tracking and identification control system modern technologies such as GSM and GPS are used in order to know the exact location of the theft vehicle alert the user so that the user can stop the vehicle by sending SMS. The users can easily identity the location of the theft vehicle which in turns saves the money and time. Further, by providing proper control signal even the direction of the vehicle, steering moment and fuel injection, acceleration and starting of the motor can be easily controlled by the user and this process can be implemented effectively.

V. REFERENCES

[1]. B.Lsmith, M.L.Pack, D.J.lovell & M.W.Setmons" Transportation management applications of anonymous mobile call sampling" in proc 80th annu.meeting Washington, DC 2001

[2]. 2.R.Hereing , A.Hofleitner , S.Amin ,T.Nasr A.Khalek, P.Abbed and A.Bayen " Using mobile phones to forelast arterial traffic through statistical learning " in proc.89th transp. Res.Board annu meeting Washington, DC Jan 10-14-2010.

[3]. 3. Schiller, Johan H. (2000)" mobile communication "Pearson

[4]. 4. S.Ajaz M.Asim,M.Ahmed, M.Siddiqui Z.Musntag " Autonomus Vehicle monitoring & tracking system " SCONEST 2005 PP 1-4.

[5]. 5. Y.B.Y.Yim and R.Cayford " Investigation of vechicles as probes using Global Positioning system and cellular phone tracking field operational test " California PATA program ,Univ calif ,Berkely ,CA, ref USBTS PWP 2001-9

High Speed Clock and Data Recovery for Serdes Applications

[1]Krishna G Namboothiri, [2]Ashok Kumar, [3]Sandip Paul, [4]R. M. Parmar

[1]Indian Institute of Space and Technology, Trivandrum
[2,3,4] Space Applications Center (Indian Space Research Organization), Ahmedabad

Abstract- In satellite systems, large amount of high speed data is required to be transmitted from one system to another. Conventional parallel data transmission techniques require a large number of cables/interface-packages and results in large weight and volume. One possible solution identified is serial interface, also termed as SERDES (SERializer/DESerializer) interface. A typical SERDES interface comprises of encoder/decoder, PLL, timing-control, multiplexer/de-multiplexer and CDR (clock and data recovery). At high speed serial data rate, synchronization between serializer and deserializer becomes very difficult; hence faithful CDR operation is a mandate. The conventional CDR methods make use of very high frequency (X10) clock to achieve this or use analog components for phase detection and subsequent correction. This paper explains an innovative approach to synchronize data with the reference clock using digital phase detectors and inbuilt reconfigurable PLL in a space grade FPGA. Input reference clock is 10 times slower than serial input data. Implemented design employs a modified version of Alexander Phase Detector to locate the position of clock with respect to data, and then use this phase information to phase-shift the serial clock. The design does not aim to latch the data at the exact mid-point, but within specified 25% data width, which provides sufficient margin for faithful serial data recovery. The design has been verified for frequency range of 20 – 200 Mbps (limited by targeted space qualified FPGA). The design consumes very less resources (<2%) of FPGA, hence same can be integrated with other functional modules of the system.

Keywords— *SERDES, CDR, PLL, Alexander Phase Detector.*

I. INTRODUCTION

Today, a typical remote sensing camera requires processing of multiple video ports. Each port is being processed to yield typically ≥7-bit digitized video data, which needs to be transmitted to other subsystems for further processing/transmission. This is conventionally done using multiple cables (parallel data transmission). Increase in number of interfaces increase weight, volume and power requirements as well.

TABLE – I: COMPARISON OF INTERFACE REQUIREMENTS

Missions/ Parameters	Previous	Future
Sampling Rate (MSPS)	4.2	10
Video Ports	16	384
Interfaces	320	8448
Interface Power (W)	1.5	90.3
Harness Weight (w/o connector) (Kg)	3.6	94.1

Table-I shows comparison of detector data parallel interface (digitized CCD video data between camera electronics and data handling system) requirement of typical previous and future missions. With increase in transmission rates and number of interfaces, problems associated with crosstalk start to become more critical. One possible solution to this problem is serial transmission i.e. to perform parallel-to-serial conversion at the transmitter end, transmit the serial stream preferably over a differential medium and convert the serial data back to parallel form at the receiver end. This interface is also termed as SERDES (SERializer at transmitter end / DESerializer at receiver end). It considerably reduces the number of interconnecting signals and overcomes the issues of crosstalk. Fig.1 shows the block diagram representation of a typical SERDES architecture.

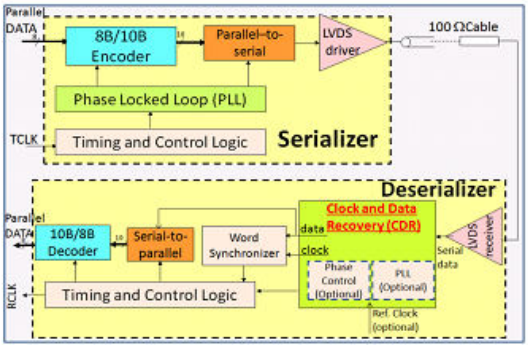

Figure 1.Block Diagram of SERDES architecture

In serializer, encoder modifies the parallel data and adds some overhead bits as well, before serializing it. This helps in synchronization and ensures data transitions in serial stream, which further helps in achieving DC balancing, clock recovery and error detection. 8B/10B encoding technique is selected for final implementation. Hence, 8-bit input data is serialized with 10X serial clock. PLL is required to generate serial rate clock (10X) from parallel clock. Serial data is transmitted over differential media.

Because of no synchronization between serializer and deserializer, recovery of serial data is very critical. So, oneof the most important functions of deserializer is clock and data recovery (CDR) form received serial data. It either extracts the synchronized clock from serial data itself or gets data synchronized with clock generated using reference parallel rate clock. PLL is mandatory for both the options. This paper investigates different CDR methods, their relative merits and demerits. This further explains design optimization and customization of selected CDR technique. The design blocks are explained in detailed. FPGA simulation and hardware results are also presented. Onboard implementation of CDR in FPGA calls for space qualified FPGA with inbuilt reconfigurable PLL. The selected FPGA's PLL operates in frequency range of 1.5 MHz to 250 MHz and it has phase control (0, 90, 180 and 270) and delay control. Design specifications are shown in table-II, which influenced from targeted FPGA.

TABLE - II
PARAMETERS AND SPECIFICATION OF CDR IMPLEMENTATION

S/N	Parameter	Specification
1	Serial Data rate	15 MHz – 250 MHz
2	Input clock Jitter value	<1.5 ns
3	Output serial clock jitter	< 2.5% of clock period peak-to-peak period jitter
3	Recovered parallel rate	1.5 MHz – 25 MHz
4	Locking time	<1 sec

II. CLOCK AND DATA RECOVERY METHODS

Clock recovery is the process of deriving a local, highly accurate, synchronized clock from a serial data stream (Fig. 2). Many serial data transmission standards such as PCI Express, IEEE1394b, Serial ATA, SAS, Fiber Channel, Gigabit Ethernet, InfiniBand, XAUI, Serial RapidIO, DVB & HDMI, HyperTransport, Common Public Radio Interface, USB 3.0 etc use CDR technique [1]. This technique is used at rates like 1.0625, 1.25, 2.5, 3.125 Gbps or even higher. Different CDR methods are investigated and explained below.

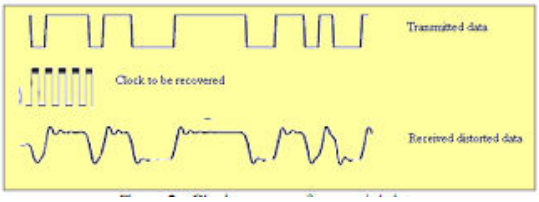

Figure 2: Clock recovery from serial data

A. Oversampling based CDR

This method performs phase detection by acquiring many samples of the data per period as shown in fig. 3. This implies that a very high frequency clock is required. If 10X frequency is considered as sampling clock, then the targeted FPGA can implement oversampling based CDR only upto 25 Mpbs serial rate. This has been verified from simulationas well. Hence this technique is found to be suitable only for low rate serial clock recovery.

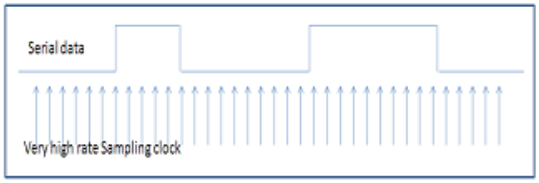

Figure 3: Clock Recovery by over sampling

B. Phase Lock Looped based CDR

PLL may be used for synchronization of serial input data with some reference serial clock. Phase Detector (PD) of PLL compares the phase of input signal with some reference signal in close loop. PLL modifies reference signal such that reference signal matches with input signal. But in CDR, input signal is NRZ random serial data, not a clock. Hence PLL could not be used straight forward way. A modified phase detector is required. Following are the two such methods for PLL based CDR implementation.

- Method-1

In NRZ serial data, there is no bit rate frequency content. For serial clock generation, spectral line at bit rate frequency is required. This spectral line can be generated by edge detection, i.e. to generate a small pulse at each transition edge. This will be fed to PLL for clock recovery. This CDR method is implemented in FPGA. Fig.4 shows the flow chart implementation. One of the main advantages of this method that input reference clock is not required. From serial data itself, serial synchronized clock is recovered.

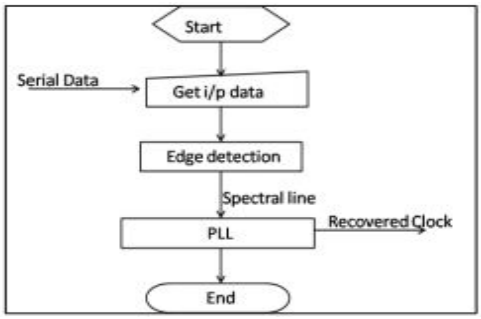

Figure 4: Clock Recovery by PLL using edge detection

Generating spectral lines at every data transition, i.e. edge detection was successfully performed by XOR-ing delayed data stream with the original data stream. But, the output of edge detector will still be random. The PLL of targeted FPGA does not lock to random data. Fig.5 shows simulation results. Clock was recovered sucessfully only when output of edge detector is periodic. For random NRZ serial data input, this method requires some different type of PLL (e.g.PLL with inbuilt Hogge phase detector), which is not available in targeted FPGA . Hence this option was not pursued further.

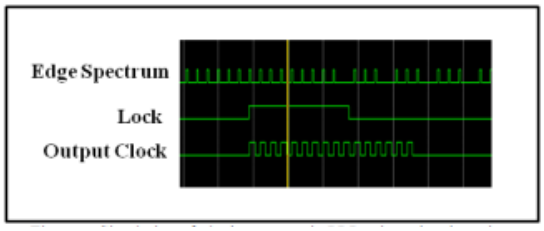

Figure 5: Simulation of clock recovery in PLL using edge detection

- Method-2

Another possible solution is to use external phase detector to detect the phase-error between serial data and reference clock and use this in a feedback loop to synchronize data with the clock (fig 6). Here, a reference clock is required, having frequency correlation with serial data. Only phase matching is required for data latching.

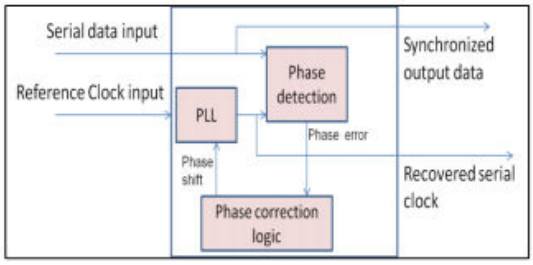

Figure 6: Clock Recovery by PLLz

For phase detection operation, two phase detectors named Hogge phase detector and Alexander phase detectors were explored. Hogge PD is analog in nature and it was not considered for present implementation. Alexander PD is fully digital in nature. This is also referred to as Bang-Bang detector. It provides only early/late information. Hence it has been modified in this design to give more accurate position of clock.

III. MODIFIED ALEXANDER PHASE ETECTOR

Alexander PD samples the data at three consecutive clock edges (S1, S2, S3) and performs simple logical operations on them to obtain early/late information as shown in fig. 7 (tabulated in table-III also). With NRZ random data, three conditions are possible i.e. early, late or hold (no transitions).

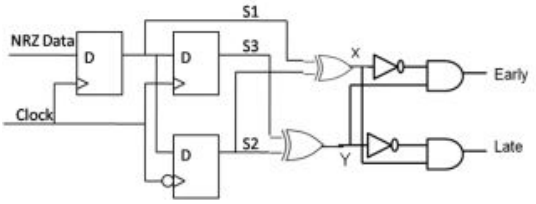

Figure 7: Alexander PD logic design

TABLE - III
ALEXANDER PHASE DETECTOR OPERATION

No data transition	Data transition with early clock	Data transition with late clock
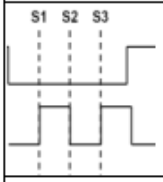	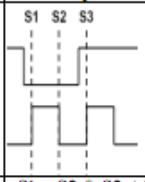	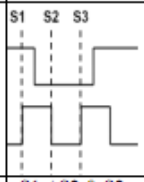
S1 = S2 = S3	S1 = S2 & S2 ≠ S3	S1 ≠ S2 & S2 = S3
Find X = S1 ⊕ S2 and Y = S2 ⊕ S3		
X = 0 = Y	X = 0 & Y = 1	X = 1 & Y = 0

Alexander PD divides the data periods in two halves. If clock rising edge is lying in first half of data period, it will be detected as ‗early'. If it is lying in second half of data period, it will be detected as late. Hence, Alexander PD does not provide sufficient phase resolution. A modified phase detector is presented keeping the basic operation same. Phase detection is done two times; one with original clock and later with 90° phase-shifted clock. This helps in locating the position of clock in one of four quadrants instead of two halves (figure 8).

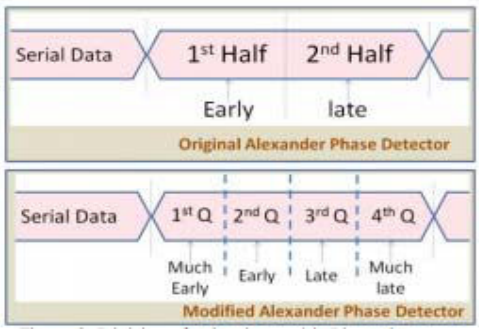

Figure 8: Division of a data interval in Phase detectors

Instead of just early/late detection, position of clock can be identified as much-early/early/late/much-late, belonging to one of the four quadrants as per the look up table Table-IV. After phase detection, final clock location (rising edge) needs to be shifted to third quadrant. Third quadrant is selected for final clock location taking into account the rise time and set-up time of high bit rate data. This is also mentioned in table-IV.

TABLE – IV: LOOK UP TABLE FOR QUADRANT IDENTIFICATION

Detected $Phase_{0°}$	Detected $Phase_{90°}$	Detected Quadrant	Detected Phase	Phase shift req. to have 3rd Quadrant
Early	Early	1	Much early	180°
Early	Late	2	Early	90°
Late	Late	3	Late	0°
Late	Early	4	Much late	270°

IV. DESIGN IMPLEMENTATION

Fig. 9 shows the block diagram representation of the design. The input to the CDR section is serial data (over a differential medium). The CDR block is supplied with reference clock having parallel rate (1/10 of serial data rate). Serial clock is generated by frequency multiplication of this parallel clock in a PLL and is later phase-shifted to obtain the recovered synchronized clock.

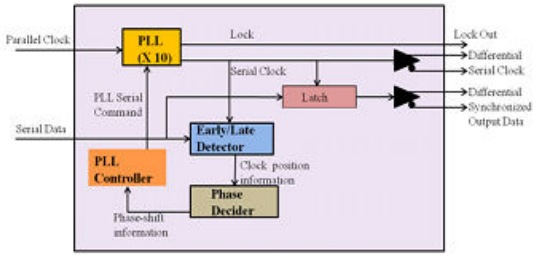

Figure 9: Design block diagram

The core available in the chosen FPGA has a programmable PLL with configurable multiply/divide frequency, phase-shifts and delays. Configuration of PLL requires serial programming (similar to JTAG). Based on the quadrant information of the clock and the corresponding phase-shift required, PLL serial programming is performed. Fig 10 shows the flowchart of the design algorithm. PLL is initialized to have 10X serial clock. Then for phase detection, original clock and 90° shifting clock is supplied. As per the detected phase, phase decider block alculates the required phase shift to have 3rd quadrant as final clock location. Again PLL is programmed for this phase shifting. In static timing analysis, 213 Mbps serial rate frequency is achieved as maximum frequency. Datasheet specifies PLL's maximum frequency as 250 MHz. Same is verified in simulation as well (given in next section). In targeted FPGA only 342 out of 13824 (2%) core cells are sed.

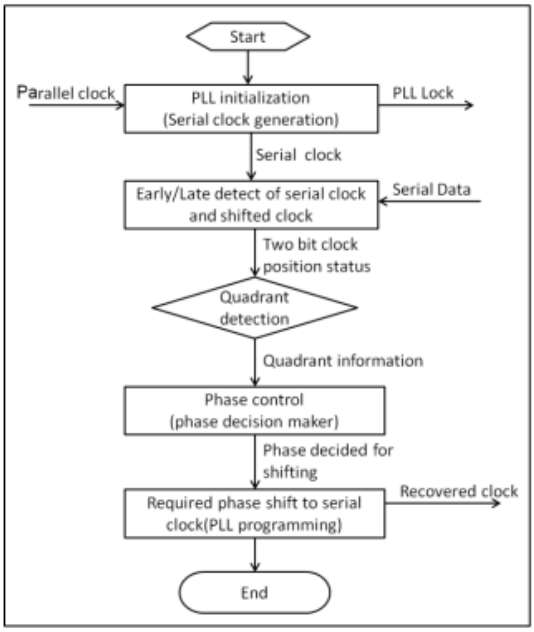

Figure 10: Algorithm of the design

TABLE VI
FREQUENCY ATTAINED IN DESIGN

Design stage	Serial clock constraint	
	Frequency requested	Frequency attained
Post-synthesis	250 MHz	204 MHz
Post-layout	250 MHz	213 MHz

V. RESULTS

Same design is verified with simulation and hardware as well. For verification purpose, one data period is taken as a Unit Interval (UI) and is divided into eight regions. Clock input is shifted to each of these regions and the output is observed. Functionality was manually verified from waveform for frequency range shown in table VII.

TABLE VII
FREQUENCY RANGE ACHIEVED

SDF Delay setting	Maximum frequency	Minimum frequency
Worst	200 MHz	20.20 MHz
Best	250 MHz	20.20 MHz

The initial and final positions of clock with respect to data have been plotted in fig.11. As per design, the final clock should fall in between 0.5 and 0.75 UI for proper functioning of the design.

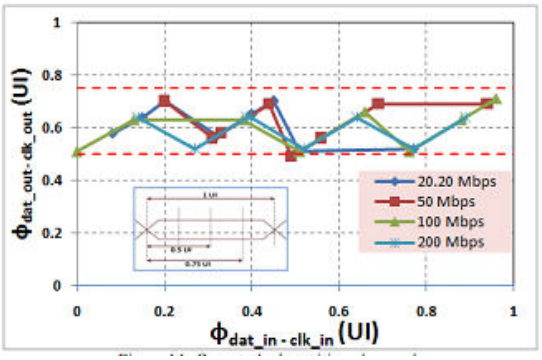

Figure 11: Output clock position observed

Same design was fused in equivalent commercial grade FPGA as well and the functionality was verified success fullyupto 160 Mbps. Fig.12 shows one of the outputs.

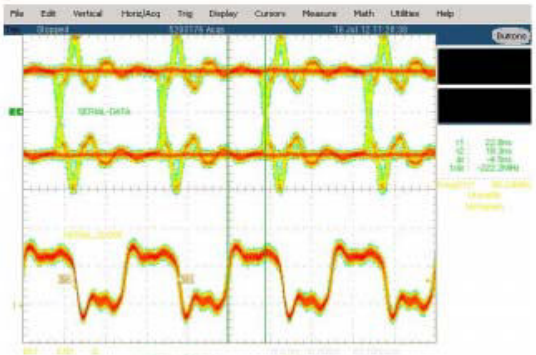

Figure 12: Synchronized data and recovered clock at 80 Mbps serial data

VI. CONCLUSION AND FUTURE SCOPE

Various Clock and Data Recovery designs were studied and relative merits understood. A modified Alexander Phase Detector based CDR is mplemented. The implementation uses inbuilt PLL function of FPGA. The design occupies only a small portion of the available logic resources, indicating that it can be integrated with other functional blocks of the system. The frequency achieved was close to the maximum frequency supported by the PLL. The clock was found to be recovered within 25 % of the expected deviation for 20 – 250 Mbps serial data rate. For data rate of <20 Mbps, oversampling based method is found to be useful and simulated successfully. For wide data rate range, both methods can be fused in hardware and implemented selectively as per input serial data rate. Hardware implementation of modified Alexander based CDR method was verified up to 160 Mbps serial data rate.

REFERENCES

[1]. Rick Walker, ―Clock and Data Recovery for Serial Digital Communication‖, Hewlett-Packard Company Palo Alto, California, ISSCC Short Course, February 2002

[2]. Istvan Haller and Zoltan Francise Baruch, High-Speed Clock Recovery for Low-Cost FPGAs‖, Computer Science Department, Technical University of Cluj-Napoca, Romania, 2012

[3]. Paulo Moreira, pllsApplicationsWithNotes.pdf‖, Paulo.Moreira@cern.ch

[4]. Steve Scroggs and Zachary Pfeffer, ―Clock and Data Recovery PLL Design Considerations in 0.1 um CMOS‖, Department of Electrical and Computer Engineering, UCB 425, University of Colorado

[5]. J. Lee, K. S. Kundert, B. Razavi, ―Analysis and Modeling of Bang-Bang Clock and Data Recovery Circuits,‖ IEEE J. Solid State Circuits, vol 39, no. 4, Apr. 2004, pp. 613-621

[6]. Radiation-Tolerant ProASIC3 Low Power Spaceflight Flash FPGAs Datasheet

AUTHORS BIO-DATA

Krishna G Namboothiri is pursuing B. Tech in Avionics Engineering from Indian Institute of Space Science & Technology (IIST), Thiruvananthapuram. Phone – 09746685721

Email: krish.kgn@gmail.com

Ashok Kumar, Sci/Engr. ‘SD’ passed his B.E. (E&C) from University of Rajasthan and joined SAC in 2008. He is involved in development of high resolution camera electronics for IRS Payloads. Contacts: 3877/67/65, SFED/SEG/SEDA, Space Applications Centre, Ahmedabad-380015, Phone- 91-79-26913877/67/65

Email: ashokkumar@sac.isro.gov.in

Sandip Paul, Sci/Engr. ‘SG’ received his B.Tech (E&C) in 1992 from NERIST and joined SAC in 1993. He is currently Head of the division for the Sensor Front End Electronics Division

Email:san@sac.isro.gov.in

R. M. Parmar, Sci/Engr. ‘G’ received his M. Tech. in Instrumentation & Control from IIT Bombay and joined SAC in 1983. He is currently Group Head, Sensors Electronics Group, SEDA/ SAC

Email: rmparmar@sac.isro.gov.in

Comparison of different digital relay algorithms for transformer protection using Matlab

[1]**Saurabh Kumar Gautam &** [2]**Ramesh Kumar,**

[1&2]NIT Patna, Patna, India

Abstract - This paper describes application of Discrete Fourier Transform and Block Pulse Functions for digital protection of power transformers. Digital relay algorithms are developed to extract fundamental, second harmonic and fifth harmonic components. These components are then used for harmonic restraint differential protection of power transformers. The Block Pulse Function based method is computationally simple and flexible to use with any sampling frequency. Off-line testing of the method with simulated inrush, over-excitation and internal fault current data clearly indicate that the Block Pulse Functions method can provide fast and reliable trip decision.

Key Words-Block Pulse Functions, Power Transformer Protection, Digital Differential Relay.

I. INTRODUCTION

The differential relaying principle is commonly used for the protection of power transformers [1]. Various developments in digital protection algorithms of power transformer up to 1988 have been reviewed by Rahman and Jeyasurya in [2]. Application of Walsh functions for microprocessor based transformer protection has been described in [3]. Fakruddin et al. have investigated the application of Haar function for differential protection [4]. All the digital filtering algorithms for differential relaying of power transformer till 2000 have been reviewed in [5] by Moravej et.al in last two decades use of artificial neural network in this area has increased rapidly. Many paper have been published describing application of Artificial Neural Networks (ANNs) in power systems [6]. Another popular algorithm recently is wavelet transform based transformer protection [7-12].

Wavelet transform became very popular lately, but researches show that they are much affected by noise [18]. Also wavelet co-efficient are complex numbers and difficult to calculate. ANN based method although gives very good result, for different systems different training sets has to be prepared so this kind of protection is subjective [7]. A recent paper which has implemented online protection highlights the need of high speed algorithms for online protection [11].

Schemes for differential protection of power transformers using DFT and BPF have been compared. The logic used to issue a trip decision in the transformer differential protection scheme is the relative amplitude of fundamental component compared to the second and fifth harmonics in the differential current. The technique is evaluated using simulated inrush and internal fault current signals. The test results clearly show that the BPF based technique can provide fast and accurate trip decisions.

II. DISCRETE FOURIER TRANSFORM

Discrete Fourier Transform is one of the most popular methods to study the discrete time signal in frequency domain. The sampled simulated data have been processed using Fast Fourier Transform and taking 16 samples per cycle.

Let us assume

$$Wn = e^{-j2\pi/N}$$

The flow graph showing the process of DFT computation has been given in figure 1.

III. BLOCK PULSE FUNCTIONS

The algorithm based on BPF is computationally simple and flexible to use with any sampling frequency. The BPF coefficients are obtained by merely calculating the values of current samples. The current samples acquired over a full cycle data window at the sampling rate of 12 samples per cycle.

Relationship between Fourier and BPF coefficients have been established

Current $i(t)$ which is given by time function can be expressed in terms of Fourier coefficients as :

$$i(t) = A_0 + \sqrt{2}\,A_1 \sin(2\pi t) + \sqrt{2}\,B_1 \cos(2\pi t) + \sqrt{2}\,A_2 \sin(4\pi t) + \sqrt{2}\,B_2 \cos(4\pi t) + \ldots\ldots \ldots + \sqrt{2}\,A_5 \sin(10\pi t) + \sqrt{2}\,B_5 \cos(10\pi t) \quad (1)$$

In terms of BPF coefficient a_n:

$$A_1 = 0.0302(a_1 + a_6 - a_7 - a_{12}) + 0.0824(a_2 + a_5 - a_8 - a_{11}) + 0.1125\,(a_3 + a_4 - a_9 - a_{10})$$

… (2)

$$B_1 = 0.1125\,(a_1 - a_6 - a_7 + a_{12}) + 0.0824\,(a_2 - a_5 - a_8 + a_{11})$$

$$+ 0.0302\,(a_3 - a_4 - a_9 + a_{10}) \quad \text{..... (3)}$$

$$A_2 = 0.05626\,(a_1 + a_3 - a_4 - a_6 + a_7 + a_9 - a_{10} - a_{12})$$

$$+ 0.1125\,(a_2 - a_5 + a_8 - a_{11}) \qquad (4)$$

$$B_2 = 0.09746\,(a_1 - a_3 - a_4 + a_6 + a_7 - a_9 - a_{10} + a_{12})$$

(5)

$$A_5 = 0.0225\,(a_3 + a_4 - a_9 - a_{10})$$

$$+ 0.06149\,(-a_2 - a_5 + a_8 + a_{11})$$

$$+ 0.084\,(a_1 + a_6 - a_7 - a_{12}) \qquad (6)$$

And

$$B_5 = 0.0225\,(a_1 - a_6 - a_7 + a_{12})$$

$$+ 0.06149\,(-a_2 + a_5 + a_8 - a_{11})$$

$$+ 0.084\,(a_3 - a_4 - a_9 + a_{10}) \qquad (7)$$

IV. APPLICATION OF DIFFERENTIAL PROTECTION OF TRANSFORMERS

In these schemes, the trip decision is based on the relative amplitude of the fundamental component compared to the second-harmonic and fifth harmonic components in the differential current. Two indices are used to obtain the relative amplitudes. The first index is defined as

K2= ((A2)2+ (B2)2)1/2 / ((A1)2+ (B1)2)1/2 ……. (8)

The second index is defined as

K5= ((A5)2+ (B5)2)1/2 / ((A1)2+ (B1)2)1/2 …….. (9)

Pre defined value for K2 is 0.15 and for K5 is 0.08 for restraining relay action.

Testing of the schemes

A 132kv/11kv three phase wye-wye transformer system has been simulated during present work.

Table 1 gives the value of transformer parameters in present simulation and table 2 gives the value of transmission line parameters. Fig 2 shows basic simpowersystem model of transformer.

TABLE 1 Transformer parameters

Transformer nominal frequency and power	10 MVA and 50Hz
Transformer winding parameters	R=.002 pu, L=.08 pu
Transformer core loss resistance	500 pu

TABLE 2 Transmission line parameters

Length	300 km
Frequency used for RLC specification	50 Hz
Positive and zero sequence resistances (Ohms/km)	0.01273 and 0.3864
Positive and zero sequence inductances (H/km)	0.9337e-3 and 4.1264e-3
Positive and zero sequence capacitance (F/km)	12.74e-9 and 7.751e-9

V. RESULTS

INRUSH CONDITION

The plots provide values of phase A, similar results have been obtained for other phases as well

RESULT FROM FFT

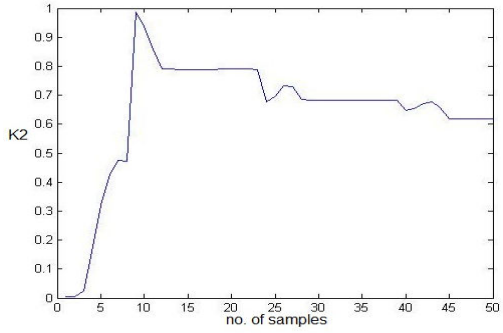

Fig. 3

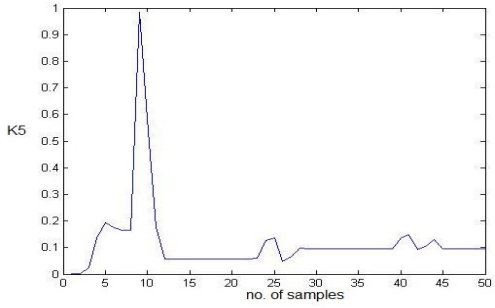

Fig. 4

RESULTS FROM BPF

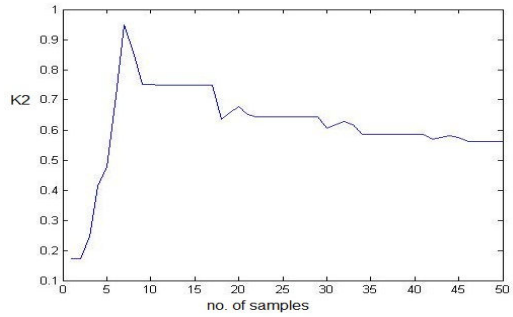

Fig. 5

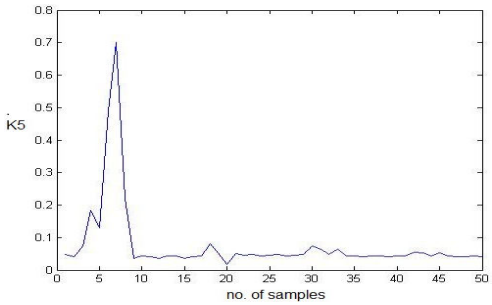

Fig.6

OVEREXCITATION CONDITION

Plots given below show condition for phase A similar results were obtained for other phase

RESULTS FROM FFT

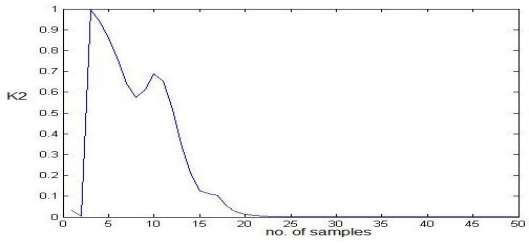

Fig. 7

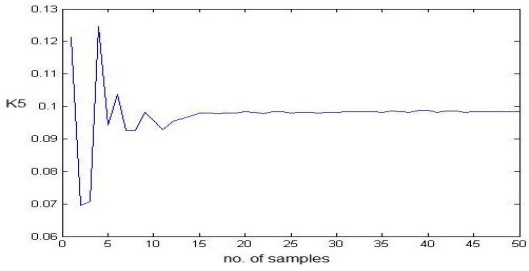

Fig. 8

RESULTS FROM BPF

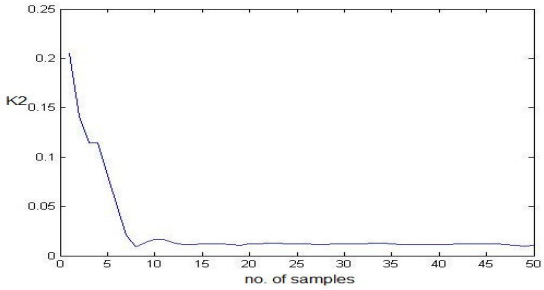

Fig. 9

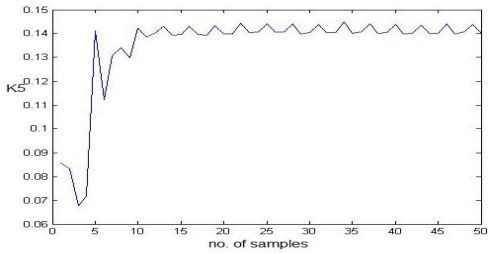

Fig. 10

INTERNAL FAULT CONDITION

Phase A condition has been depicted in plots

RESULT FROM FFT

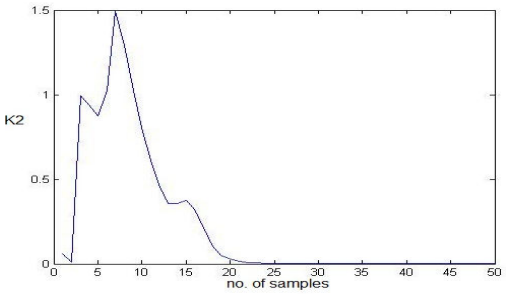

Fig.11

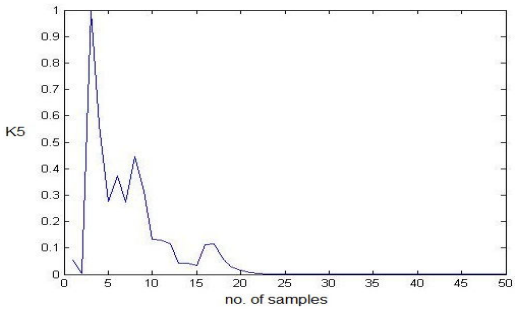

Fig. 12

RESULTS FROM BPF

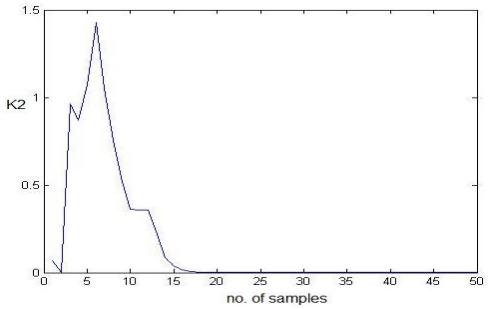

Fig. 13

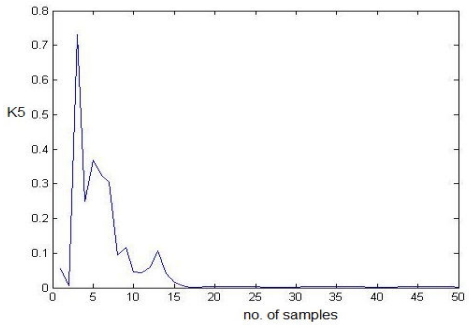

Fig. 14

VI. CONCLUSIONS

i) Simulation results from MATLAB sim power system reveal that differential current is negligible in case of normal condition and external fault condition.
ii) The differential current is high in case of inrush current, over excitation and internal fault current.
iii) The post fault current from all the cases have been processed with two algorithms. The coding has been done manually for Block Pulse Function method, while Discrete Fourier Transform has been performed using inbuilt code in MATLAB using standard command. .
iv) Fault conditions can be distinguished from non fault conditions within a cycle in both algorithms. In non fault conditions either K2nd or K5th are above their respective threshold values, restraining trip action of protective relay. In internal fault condition neither of the indices are above the threshold value and tripping action takes place.
v) Processing time in case of block pulse function algorithm is least.
vi) Block Pulse Function requires lesser number of samples per cycle. It gives satisfactory result at sampling rate of 12 samples per cycle whereas DFT require at least 16 samples per cycle to provide appropriate result

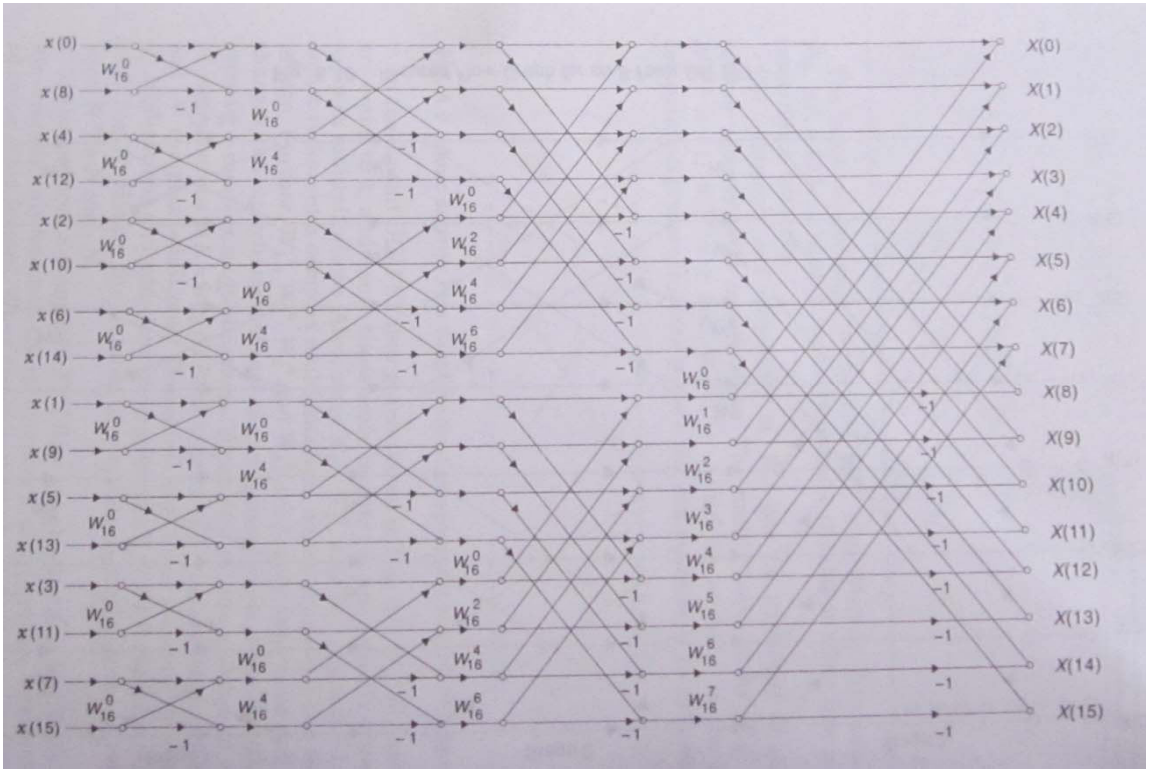

Fig.1 flow graph of the 16 –point DIT FFT algorithm

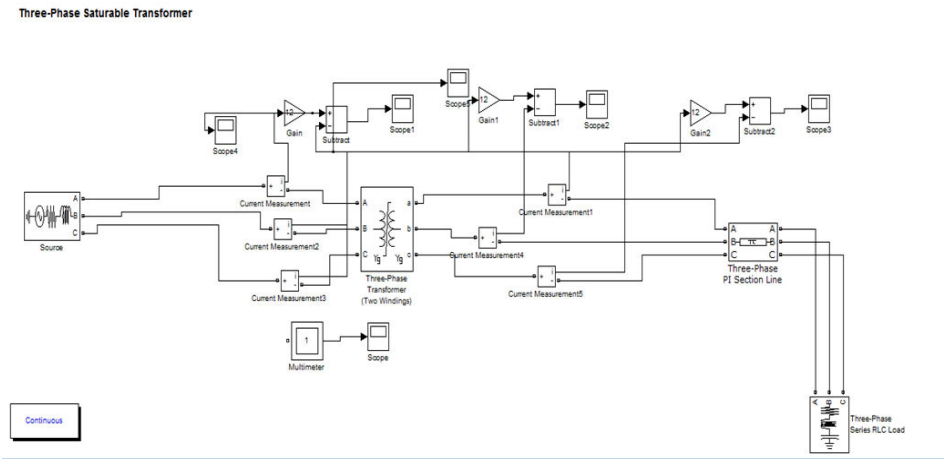

Fig. 2 Transformer model

REFERENCES

[1]. Horowitz, S.H. and Phadke , A.G. (2008) "Power System Relaying", John Wiley & Sons, England.

[2]. Rahman, M.A. and Jeyasurya, B. (1988) "A state-of-the-art review of transformer protection algorithms". IEEE Trans. Power Delivery, vol. 3, pp. 534–544

[3]. Rahman, M.A. and Jeyasurya, B.(1985) "Application of Walsh function for microprocessor based transformer protection". IEEE Trans. on Electromagnetic Compatibility, Vol. EMC-27, No. 4, pp. 221-225

[4]. Fakruddin, D.B. and Parthasarathy, K. (1985) , "Simplified algorithms based on Haar transforms for signal recognition in protective relays" Proceedings of the IEEE Volume: 73 , Issue: 5 Page(s): 940 - 942

[5]. Moravej, Z. and Vishwakarma, D.N. and Singh, S.P.(June 2000) , "Digital Filtering Algorithms for Differential Relaying of Power Transformer An Overview", Electric Machines and Power Systems, Vol.28, No.6, pp. 485-500.

[6]. Moravej, Z. and Vishwakarma, D.N. and Singh, S.P(June 2002), "Intelligent differential relay for power transformer protection", Journal of The Institution of Engineers ,vol.83pp.28-32,India

[7]. Vittal, K.P. and Gaonkar, D.N. and Fakruddin (2003), "Development of wavelet transform based numeric relay for differential protection of power transformer", IEEE TENCON, vol.4, pp.1580-1584,India.

[8]. Saleh, A. and Rahman, M. A.(2005), "Modeling and protection of a three-phase power transformer using Wavelet Packet transforms", IEEE transactions on power delivery, VOL. 20, NO. 2, pp. 1273-1282

[9]. Mozina, Charles J. (1999)," Protection of power plant transformers using digital technology", IEEE Transmission and distribution conference, vol.1,pp.421-432

[10]. Vazquez, E. and Mijares, I.I. and Chacon, O.L. and Conde, A.(2006), "Transformer differential protection using principal component analysis", IEEE Power Engineering Society General Meeting,pp.1-6

[11]. Aktaibi, A. and Rahman, M.A. (2011), "A software design technique for differential protection of power transformers", IEEE International Electric Machines & Drives Conference (IEMDC), 2011 , pp.1456-1461,USA

[12]. Srinivasulu, K. and Vishwakarma, D. N. and Sinha , Amrita (2010) **, "**Wavelet and ANN based differential protection of power transformer**"**16th national power systems conference, pp.675-680

[13]. Tallia, Raimondo and Morello, Piero and Castellano, Giancarlo (1984), "The Walsh-Hadamard Transform: An Alternative Means of Obtaining Phase and Amplitude Maps", Journal of nuclear medicine, vol.25, pp.-608-612

[14]. Rao, K.R. and Jalali, A. (1977), "Rationalized Hadamard-Haar Transform 11th Annual Asilomar Conference On Circuits, Systems and Computers", On Page(s): 194 - 203

[15]. Mekic, Fahrudin and Girgis, Ramsis and Gajic, Zoran and teNyenhuis, Ed (2007), "Power Transformer Characteristics and Their Effect on Protective Relays"**,** 60th Annual Conference for Protective Relay Engineers, 2007, pp 455-466

[16]. Kulidjian,A. and Kazstenny, B. and Campbell, B.(2001)"New magnetizing inrush restraining algorithm for power transformer protection", Development in power system protection conference publication no.479 IEE 2001,pp.181-184. (Canada)

[17]. Castro, C.R.T. and Barbosa, S.R. and Ferreira, H.L. and Samico, L.E. and Lopes, I.J.S. and Toshiba S.R.S. (2004), "Power transformer loading studies considering over-excitation", IEEE/PES Transmission & Distribution Conference & Exposition pp. 651-656 Latin America

[18]. Ashrafian, A. and Rostami, M. and Gharehpetian, G. B. and Gholamghasemi, M. (April 2012) "Application of Discrete S-Transform for Differential Protection of Power Transformers" *International Journal of Computer and Electrical Engineering, Vol.4, No.2.*

Achieving Wireless Data Transfer using Visible Light

[1]Jimesh Chokshi, [2]Nimit Gala & [3]Hrushit Parikh.

[1,2&3]Department Of Electronics and Telecommunication,
Dwarkadas J.Sanghvi College of Engineering, Mumbai.

Abstract—The prime source of communication since many decades has been radio communication. Its use is unchallenged partly due to usage practicality and also due to no effective alternative. However, due to the advent of data hungry smart phones and tablet computers and their sheer volume, the available radio spectrum is fast dwindling. Through this paper we wish to show that a very efficient alternative exists in the form of Visible Light! We wish to show how visible light can be used for cheap, secure, ultra-fast and beautiful communication. LED bulbs are used as transmitters and the intensity of the LED s is varied at very high rate, using the high capacity (almost reaching Shannon's limit) OFDM modulation technique to encode the data, such that the intensity appears constant to the human eye. So to an observer the bulb will appear to be doing what it always does - providing Illumination, however it is also transmitting data at unbelievable rates. The sensitive receiver circuit is designed to detect these small instantaneous changes in the LED intensity and hence decode the received data. The integration of high response Silicon PIN Photodiodes with signal processing tools makes this possible. Specific design measures prevent ambient light from interfering with the demodulation process at the receiver. Although this method can be currently used for short range, future developments can really expand its scope.

Index Terms— *Visible Light wireless communication, OFDM, Very high speed data transfer, PIN Photodiodes.*

I. INTRODUCTION

Visible light has been around us since almost the origin of the universe and will always be there. It is inherently safe, so to harness it for the purpose of communication would be phenomenal. Through this paper we propose a model which can be used to achieve this. In our study we realised the speeds which can be attained and this showed us the true potential of this method. Certain superior characteristics of visible light over radio waves which we would like to harness are:

- Supremely high transfer speeds; theoretically of the order of 10gbps
- 10,000 times greater spectrum than radio waves (Radio waves correspond to a frequency band of ~300GHz to ~3kHz, while the visible light correspond to a frequency band of ~400 THz to ~780 THz.)
- This technique has greater efficiency than radio communication. LEDs have proven operational efficiency and since visible light is used for communication, the data transfer is almost free of cost.

Commercially available PIN photodiodes are used to detect the light being transmitted. The diodes have rise and fall times ranging from a few nanoseconds to picoseconds. This corresponds to decoding rates of Gbps. At the transmitter end conventional modulation techniques can easily match up to these rates. What is needed is error free data transmission at such high rates. We wish to propose a model which we believe can ensure this. Data is modulated using the high channel capacity OFDM technique and the modulated data is transmitted in the form of intensity variations of an LED bulb. Steps are taken to ensure high SNR and low bit error rate. While it is obvious that this technology will be limited by line of sight, however, it is ideal for purposes such as secure indoor communication and as a wireless access point as we shall see in due course.

II. MODULATION AND TRANSMITTER BLOCK

A. Signal Representation

An OFDM signal is a sum of subcarriers that are individually modulated by phase shift keying (PSK) or quadrature amplitude modulation (QAM). [1] The symbol can be written as:

$$s(t) = \mathrm{Re}\left\{ \sum_{i=-\frac{Ns}{2}}^{\frac{Ns}{2}-1} d_{i+\frac{Ns}{2}} \exp(j2\prod(f_c - \tfrac{i+0.5}{T})(t-t_s)) \right\}, t_s \qquad (1)$$

$s(t) = 0$, $t<t_s$ and $t>t_s + T$

N_s is the number of Subcarriers
T_s is the symbol duration
F_c is the carrier frequency

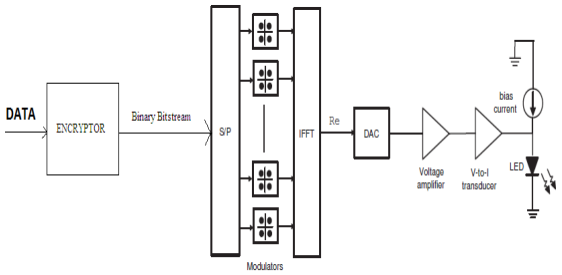

Fig. 1 Modulation and transmission. The LED is biased before applying the OFDM signal.

The encrypted data to be transmitted is OFDM modulated in the following manner. The serial data and redundancy bits are demultiplexed into parallel streams, each of which is transmitted on a separate sub-carrier as shown in fig. Phase shift keying (PSK), and m-ary quadrature amplitude (M-QAM) modulation methods can be used [2] . The Inverse fast Fourier transform (IFFT) operation is used to modulate the sub-carriers and generate the time domain OFDM signal,

$$x_k = \frac{1}{N}\sum_{n=0}^{N-1} X_n \exp\left(j\frac{2\Pi}{N}nk\right) \qquad (2)$$

Where x_k with k = 0, · · · ,N −1, are the N time-domain output samples, and X_n with n =0, · · · ,N − 1, are the input symbols. To modulate the LED intensity, the time-domain OFDM samples must be real. To ensure this complex conjugate input data symbols (e.g. Xn =X^*_{N-n}) are input to the IFFT block. A CP (Cyclic prefix) is needed due to multipath propagation. The CP acts as a guard interval to avoid ISI. To realize the CP, the last G samples of the OFDM symbol in eqn. (1) are repeated at the beginning so that N+G samples are transmitted. The measured channel delay spread in Optical Wireless(OW) systems is significantly less than that of RF based systems. Hence, the effect of the CP length on the bandwidth efficiency and SNR is insignificant in optical systems. [2]

B. Fixing the bias of LED and effects of its non-linearities

The digital OFDM signal is converted to its analog equivalent, amplified and this signal intensity modulates the LED as shown in Fig.1. Since the output OFDM signal is bipolar and optical intensity cannot be negative, the LED should be biased before applying the OFDM modulating signal. This DC component is removed through a DC restoration circuit at the receiver side. At high frequencies the LED behavior is non-linear. In RF systems, the main device causing 'nonlinear' distortions is the transmit power amplifier (PA) which is linear only over a finite range of input amplitudes. Fig 2 provides the comparison between the two and shows the non-linearity is less prominent in Optical Systems.

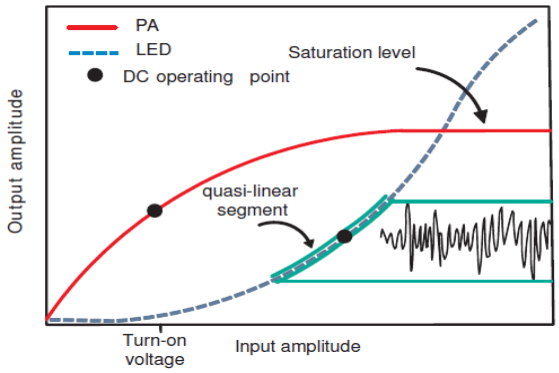

Fig. 2 Non linearities of Power Amplifier and LED [2]

The OFDM signal exhibits high Peak to average power ratio (PAPR). Therefore, the signal is very sensitive to nonlinearities. In optical systems, the OFDM signal envelope variations are utilized to intensity modulate the LED with its nonlinear characteristics. Selecting the correct bias point of the LED the distortion level s can be minimized. [2] The biasing point should be carefully selected to set the maximum forward current of the LED, to minimize signal clipping at the turn-on voltage and to minimize magnitude distortion which is influenced by the LED operating segment of its characteristics.

III. RECEIVER BLOCK

The first stage in the optical receiver design is the optical to electrical conversion which is shown in Fig. 3. This conversion is provided by the Photo detector (PD) and a transimpedance amplifier. The amplifier is used to amplify and convert the small PD current into a readable voltage.

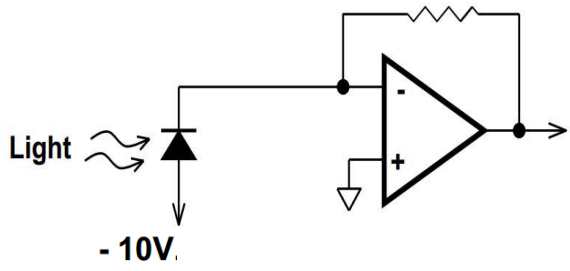

Fig. 3 Receiver and amplifier.

This voltage is additionally amplified and the DC component is eliminated. The signal is filtered by a low pass filter (anti-alias filter) and then sampled by the ADC. The amplifier at the photo detector stage is absolutely necessary because the photocurrent

produced by the PD is extremely small (of the order of nA) and also to convert this current into a voltage which is always easier for further processing.

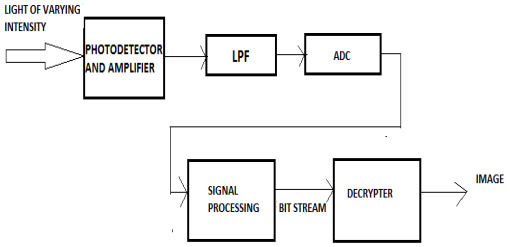

Fig. 4 Receiver block diagram

Fig. 4 shows a block diagram of the receiver. After down conversion and analog-to-digital conversion, the fast Fourier transform (FFT) is used to demodulate the N subcarriers of the OFDM signal. This happens in the signal processing block. After this process, the data is in the form of a binary bitstream. The conversion from the bit stream to the actual output data is then done by using the relevant decryptor.

IV. THE SI PIN PHOTODETECTOR

We make use of PIN photodiodes as Photo detectors .PIN diodes have operating wavelength range of 400-1000nm and hence are perfect for visible light application.

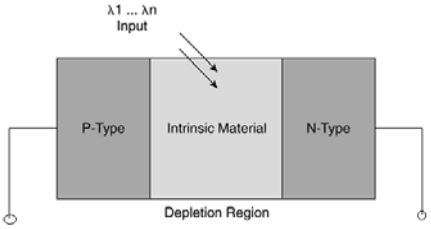

Fig. 5 PIN photodiode structure.

Fig. 5 shows the PIN diode structure. For high speed operation they are reverse biased. This draws current out of the central depleted region, blocking current flow unless light frees electrons and holes to carry current. The current is proportional to the amount of light absorbed which in turn increases with the thickness of the depleted region. The light absorption is concentrated in the middle intrinsic region which avoids the noise and slow response that would occur if ordinary PN photodiode was used. The typical reverse biases are 5-20V and typical response times range from a few nanoseconds to about 10 picoseconds. Sensitivity is about 0.7A/W at 800nm.

The device active area influences the detector speed and sensitivity. If the transmitting source has a cone of emission of diameter d, half-acceptance angle Θ and is at a distance S from the receiver; then it will project onto the detector a spot of diameter D [5]

$$D = d + 2S \tan \Theta \qquad (3)$$

Another important factor is the dark current which can introduce error in the receiver. It needs to be mitigated by proper device fabrication and in applications at room temperature it is negligible.

Avalanche Photodiodes (APDs) can be used and have faster response as they have internal gain mechanism by the process of photon multiplication which produces a veritable avalanche of carriers. Though they are extremely fast, the uneven nature of multiplication produces noise. Further, they need reverse biases of 10s-100s of volts which increases receiver complexity to the point of being impractical for our purpose.

VI. SYSTEM SNR and ADC RESOLUTION CONSIDERATIONS

Many sources of noise and non-linearities exist in this technology. The main source of errors is the error due to reduction in the SNR ratio due to quantization error from the ADC. It is given by [3]:

$$SNR = (1.763 + 6.02q)\ \text{dB} \qquad (4)$$

Where, q is the data converter bit resolution

However, the SNR values of a practical ADC are lower than the theoretical value of (3) because of the on-chip noise such as thermal noise, and shot noise and so on. Importantly, both sources are functions of the highest frequency of the signal being sampled. Therefore, the SNR of the ADC degrades as the OFDM signal bandwidth increases. Furthermore, by taking the square root of the sum of the squares for uncorrelated noise sources, the overall system SNR can be determined using:

$$SNR_{system} = -20\log_{10}\sqrt{10^{\frac{-SNR_1}{10}} + \ldots + 10^{\frac{-SNR_k}{10}}} \qquad (5)$$

This means that individual stage SNR figures combine so that the overall system SNR is lower than the SNR of the component with the lowest SNR. This is a serious issue which can only be addressed by choosing an ADC with an appropriate resolution based on empirical observations so as to achieve the required SNR to obtain faithful reproduction of data.

VII.APPLICATIONS

The applications for this technology are limitless owing to the fact that light is probably the safest source of energy there is.

- This technique can be used for almost all unidirectional communication within the same enclosure such as Indoor communication for office environments
- Wireless access points
- Smart streetlamps which can transmit weather forecasts, news, traffic updates to passing cars.
- Intra aircraft communications since visible light doesnot interfere with the radio communication of the cockpit.
- In hazardous environments such as petrochemical plants, where RF is prohibited.
- Radio waves do not propagate in water but light does and hence this technique can revolutionize underwater communication.
- This technology when implemented in mobile phones can be used for mobile to mobile communication and can replace existing technologies like Bluetooth and infrared because of superior data rates.
- The data being transferred cannot be tapped into from a remote location as in the case of RF because light does not propagate through opaque media.

VIII. CONCLUSION

We have presented a feasible method to use visible light for safe and cheap data transfer. The various steps to achieve transmission and faithful reproduction of data have been described. .OFDM modulation is used due to great efficiency at high speeds. This methods greatest challenge, the noise consideration, has been highlighted and we have proved that to improve SNR a trade-off in ADC resolution is necessary. The overwhelming advantages of this communication technique make this technology exciting. Though, this technology is still in its infancy, with further studies and development its far-reaching applications will only get better.

ACKNOWLEDGMENT

We gratefully acknowledge the insight and material provided to us by our research guide Prof. Tanaji D. Biradar at every step. In addition, we acknowledge the support of the faculty members of the department of Electronics and Telecommunication, Dwarkadas J. Sanghvi College of Engineering especially that of Prof. Dharmesh Mistry.

REFERENCES

[1] A.L. Intini " Orthogonal frequency division multiplexing for wireless networks" ,Graduate student UCSB, December 2000, unpublished. retrieved from Centre for research in art technology (CREATE) website www.create.ucsb.edu

[2] H. Elgala, R. Mesleh and H. Haas " Practical Considerations for Indoor wireless Optical System Implementation using OFDM ", downladable paper from www.see.edu.ac.uk

[3] Baker. B., Microchip Technology Inc, "Article: What does the ADC SNR mean?" Retrieved from http://www.edn.com, Feb 08. [4] Jeff Hecht, Understanding fibre optics, BPB publication, second edition, Indian subcontinent, pp. 137-149.

[5] J. Kahn, J. Barry, W. Krause, M. Audeh, J. Carruthers, G. Marsh, E. Lee, and D. Messerschmitt, "High–Speed Non–Directional Infrared Communication for Wireless Local-Area Networks," in *Proc. of the 26th Asilomar Conference on Signals, Systems and Computers*, vol. 1, California, USA, Oct. 26–28, 1992, pp. 83–87.

[6] Y. Tanaka, T. Komine, S. Haruyama, and M. Nakagawa, "Indoor Visible Communication Utilizing Plural White LEDs as lighting" in *Proc. of the 12th IEEE International Symposium on Personal, Indoor and Mobile Radio Communications*, vol. 2, San Diego, USA, Sep. 30 – Oct. 3, 2001, pp. 81–85.

[7] Mosier, R. R., and Clabaugh, R.G., "A Bandwidth Efficient Binary Transmission System", IEEE Trans., Vol. 76, pp. 723-728 Jan 1958.

[8] Schmidl, T. M., and Cox, D.C., "Robust frequency and timing synchronization OFDM", IEEE Trans. on Comm., Vol. 45, No. 12, pp. 1613-1621, Dec 1997.

[9] J. Grubor, S. Randel, K. Langer, and J. Walewski, "Bandwidth Efficient Indoor Optical Wireless Communications with White Light emitting Diodes," in *Proc. of the 6th International Symposium on Communication Systems, Networks and Digital Signal Processing* vol. 1, Graz, Austria, Jun. 23–25, 2008, pp. 165–169.

◈◈◈

Adaptive Steganography based on Spatial and Transform domain Techniques

[1]H S Manjunatha Reddy, [2]Vijaya lakshmi Patil & [3]K B Raja

[1]Department of ECE, Global Academy of Technology Bangalore, India
[2&3]Department of ECE, University Visvesvaraya College of Engineering
Bangalore University, Bangalore, India

Abstract— The Steganography is used in covert communication by embedding secrete information into cover object. In this paper, we propose Adaptive Steganography based on Spatial and Transform domain Techniques (ASSTD). The payload is segmented into two equal parts say part 1 and part 2. The pixels of payload (PL) Part I intensity values with less than 128 are considered and square root is applied to covert 8 bits to 4 bits length. The 4 bits of payload Part I is embedded into cover image pixels with intensity values less than 128 using LSB replacement method to generate LSB stego object. The cover and PL Part I with intensity values more than or equal to 128 are considered and Bit plane slicing (BPS) is employed to convert gray scale into binary images. The four LSB planes of cover image are replaced by four MSB planes PL Part 1 to generate BPS stego object. The IWT is applied on intermediate stego object obtained by merging BPS and LSB stego objects. The PL Part 2 is embedded into LL subband of intermediate stego object to generate final stego object. It is observed that the PSNR values are better is the case of proposed algorithm compared to existing algorithms.

Keywords- *Steganography, BPS embedding, IWT, Payload, Cover Image.*

I. INTRODUCTION

The growth of high speed networks and in particular use of the internet has increased the ease of information exchange through network using digital formatted data. Digital media offers high quality, easy editing, high fidelity copying, compression etc [1]. The advancement in the field of data communication, Security of information is becoming an integral part of it. Therefore, the confidentiality and data integrity are required to protect against unauthorized access and the security of information has become a fundamental issue. The security is also important issue to prevent extraction of hidden image or information by any third party [2]. In contrast to cryptography, the message or information is embedded in a digital host before passing it through the network, thus the existence of the message is unknown leads to steganography.

Steganography plays an important role in information security; it includes techniques to hide an image, messages, a text file and even an executable program inside a cover image without distorting the cover image. The digital mediums used for information hiding are text, software, images, audio, video et al., The digital images are widespread on the internet and can be used as a cover objects without much suspicion. The main purpose of steganography is having a covert communication between sender and receiver whose existence is unknown to a possible attacker. The steganography consists of two steps: (1) the cover image is analyzed to determine up to what extent it can be modified and (2) the information bits are inserted into cover image to derive the stego image. Steganography and Cryptography are closely related and complementary to each other. Cryptography scrambles the messages, where as steganography will hide the message in the host medium. Hence steganography is most secure and reliable compared to cryptography, since the observer can detect the presence of any secret message that has been transmitted using cryptography technique. Steganography replaces unused parts of cover image with the secret information. Information hiding is an emerging research area, which encompasses applications such as Copyright protection for digital media, watermarking, fingerprinting and steganography.

Contribution: In this paper ASSTD algorithm is proposed. The payload is decomposed into two equal Parts 1 and 2. The PL Part I with intensity values of less than 128 are embedding into cover image pixels with intensity values of less than 128 using LSB techniques. The PL Part I with intensity values of more than or equal to 128 are embedding into cover image pixel of intensity values more than or equal to 128 using BPS techniques. The PL Part 2 is embedded into LL subband of intermediate stego object to derive final stego object.

Organization: This paper is organized into following sections. Section 2 is an overview of related work. The steganography definitions, proposed embedding model and extraction model are discussed in section 3. The algorithms used for embedding and extracting are discussed in section 4. In section 5 Performance analyses are discussed.

II. LITERATURE OF SURVEY

Souvik Bhattacharyya et al., [3] proposed a specific image based steganography technique for communicating information between two locations. The secret information has been permuted, encoded through integer wavelet transformation by lifting scheme and segmented in different parts and then finally each part has been embedded through modified LSB embedding method on different objects of the cover image to form different stego objects. Finally stego image is formed by combining different stego objects and transmit to the receiver side. El Safy, R.O. et al., [4] proposed a technique to optimized high hiding capacity and imperceptibility. For hiding data in digital images by combining the use of adaptive hiding capacity function that hides secret data in the integer wavelet coefficients of the cover image with the Optimum Pixel Adjustment (OPA) algorithm. The coefficients used are selected according to a pseudorandom function generator to increase the security of the hidden data. The OPA algorithm is applied after embedding secret message to minimize the embedding error.

Sathisha et al., [5] proposed Spatial Domain Steganography using 1-Bit Most Significant Bit (MSB) with chaotic manner. The cover image is decomposed into blocks of 8*8 matrix of equal size and the first block of cover image is embedded with 8 bits of upper bound and lower bound values required for retrieving payload at the destination. The mean of median values and difference between consecutive pixels is determined to embed payload in 3bits of Least Significant Bit (LSB) and one bit of MSB in chaotic manner. Shiva Kumar et al., [6] proposed Hybrid Domain Steganography which is an integration of both spatial and transform domains. Both cover image and the payload is divided into two cells each. The RGB components of cover image cell1 are separated and then transformed individually from spatial to transform domain using DCT/DWT/FFT and then embedded. The components of cell 2 retained in spatial domains itself.

Kumar S. and Muttoo [7] proposed Data Hiding Techniques Based on Wavelet-like Transform and Complex Wavelet Transforms. The algorithms based on Slant Transform and Dual Tree Complex Wavelet Transforms (DTCWT) using wavelet based fusion method and threshold method and compared DWT in terms of visual quality and embedding capacity. Hu-Yu Huang and Shih-Hsu Chang [8] proposed a Lossless data hiding based on Discrete Haar Wavelet Transform Using the quantized DWT-based method. The secret data embedded into the successive zero coefficients of the medium-high frequency components in each reconstructed block for 3-level 2-D DWT of a cover image.

III. PROPOSED MODEL

In this section, the definitions and proposed model are discussed.

3.1 Definitions of Performance Analysis:

3.1.1 Capacity: It is the size of the data in a cover image that can be modified without deteriorating the integrity of the cover image. The steganography embedding operation needs to preserve the statistical properties of the cover image in addition to its perceptual quality. Capacity is represented by bits per pixel (bpp) using Equation 1.

$$Capacity = \frac{No\ of\ bits\ embedded\ \text{cover image}}{Total\ No.\ of\ pixel\ in\ \text{cover image}} \quad (1)$$

3.1.2 Mean Square Error (MSE): It is defined as the square of error between cover image and the stego image. The distortion in the image can be measured by using Equation 2.

$$MSE = \sum_{i=1}^{all\ pixels} \sum_{j=1}^{all\ pixels} \frac{[C(i,j) - S(i,j)]^2}{N * N} \quad (2)$$

Where C (i, j) is the cover image pixel
S (i, j) is the stego image pixels
N ∗ N is the image size.

3.1.3 Peak Signal to Noise Ratio (PSNR): It is the ratio of the maximum signal to noise between stego image and cover image can be measured in db using Equation 3.

$$PSNR = 10 \log_{10} \left(\frac{255^2}{MSE} \right) \quad (3)$$

3.2 Proposed Model:

The payload is embedded into cover image using LSB, BPCS and IWT to generate stego image with high PSNR and Capacity.

3.2.1 EMBEDDING MODEL

The block diagram of embedding model is shown in Figure 1. The payload is more secure in the proposed model since

(i) The BPS embedding technique is used for cover image pixel intensity values more than or equal to 128.

(ii) The LSB embedding technique is used on square root intensity values less than 128 of PL part 1.

(iii) The IWT is applied on both BPS stego object and LSB stego object. The spatial domain PL part 1 is embedded into coefficient of transform domain stego object.

3.2.1.1 Payload (PL): The gray scale image of suitable sizes and different formats which is to be transmitted in covert way is considered as a payload.

3.2.1.2 Cover Image (CI): The cover image can either be color or grayscale image, provided color image is converted into gray scale image, before secret image

is hidden. The cover images of any size and formats are considered.

3.2.1.3 Segmentation: The payload is equally decomposed into two parts say part-1 and part-2.

3.2.1.4 Bit Plane Slicing Embedding: The gray scale image is represented by pixels with intensity values vary between zero and 255 with each pixel are represented by 8 bits. In bit plane slicing, the eight bits of a pixel are split into its constituent binary planes varying from MSB to LSB. For example, the gray scale matrix of size 4*4 is converted into 8 matrices of single bit planes using bit plane slicing as shown in Figure 2.

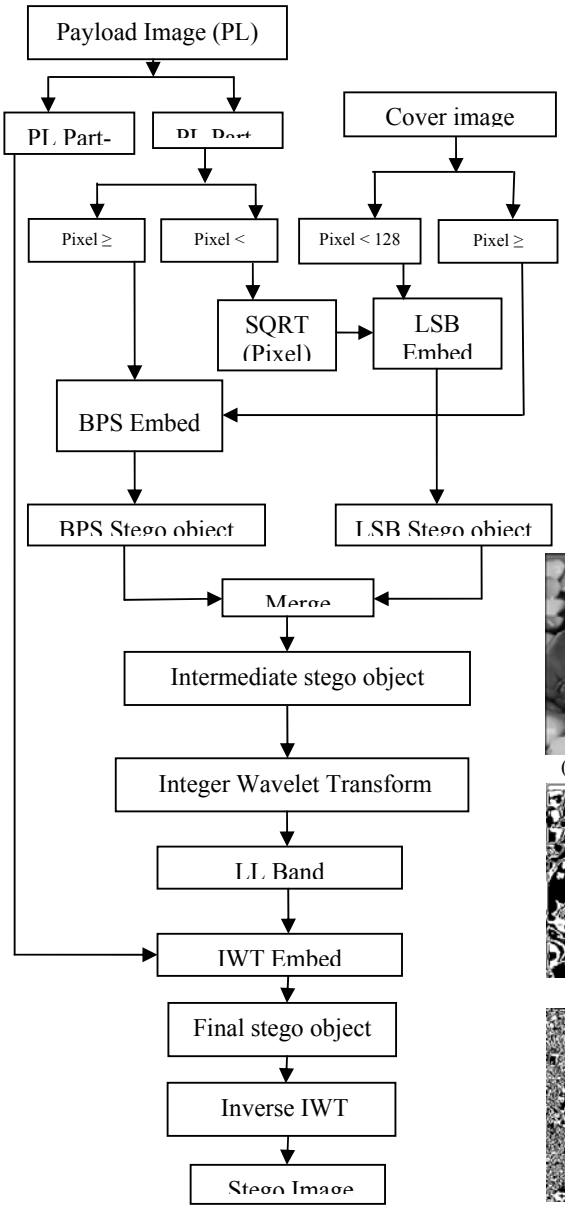

Figure1. Flowchart for embedding system of ASSTD.

The part 1 of payload and cover image is considered and the intensity values of each pixel is observed and if intensity value of a pixel is greater than or equal 128, then consider those pixels for BPS embedding. The intensity values greater than or equal 128 of both PL part 1 and cover image are split in 8 bit planes using BPS. The four LSB bit planes of cover image are replaced with four MSB bit planes of PL part 1 respectively to generate BPS stego object. The eight bit planes of BPS stego object are merged to obtain single BPS stego object with 8 bits per pixels.

$$\begin{bmatrix} 98 & 255 & 55 & 28 \\ 00 & 127 & 48 & 128 \\ 128 & 212 & 240 & 11 \\ 212 & 171 & 130 & 161 \end{bmatrix}$$

(a)

$$\begin{bmatrix} 0 & 1 & 0 & 0 \\ 0 & 0 & 0 & 1 \\ 1 & 1 & 1 & 0 \\ 1 & 1 & 1 & 1 \end{bmatrix} \quad \begin{bmatrix} 1 & 1 & 0 & 0 \\ 0 & 1 & 0 & 0 \\ 0 & 1 & 1 & 0 \\ 1 & 0 & 0 & 0 \end{bmatrix} \quad \begin{bmatrix} 1 & 1 & 1 & 0 \\ 0 & 1 & 1 & 0 \\ 0 & 0 & 1 & 0 \\ 0 & 1 & 0 & 1 \end{bmatrix} \quad \begin{bmatrix} 0 & 1 & 1 & 1 \\ 0 & 1 & 1 & 0 \\ 0 & 1 & 1 & 0 \\ 1 & 0 & 0 & 0 \end{bmatrix}$$

(b) (c) (d) (e)

$$\begin{bmatrix} 0 & 1 & 0 & 1 \\ 0 & 1 & 0 & 0 \\ 0 & 0 & 0 & 1 \\ 0 & 1 & 0 & 0 \end{bmatrix} \quad \begin{bmatrix} 0 & 1 & 1 & 1 \\ 0 & 1 & 0 & 0 \\ 0 & 1 & 0 & 0 \\ 1 & 0 & 0 & 0 \end{bmatrix} \quad \begin{bmatrix} 1 & 1 & 1 & 0 \\ 0 & 1 & 0 & 0 \\ 0 & 0 & 0 & 1 \\ 0 & 1 & 1 & 0 \end{bmatrix} \quad \begin{bmatrix} 0 & 1 & 1 & 0 \\ 0 & 1 & 0 & 0 \\ 0 & 0 & 0 & 1 \\ 0 & 1 & 0 & 1 \end{bmatrix}$$

(f) (g) (h) (i)

Figure 2. (a)Original matrix, (b)-(i)Constituent bit plane of (a)

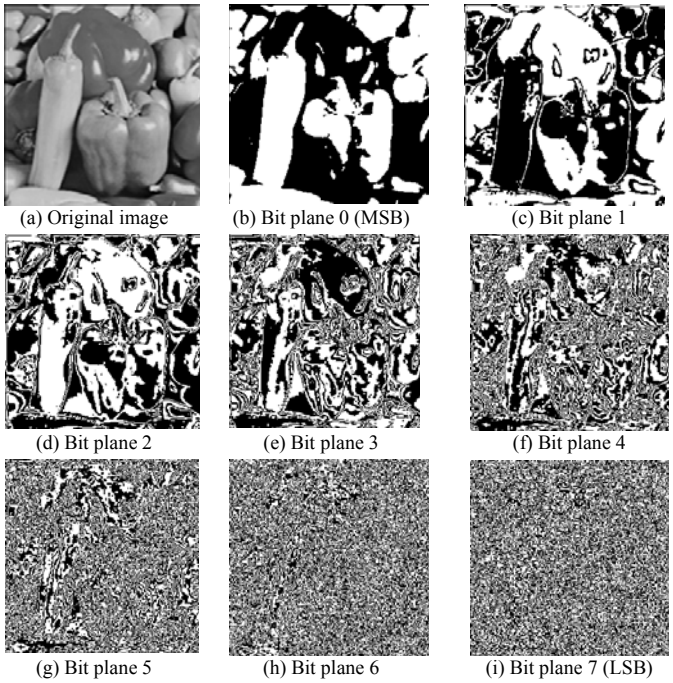

(a) Original image (b) Bit plane 0 (MSB) (c) Bit plane 1

(d) Bit plane 2 (e) Bit plane 3 (f) Bit plane 4

(g) Bit plane 5 (h) Bit plane 6 (i) Bit plane 7 (LSB)

Figure 3. BPS Technique

The BPS is applied an image Pepeer.jpg to derive corresponding binarized 8 bit planes as shown in Figure 3. The MSB bit plane image has significant information of original image compare to other 7 bit plane images. The LSB bit plane image has no information/insignificant information of original image.

3.2.1.5 LSB Embedding: The intensity values of each pixel of PL part 1 and cover image are observed and if intensity values are less than 128, then consider the pixels for LSB embedding. The square root is applied on each pixel value of PL part 1to compress 8 bits into 4 bits. The four LSB bits of cover image pixels are replaced by four bits of PL part 1 to generate LSB stego object.

3.2.1.6 Merge: BPS Stego object and LSB Stego object are added to generate intermediate stego object.

3.2.1.7 IWT Embedding: The two- dimensional integer wavelet transform is applied on intermediate stego object to generate four sub bands such as LL, LH, HL, and HH. The LL band represents the low frequency coefficients and three other bands represent the high frequency coefficients. The PL part 2 is embedded into the LL band coefficients using 4 bit LSB replacement method. The four MSB's of PL part 2 are embedded into four LSB bits of LL band coefficient of intermediate stego object to generate final stego object. The inverse IWT is applied on final stego object to derive stego image in spatial domain.

3.2.2 PROPOSED EXTRACTION MODEL

The embedded payload is extracted from stego image at the destination by applying reverse process of embedding. The extraction model is as shown in Figure 4. The IWT is applied on stego image to generate four sub bands say LL, LH, HL and HH. The four LSB coefficient of LL band has the MSB bits of PL part 2, hence extract to get PL part 2. The inverse IWT is applied on MSB coefficients of LL band along with all three sub bands LH, HL and HH to generate intermediate stego image. The intensity values of intermediate stego image are observed, if values are less than 128 then apply square to decompress to generate pixel length to 8 bits. The four MSB's are extracted to generate part of PL part 1. If pixel values are more than or equal to 128 then apply BPS to generate 8 bit planes. The four LSB bit planes are considered to obtain MSB part of PL part 1. The matrix of part of PL part 1 of LSB method is merged with the matrix of part of PL part 1 BPS method to derive final PL part 1 image. The final PL part 1 image is merged with PL part 2 images to extract original payload.

IV. ALGORITHM

Problem definition: The payload is embedded into cover image using BPS, LSB and IWT to generate stego image for secure communication

The objectives are

(i) To increase capacity.

(ii) To increase PSNR

Assumptions:

(i) Both cover and payload objects are gray scale images with different dimensions and formats.

(ii) The stego image is transmitted over an ideal channel.

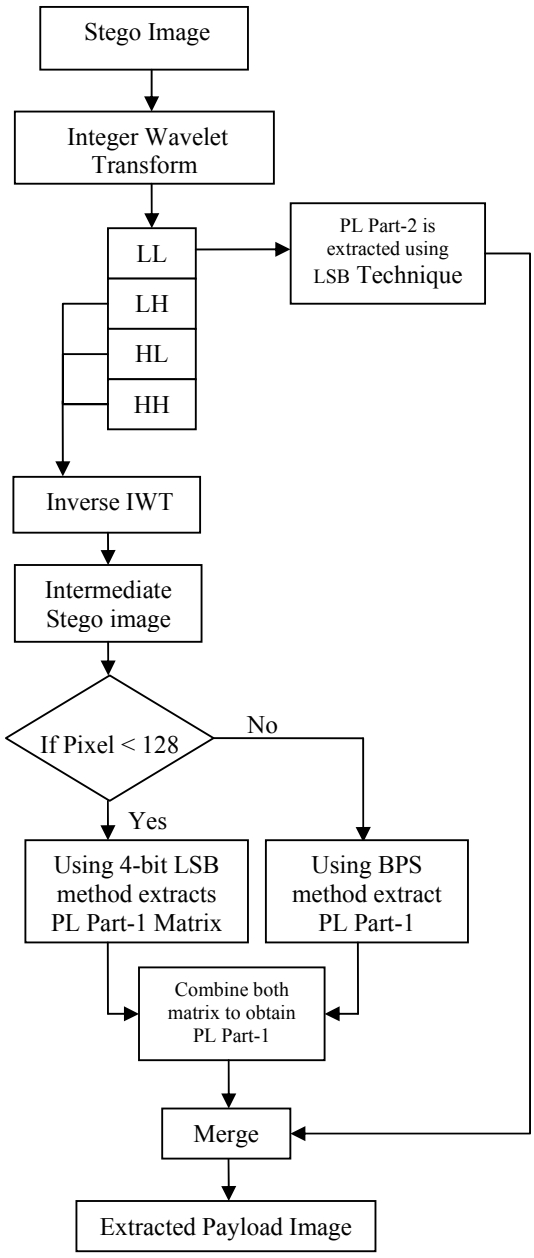

Figure 4. Flowchart of Extraction Process of ASSTD

4.1Embedding algorithm: The payload is embedded into the cover image using spatial domain and transform domain techniques are given in the table 1. The proposed stenography algorithm is more secured as three different techniques are used to embed payload along with some part of payload and cover image are compressed.

TABLE 1: EMBEDDING ALGORITHM OF ASSTD

Input**:** Cover image and Payload
Output: Stego image.
1. Read the cover image and payload.
2. Decompose payload into PL part 1 and PL part 2.
3. Check intensity values of PL part 1 and cover image.
4. If intensity values less than 128 then apply square root to compress pixel length from 8 to 4 bits.
5. The 4 bits of cover image are replaced by 4 bits of PL part 1 to generate LSB stego object.
6. The BPS embedding is applied on pixels having intensity values greater than or equal to 128 of PL part 1 and cover image.
7. The 4 LSB planes of cover image are replaced by 4 MSB planes of PL part 1 and convert 8 bits per pixel to generate Bps stego object.
8. The intermediate stego object is obtained by merging BPS and LSB stego object.
9. IWT is applied on intermediate stego object and consider LL band.
10. The MSB bits of PL part 1 are embedded into four LSB's of LL band coefficient to generate final stego object.

Apply inverse IWT to generate stego image.

*4.2 Extracting Algorithm***:** The payload is extracted from the stego image by the reverse process of embedding as given in table 2.

TABLE 2 EXTRACTING ALGORITHM OF ASSTD

Input : Stego Image
Output : Extracted Payload Image
1. Read the stego image.
2. IWT is applied to generate four sub bands and extract four LSB coefficient of LL band which has the MSB bits of PL part 2.
3. The inverse IWT is applied on MSB coefficients of LL band along with all three sub bands LH, HL and HH to generate intermediate stego image.
4. The intensity values of intermediate stego image are less than 128 then square it to decompress to generate pixel length to 8 bits
5. The four MSB's are extracted to generate part of PL part 1.
6. If pixel values are greater than or equal to 128 then apply BPS to generate 8 bit planes
7. The 4 LSB bit planes are considered to obtain MSB part of PL part 1.
8. Both LSB and BPS matrices are merged to derive final PL part 1 image.
9. The final PL part 1 image is merged with PL part 2 images to extract original payload.

V. PERFORMANACE ANALYSIS

The several cover images such as peppers, house, old image and goldhill shown in Figure 5 and payload images of different sizes and different formats are considered for performance analysis. The payload Lena image is embedded in the cover image Barbara using proposed algorithm to generate stego image Barbara as shown in Figure 6. It is observed that perceptibility of stego image and cover image are same. The quality of stego image is same as cover image by appearance and also statistical characteristic of stego image is almost same as cover image, since the PSNR value in the proposed algorithm is more than 40 dB.

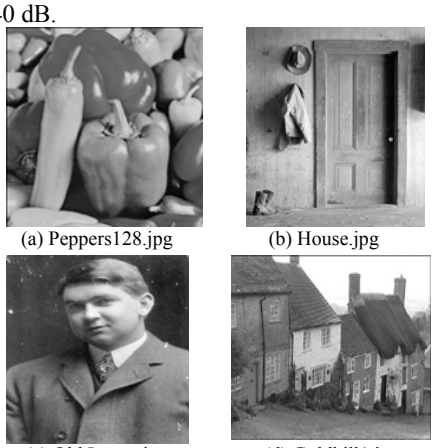

(a) Peppers128.jpg (b) House.jpg
(c) Old Image.jpg (d) Goldhill1.jpg

Figure 5. Cover images

(a) CI Barbara (b) Payload Lena (c) SI Barbara

Figure 6. CI, PL and SI

The PSNR values between cover image and stego image as well as PSNR values between original payload and extracted payload for different payload sizes with constant cover image size are tabulated in Table 3. The payload image Lena. jpg is embedded into cover image Barbara.bmp (512 * 512) to generate stego image Barbara.bmp. The PSNR of cover image and stego image values are decreases as capacity increases where as the PSNR values between payload and extracted payload are almost constant with respect to the capacity.

The variation of PSNR between cover image and stego image with capacity are plotted in the Figure 7. The PSNR values decreases as capacity increases. The variation of PSNR of cover image Barbara.bmp (512*512) and stego image Barbara.bmp (512*512)

and PSNR between original payload with different image formats having size of 64*64 with extracted payload are tabulated in Table 4. It is observed that the payload formats does not affect the quality of stego image i.e., PSNR between cover image and stego image having value around 43 dB and the PSNR between original payload and extracted payload having value of around 31 dB are almost constant for different payload image formats.

The PSNR value between cover image & stego image and payload & extracted payload for different cover image formats with constant capacity are given in Table 5. It is seen that different cover image formats has least effect on the quality of stego image as PSNR values are almost constant. The PSNR value between cover & stego image and payload & extracted payload for different cover images is almost constant are given in Table 6.

TABLE 3: PSNR VARIATIONS FOR DIFFERENT PAYLOAD SIZES WITH COVER IMAGE BARBARA.BMP (512 X512)

Payload Image size[lena.jpg]	PSNR of CI and SI	Capacity	PSNR of PL and EPL
64 X 32	45.8296	0.0078	30.9900
64 X 64	42.7816	0.0156	30.7907
64 X 128	39.7085	0.0313	30.8540
128 X 128	36.6551	0.0625	30.7849
128 X 256	33.6315	0.125	30.8326

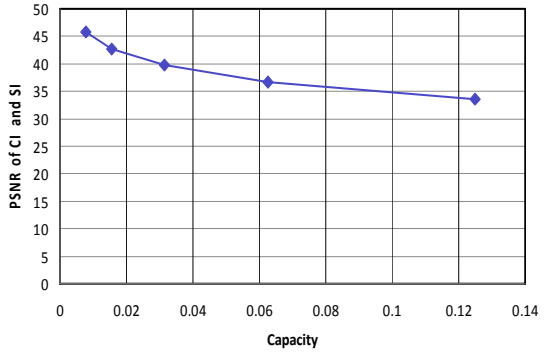

Figure 7. PSNR variations with Capacity

TABLE 4: PSNR VARIATIONS FOR DIFFERENT PAYLOAD FORMATS WITH COVER IMAGE BARBARA.BMP (512 X 512)

Payload Image formats Lena(64 x 64)	PSNR of CI and SI	PSNR of PI and EPL
Png	42.8781	30.4224
Jpg	42.7816	30.7907
Bmp	42.9250	30.3722
Tif	42.9215	30.5171
Gif	42.9198	30.4496

TABLE 5: PSNR VARIATIONS FOR DIFFERENT COVER IMAGE FORMATS WITH PAYLOAD IMAGE LENA.JPG (64 X 64)

Cover Image formats	PSNR of CI and SI	Capacity	PSNR of PL and EPL
Bmp	42.5629	0.0156	29.6189
Tif	42.5753	0.0156	29.6189
Gif	42.5906	0.0156	29.6189
Png	42.9973	0.0156	29.6189
Jpg	43.4194	0.0156	29.6189

TABLE 6: PSNR VALUES FOR DIFFERENT COVER IMAGES

Cover image (512 x 512)	Payload (64 x 64)	PSNR (CI & SI)	PSNR(PL & EPL)
Goldhill1.jpg	Lena.png	41.276	30.96
House.jpg	Lena.png	42.719	30.962
Old Image.jpg	Lena.png	42.6646	30.837
Peppers128.jpg	Lena.png	42.5471	29.05
Barbara.bmp	Lena.png	42.8781	30.422

TABLE 7: COMPARISON OF PSNR FOR EXISTING AND PROPOSED TECHNIQUE

Methods	PSNR
El.Sayed M El. Alfy et.al [9]	38.354
Elham Ghasemi et.al.[10]	35.17
Sivajanakiraman et.al.[11]	34.8605
Yedla Dinesh and Addanki Purna Ramesh [12]	26.30
Proposed method	43.4194

The value of PSNR for existing methods and proposed ASSTD method are compared in Table 7. It is observed that the value of PSNR is better in the case of proposed algorithm compared to existing algorithms. The security to the payload in the propose algorithm is better since (i) Spatial domain and Transform domain concepts are used (ii) The part of the payload is compressed using square root before embedding.

VI. CONCLUSION

The stenography is technique to hide secrete information into cover object for secure communication. In this paper ASSTD algorithm is proposed. The payload is decomposed into two equal parts say Part 1 and Part 2. The PL Part 1 pixels with intensity values less than 128 are square rooted to compress 8 bit pixel length to 4 bit pixel length. The 4bits of PL Part I are embedded into cover image pixels with intensity values less than 128 using LSB technique to generate LSB stego object. The intensity values more than or equal to 128 of cover image and payload Part I are considered to convert into bit planes. The LSB planes of cover image are replaced by MSB planes of PL Part 1 to generate BPS stego object. The intermediate stego image is obtained by merging LSB and BPS stego object and IWT is applied. The PL Part 2 is embedded into LL subband of intermediate stego object to generate final stego object. It is observed that, the PSNR values in the proposed algorithm are better compared to existing algorithms. In future the algorithm can be tested with different transform domain techniques.

REFERENCES

[1] Samir K Bandyopadhyay and Indra K Maitra, "Hiding of Data using Reserved Field of Palette for Steganography", *Journal of Computer science and Engineering*, pp.1-6, vol.1 (2), June 2010.

[2] S.K.Muttoo and sushil kumar, "A Multilayered Secure, Robust and High Capacity Image Steganographic Algorithm," *World of Computer Science and Information Technology Journal,* pp.239-246, vol.1, no.6, 2011

[3] Souvik Bhattacharyya, Avinash Prasad kshitij and Gautom sanyal Samir K Bandyopadhyay and Indra K Maitra", Novel Approach to Develop a Secure Image based Steganographic Model using Integer Wavelet Transform," *International Conference on Recent Trends in Information, Telecommunication and Computing* pp.173-178, 2010.

[4] El Safy R O, Zayed H H, El Dessouki A and Benha Univ Banha "An Adaptive Steganographic Technique based on Integer Wavelet Transform," *International Conference on Networking and Media Convergence*, PP.111-117, 2009.

[5] Sathisha N, Madhusudan G N, Bharathesh S, Suresh Babu K, Raja K B and Venugopal K R, "Chaos based Spatial Domain Steganography using MSB", *International Conference on Industrial and Information Systems*, pp.11-117, 2010.

[6] K B Shiva Kumar, K B Raja, Sabyasachi Pattnaik "Hybrid Domain in LSB Steganography", *International Journal of Computer Applications,* pp.35-40, vol.19, no.7, April 2011.

[7] Kumar S and Muttoo S K, "Data Hiding Techniques Based on Wavelet-like Transform and Complex Wavelet Transforms," *International Symposium on Intelligence Information Processing and Trusted Computing,* pp. 9-14, october2010.

[8] Hu-Yu Huang and Shih-Hsu Chang, "A Lossless Data Hiding based on Discrete Haar Wavelet Transform," *International Conference on Computer and Information Technology,* pp.1554-1559, July 2010.

[9] El-Sayed M El-Alfy, Azzat A and Al-Sadi "A Comparative Study of PVD-Based Schemes for Data Hiding in Digital Images", *IEEE International Conference on Computer Systems and Applications*, pp. 144-149, 2011.

[10] Elham Ghasemi, Jamshid Shanbehzadeh and Bahram Zahir Azami "A Steganographic Method Based on Integer Wavelet Transform and Genetic Algorithm," *International Conference on Communications and Signal Processing*, pp. 42-45, 2011.

[11] Siva Janakiraman, Anitha Mary A and Jagannathan Chakravarthy, "Pixel Bit Manipulation for Encoded Hiding - An Inherent stego," *International Conference on Computer Communication and Informatics,* pp. 1-6 January 2012.

[12] Yedla Dinesh and Addanki Purna Ramesh, **"**Efficient Capacity Image Steganography by Using Wavelets," International Journal of Engineering Research and Applications, vol. 2, issue 1, pp. 251-259 February 2012.

◈◈◈

Comparative Performance Analysis Of Linear Inverted Pendulum With LQR And Fuzzy Logic Controller

[1]Nabanita Bisoyi, [2]P.K.Roy & [3]Rekha Jha

[1,2&3]Deptt. Electrical Engg. B.I.T. Sindri, Dhanbad, India

Abstract— with advancement of technology there is an urgent need to design control systems that are able to maintain acceptable performance levels under significant unanticipated uncertainties. Recent advances in intelligent control methodologies have enable us to address this issue better. Fuzzy logic control is one of the important intelligent controllers. In this study a fuzzy logic controller tuned by an artificial neural network called as ANFISC (Adaptive Neuro Fuzzy Inference System controller) is designed for the control of linear inverted pendulum. Two parameters i.e. the position and the angle of the inverted pendulum is controlled with the fuzzy logic controller. The performance is compared with the linear quadratic regulator based controller. The simulation results are well studied and clearly indicate that the performance of fuzzy logic controller tuned by ANFIS is very much better compared to its counterparts in terms of its time response parameter.

Keywords-*linear inverted pendulum; fuzzy logic controller; ANFIS;*

I. INTRODUCTION

The inverted pendulum system has the property of unstable, higher order, multi variable and higher coupled, which can be treated as a typical nonlinear problem [1-2]. The system's characteristic are an unstable equilibrium point at the upright position of the pendulum, a stable equilibrium point at the pendant position, as well as two uncontrollable points when the pendulum is at the horizontal position [3-4]. Although many investigations have been carried out on the inverted pendulum problem, like proportional derivative (PD), hybrid PD + Fuzzy, FLC, ANFIS and so on, each investigation has its own merits [1-8]. One most popular method is the fuzzy inference system (FIS) tuned with the help of ANFIS.

In this paper a fuzzy logic controller has been designed tuned by ANFIS and is used for both position and angle control of inverted pendulum (IP). The performance of FLC is compared with linear quadratic regulator (LQR) based control of inverted pendulum.

This paper is organized as follows. In Section II, mathematical model of IP is discussed. Section III briefs about LQR theory. ANFIS is presented Section IV. Simulation results are discussed in Section V. And finally the conclusion is presented in Section VI.

II. MODELING OF LINEAR INVERTED PENDULUM

Single stage linear IP can be simplified as a system of cart and even quality rod, as shown in Figure 1.

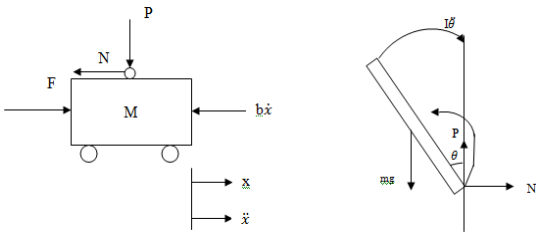

Figure 1. Cart and Rod Force Analysis

From the forces in the horizontal direction

$$M\ddot{x} = F - b\dot{x} - N \quad (1)$$

From the force acting on the rod in horizontal direction

$$N = m\frac{d^2}{dt^2}(x + l\sin\theta) \quad (2)$$

$$\text{i.e } N = m\ddot{x} + ml\ddot{\theta}\cos\theta - ml\dot{\theta}^2\sin\theta \quad (3)$$

Combining equation (1-3) the first dynamic equation is obtained as

$$(M+m)\ddot{x} + b\dot{x} + ml\ddot{\theta}\cos\theta - ml\dot{\theta}^2\sin\theta = F \quad (4)$$

To get the second dynamic equation, analyze the force in the vertical direction

$$P - mg = m\frac{d^2}{dt^2}(l\cos\theta) \quad (5)$$

$$P - mg = -ml\ddot{\theta}\sin\theta - ml\dot{\theta}^2\cos\theta \quad (6)$$

By moment conservation

$$-Pl\sin\theta - Nl\cos\theta = I\ddot{\theta}$$

It is to be noted that the direction of moment is negative because θ=π+Φ,cosΦ=-cosθ, sin Φ = -sin θ.

Combining the above two equation, the second dynamic equation is obtained as:

$$(I+ml^2)\ddot{\theta} + mgl\sin\theta = -ml\ddot{x}\cos\theta$$

Let θ = π + Φ (Φ is the angle between the rod and vertically upward direction), assume Φ is relatively small to 1 (unit in radian), which means Φ << 1, then following approximation can be obtained: cosθ = -1, sinθ = -Φ, $\left(\frac{d\theta}{dt}\right)^2 = 0$. Let u denote the input force of the object, linearize the two dynamics equations.

$$\begin{cases}(I+ml^2)\ddot{\phi} - mgl\,\phi = ml\ddot{x}\\ (M+m)\ddot{x} + b\dot{x} - ml\ddot{\phi} = u\end{cases}$$

The Laplace transformation of equation (9) is as follows

$$\begin{cases}(I+ml^2)\Phi(s)s^2 - mgl\,\Phi(s) = mlX(s)s^2\\ (M+m)X(s)s^2 + bX(s)s - ml\Phi(s)s^2 = U(s)\end{cases}$$

Here the initial condition is assumed to be 1 when deducing the transfer function.

The output angle is Φ, solving the first equation

$$X(s) = \left[\frac{(I+ml^2)}{ml} - \frac{g}{s^2}\right]\Phi(s)$$

or $$\frac{\Phi(s)}{X(s)} = \frac{mls^2}{(I+ml^2)s^2 - mgl}$$

Let $v = \ddot{x}$, then

$$\frac{\Phi(s)}{V(s)} = \frac{ml}{(I+ml^2)s^2 - mgl}$$

Substituting the above equation to the second one in equation (10)

$$(M+m)\left[\frac{(I+ml^2)}{ml} - \frac{g}{s}\right]\Phi(s)s^2 + b\left[\frac{(I+ml^2)}{ml} + \frac{g}{s^2}\right]\Phi(s)s - ml\Phi(s)s^2 = U(s)$$

(14)

The transfer function is obtained after simplification

$$\frac{\Phi(s)}{U(s)} = \frac{\frac{ml}{q}s^2}{s^4 + \frac{b(I+ml^2)}{q}s^3 - \frac{(M+m)mgl}{q}s^2 - \frac{bmgl}{q}s}$$

(15)

in which

$$q = (M+m)(l+ml^2) - (ml^2)$$

Assume the system state space equations are

$$\dot{X} = AX + Bu$$
$$y = CX + Du$$

Solving the algebraic equations

$$\begin{cases}\dot{x} = \dot{x}\\ \ddot{x} = \frac{-(I+ml^2)b}{I(M+m)+Mml^2}\dot{x} + \frac{m^2gl^2}{I(M+m)+Mml^2}\phi + \frac{(I+ml^2)}{I(M+m)+Mml^2}u\\ \dot{\phi} = \dot{\phi}\\ \ddot{\phi} = \frac{-mlb}{I(M+m)+Mml^2}\dot{x} + \frac{mgl(M+m)}{I(M+m)+Mml^2}\phi + \frac{ml}{I(M+m)+Mml^2}u\end{cases}$$

(17)

The state space equation can then be written as

$$\begin{bmatrix}\dot{x}\\ \ddot{x}\\ \dot{\phi}\\ \ddot{\phi}\end{bmatrix} = \begin{bmatrix}0 & 1 & 0 & 0\\ 0 & \frac{-(I+ml^2)b}{I(M+m)+Mml^2} & \frac{m^2gl^2}{I(M+m)+Mml^2} & 0\\ 0 & 0 & 0 & 1\\ 0 & \frac{-mlb}{I(M+m)+Mml^2} & \frac{mgl(M+m)}{I(M+m)+Mml^2} & 0\end{bmatrix}\begin{bmatrix}x\\ \dot{x}\\ \phi\\ \dot{\phi}\end{bmatrix} + \begin{bmatrix}0\\ \frac{(I+ml^2)}{I(M+m)+Mml^2}\\ 0\\ \frac{ml}{I(M+m)+Mml^2}\end{bmatrix}u$$

$$y = \begin{bmatrix}x\\ \phi\end{bmatrix} = \begin{bmatrix}1 & 0 & 0 & 0\\ 0 & 0 & 1 & 0\end{bmatrix}\begin{bmatrix}x\\ \dot{x}\\ \phi\\ \dot{\phi}\end{bmatrix} + \begin{bmatrix}0\\ 0\end{bmatrix}u$$

Now

$$(I+ml^2)\ddot{\phi} - mgl\phi = ml\ddot{x}$$

For a rod of even quality, the moment of inertia is

$$I = \frac{1}{3}ml^2$$

After simplification

$$\ddot{\phi} = \frac{3g}{4l}\phi + \frac{3}{4l}\ddot{x} \quad (20)$$

$$X = \{x, \dot{x}, \phi, \dot{\phi}\}, u' = \ddot{x}$$

Then

$$\begin{bmatrix} \dot{x} \\ \ddot{x} \\ \dot{\phi} \\ \ddot{\phi} \end{bmatrix} = \begin{bmatrix} 0 & 1 & 0 & 0 \\ 0 & 0 & 0 & 0 \\ 0 & 0 & 0 & 1 \\ 0 & 0 & \frac{3g}{4l} & 0 \end{bmatrix} \begin{bmatrix} x \\ \dot{x} \\ \phi \\ \dot{\phi} \end{bmatrix} + \begin{bmatrix} 0 \\ 1 \\ 0 \\ \frac{3}{4l} \end{bmatrix} u'$$

(21)

$$y = \begin{bmatrix} x \\ \phi \end{bmatrix} = \begin{bmatrix} 1 & 0 & 0 & 0 \\ 0 & 0 & 1 & 0 \end{bmatrix} \begin{bmatrix} x \\ \dot{x} \\ \phi \\ \dot{\phi} \end{bmatrix} + \begin{bmatrix} 0 \\ 0 \end{bmatrix} u'$$

(22)

Where

M - cart mass, *m* - rod mass, *b* - friction coefficient of the cart, *l* -distance from the rod axis rotation center to the rod mass center, *I* - rod inertia, *F* - force acting on the cart

x - cart position, Φ - angle between the rod and vertically upward direction, θ - angle between the rod and vertically downward direction

III. LINEAR QUADRATIC REGULATOR OPTIMAL CONTROL

The LQR optimal control principle is defined by the system equations:

$$\dot{X} = AX + Bu \quad (23)$$

Determination of a matrix K that gives the optimal control vector u(t) = -K*x(t)

Such that the performance index is minimized:

$$J = \int_0^\infty (X^* QX + u^* Ru) dt \quad (24)$$

Q is a positive definite (or semi-positive definite) hermitian or real symmetric matrix and R is a positive definite hermitian or real symmetric matrix.

The 1-stage linear IP system state space equations are

$$\begin{bmatrix} \dot{x} \\ \ddot{x} \\ \dot{\phi} \\ \ddot{\phi} \end{bmatrix} = \begin{bmatrix} 0 & 1 & 0 & 0 \\ 0 & 0 & 0 & 0 \\ 0 & 0 & 0 & 1 \\ 0 & 0 & 24.1 & 0 \end{bmatrix} \begin{bmatrix} x \\ \dot{x} \\ \phi \\ \dot{\phi} \end{bmatrix} + \begin{bmatrix} 0 \\ 1 \\ 0 \\ 2.5 \end{bmatrix} u' \quad (25)$$

$$y = \begin{bmatrix} x \\ \phi \end{bmatrix} = \begin{bmatrix} 1 & 0 & 0 & 0 \\ 0 & 0 & 1 & 0 \end{bmatrix} \begin{bmatrix} x \\ \dot{x} \\ \phi \\ \dot{\phi} \end{bmatrix} + \begin{bmatrix} 0 \\ 0 \end{bmatrix} u'$$

Applying linear feedback controller, suppose R is a impulse input acting on the cart and the four state variables $x, \dot{x}, \phi, \dot{\phi}$ represents cart position, cart velocity, pendulum rod angle and pendulum rod velocity respectively. The output $y = [x, \varphi]$ includes cart position and pendulum angle. The objective is to design a controller such that, when acting on an impulse input signal to the system, the pendulum rod will be back to vertically up after oscillation

$$Q = C' * C = \begin{bmatrix} 1 & 0 & 0 & 0 \\ 0 & 0 & 0 & 0 \\ 0 & 0 & 1 & 0 \\ 0 & 0 & 0 & 0 \end{bmatrix} \quad (26)$$

$Q_{1,1}$ is the cart position coefficient and $Q_{3,3}$ is the pendulum rod angle coefficient and the input coefficient R is 1. Using MATLAB command l LQR, the value of K is

K= [-1 -1.8241 25.6773 5.2265]

It can also be observed that in Q matrix, both the settling time and pendulum rod angle movement will decrease as $Q_{1,1}$ increase, Let $Q_{1,1}$ =1000 and $Q_{3,3}$ = 200, then

K=[-31.623 -21.3 78.846 15.80]

Using this technique the LQR controller is designed for the IP model and its performance is discussed in results section [10]

IV. ADAPTIVE NEURO-FUZZY INFRENCE SYSTEM (ANFIS)

The ANFIS is used to design the fuzzy controller. ANFIS constructs a fuzzy controller using input-output data set, known as training data set. Without loss of generality we assume two inputs, u1 and u2, and one output, y. Assume for now a first order Sugeno type of rule base with the following two rules,

If u1 is A1 and u2 is B1 then y1 = c11u1 + c12u2 + c10

If u1 is A2 and u2 is B2 then y2 = c21u1 + c22u2 + c20

Incidentally, this fuzzy controller could interpolate between two linear controllers depending on the current state. If the firing strengths of the rules are α1 and α2 respectively, for two particular values of the inputs u1 and u2, then the output is computed as a weighted average,

$$y = \frac{\alpha 1 y1 + \alpha 2 y2}{\alpha 1 + \alpha 2} = \overline{\alpha 1} y1 + \overline{\alpha 2} y2 \quad (28)$$

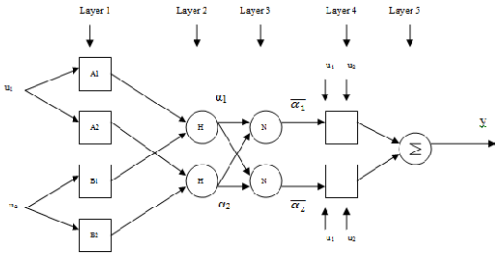

Figure 2. Structure or the ANFIS network

The corresponding ANFIS network is shown in Figure 2. A description of the layers in the network is as follows:- [9]

1. Each neuron i in layer 1 is adaptive with a parametric activation function. Its output is the grade of membership to which the given input satisfies the membership function, i.e., μA1(u1), μB1(u2), μA2(u1) or μB1(u2), An example of a membership function is the generalized Bell function

$$\mu(x) = \frac{1}{1+\left|\frac{x-c}{a}\right|^{2b}} \quad (29)$$

Where {a, b, c} are the parameter set. As the values of the parameters change, the shape of the bell-shaped function varies. Parameters in that layer are called premise parameters.

2. Every node in layer 2 is a fixed node, whose output is the product of all incoming signals. In general, any other fuzzy AND operation can be used. Each node output represents the firing strength αi of the ith rule.

3. Every node in layer 3 is a fixed node which calculates the ratio of the ith rule's firing strength relative to the sum of all rule's firing strengths,

$$\overline{\alpha}_i = \frac{\alpha_i}{\alpha_1 + \alpha_2}, \quad i = 1, 2$$

The result is a normalized firing strength.

4. Every node in layer 4 is an adaptive node with a node output

$$\overline{\alpha i} = \overline{\alpha i}(ci1u1 + ci2u2 + ci0), \quad i = 1, 2$$

where $\overline{\alpha i}$ is the normalized firing strength from layer 3 and {ci1, ci2u2, ci0}is the parameter set of this node. Parameters in this layer are called consequent parameters.

5. Every node in layer 5 is a fixed node which sums all incoming signals.

It is straight forward to generalize the ANFIS architecture in Fig. 5 to a rule base with more than two rules.

V. SIMULATION RESULTS

In this study the LQR controller is designed with the help of matlab LQR design toolbox. All the matrix parameters of LQR is calculated from the inverted pendulum data as discussed in the previous section. The simulink model used for the simulation is shown in the fig.3 . The corresponding results for both position and angle are shown in the fig. 5 and fig. 6 respectively.

The same inverted pendulum model is simulated with applying a TS fuzzy logic controller having four inputs, i.e position error and its derivative, angle error and its derivative tuned by ANFIS as disscussed in previous section, in the simulink envirionment of MATLAB.The FLC properly tuned is applied for the control of the IP and the model is shown in the fig. 4 and the cooresponding results for both position and angle is shown in the fig.7 and fig.8 respectively.

The results shown in the fig. 5 and 7 are position control plots of inverted pendulum for LQR and FLC respectively and clearly indicate that the FLC plot has negligible overshoot compared to its other two controllers and it is also settling at its reference value in 4 sec. compared to 6 sec for LQR. Similarly the results shown in the fig. 6 and 8 are angle control plots of inverted pendulum for LQR and FLC respectively and clearly indicate that the FLC plot has very less overshoot compared to its counterpart and it is also settling at its reference value in 2 sec. compared to 6 sec against LQR controller. Therefore it concludes that the fuzzy logic control based inverted pendulum has a faster position and angle controlled response compared to the LQR based controlled inverted pendulum.

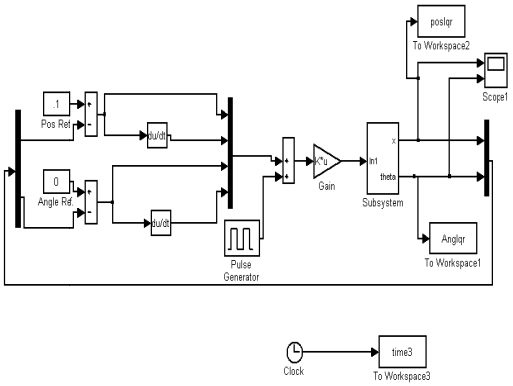

Figure 3. LQR control simulink model of inverted pendulum

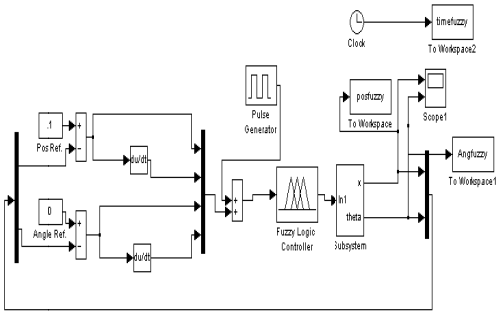

Figure 4. Fuzzy logic control simulink model of inverted pendulum

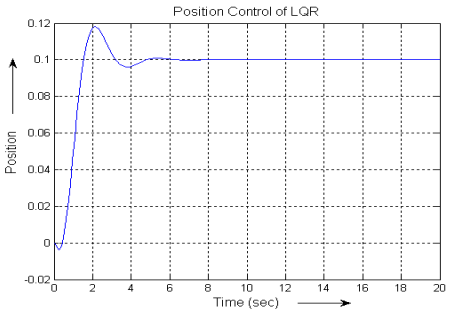

Figure 5. Position control of IP using LQR

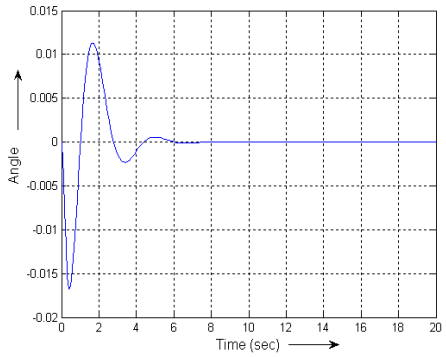

Figure 6. Angle control of IP using LQR

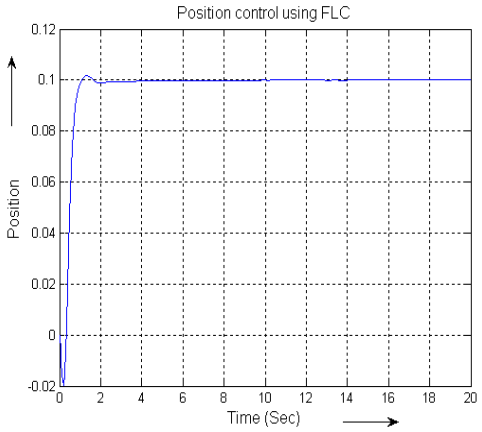

Figure 7. Position control of IP using FLC

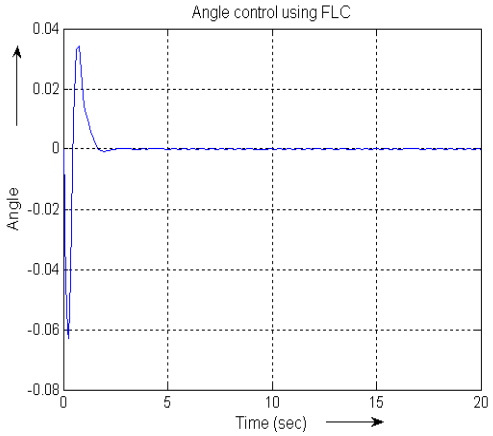

Figure 8. Angle control of IP using FLC

VI. CONCLUSION

In this research work two controllers i.e a fuzzy logic controller with four inputs and two outputs variable tuned by ANFIS and an LQR controller is designed for the control of position and angle of inverted pendulum. The fuzzy logic controlled based inverted pendulum is found to be more effective and gave faster response compared to LQR based controlled inverted pendulum in terms of less overshoot and low settling time.

REFERENCES

[1] R. C. Tatikonda, V. P. Battula and V. Kumar, "Control of inverted pendulum using Adaptive Neuro Fuzzy Inference Structure (ANFIS)", Circuit and System (ISCAS), IEEE International Symposium, pp. 1348-1351, 2010.

[2] Y. Gao, W. Chen, Z. Lu and S. Lu, "Design of parallel fuzzy neural network controller for inverted pendulum", Second IEEE conference on industrial electronics and application, pp. 856-861, 2007.

[3] M. I. EI-Hawwry, A. L. Elshafei, H. M. Emara and H. A. Abdel Fattah, "Adaptive fuzzy control of the inverted pendulum problem", IEEE Transaction on Control System Technology, vol. 14, no. 6, pp. 1135-1144, November 2006.

[4] C. E. Lin and Y. R. Sheu, "A hybrid control approach for Pendulum-Car control", IEEE Transaction on Industrial Electronic, vol. 39, no. 3, pp. 208-214, June 1992.

[5] G. Cansever, O. F. Ozguven, "Application of fuzzy set theory to stabilization of an inverted pendulum by a high speed fuzzy logic controller", IEEE Electrotechnical Confrence, vol. 3, pp. 1085-1088, April 1994.

[6] Y. Xiao-hui, L. Guo-ping, L. Guo-ping and X. Gen-fu, "Control experiment of inverted pendulum using adaptive neural fuzzy controller", IEEE International conference on electrical and control engineering, pp. 629-632, 2010.

[7] G. H. Lee and S. Jung, "Control of inverted pendulum system using a neuro fuzzy controller for intelligent control education", IEEE International conference on mechatronic and automation, pp. 965-970

[8] M. A. Lee and H. Takagi, "Integrating design stages of fuzzy systems using genetic algorithms", IEEE Transaction of Fuzzy System, pp. 612-617, 1993

[9] S N Sivanandam, S Sumathi and S N Deepa "Introduction to Neural Networks using MATLAB 6.0" Tata McGrow-Hill, ISBN-13:978-0-07-059112-7.

[10] Googol Technology, "Inverted Pendulum Experimental Manual", 2nd edition, July, 2006.

◈◈◈

Control of Multiaxis Manipulator arm with kinematic analysis for Land Mine Detection on the Unmanned Tracked Vehicle

[1]PT Lakshmi Prathibha, [2]Swarna Ramesh, [3]N. Seetharaman & [4]N.Babu

[1,2,3&4]Robotics division
Combat vehicles Research and development Establishment
(CVRDE, DRDO), Chennai, India

Abstract— Efficient unmanned mine detection system depends on the mine detection sensor for detecting the mines and method of deployment of mine detection sensor in suitable way to acquire the buried land mine data . This paper describes the configuration of the multi axis manipulator arm to carry heavy payloads and the large size Ground penetrating radar type of mine detection sensor mounted on the unmanned tracked vehicle. Manipulators are used to scan complete width of the vehicle and also side scan of the vehicle, two serial manipulators are very much preferable in the aspect of maneuverability. Also explained the complexity to control the manipulator arm for simultaneous movement of multiple joints with synchronization and less error. Forward and inverse kinematic analysis, trajectory planning, PID tuning as well as simultaneous control algorithm design for the manipulator are discussed. The hardware implementations in real time control of the two manipulator arms with the controller architecture are presented. Experiments were conducted and verified the inverse kinematics and the control algorithm for simultaneous control of the manipulator arms for the specific critical requirement of unmanned mine detection mission.

Keywords-*manipulator; unmanned vehicle; kinematics; control.*

I. INTRODUCTION

All over the world land mine detection and clearing is a significant humanitarian activity. New technologies such as improved sensors, efficient manipulators and mobile robots can help to clean mine fields.

Efficient sensors, detectors and positioning systems are needed to detect, locate and the challenging part of identifying different mines (1).Also adequate vehicles is required to carry the sensors over the infested fields. Many of the walking and wheel robots are deployed in the field of mine detection, As a combination of tracked vehicle and mobile robots provides an advantage in detection and clearance for the uneven terrain also considering the safety
(2). Conventional vehicle-mounted mine detector systems employ an array of sensor elements to achieve a detection swath typically 2 to 4m wide. Some systems employ more than one type of sensor technology. The sensors are mounted on the manipulator. The Manipulator aids in sweeping of a mine detector from side to side while moving forward to cover ground (3). The Manipulator has to follow the ground profile with the detector head parallel or close to the ground without hitting the ground or any objects on it. Otherwise mine detection sensor output leads to error or offset (4) .As the process involves sweeping of 3 to 4 m width, two serial manipulators are used. Most challenging part of this Manipulator in the moving vehicle is arm has to carry a high payload and both the arm has to move simultaneously with less error, else it will lead to breaking of joints and also causes damage to the sensor. Hence to move the arm synchronously during the real time application, forward and inverse kinematics joint angle and end effectors position, trajectory planning for one point to another, motion control algorithm has to be implemented in the real time hardware system.

II. CONFIGURATION OF MANIPULATOR

There are two serial arm manipulator has to be fitted in front of the vehicle. The each arm has five degrees of freedom such as base turret rotation, back arm rotation, fore arm rotation and fore arm linear actuation and roll rotation. A correct combination of Angular movement of Back Arms, Fore Arms and Linear Actuator through their Brushless DC motors can position the mine detection platform, parallel to the ground contour. This will be facilitated by the signals received from the distance sensors. The mine detection sensor such as Ground penetrating Radar will be utilized for mine detection purpose. The mine detection sensor is a rectangular structure which covers the whole width of the vehicle. Then the rectangular array sensor is connected to the two arm manipulator with a suitable joint as shown in Fig.1. The position of the each link can be continuously monitored by the respective encoder in each joint. This will facilitate to control the corresponding actuator accurately.

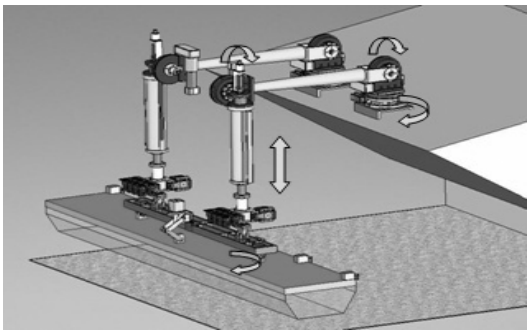

Figure 1. Shows the configuration of manipulator system

III. KINEMATICS OF THE MANIPULATOR

The forward kinematics problem for a serial-chain manipulator is to find the position and orientation of the end-effectors relative to the base given

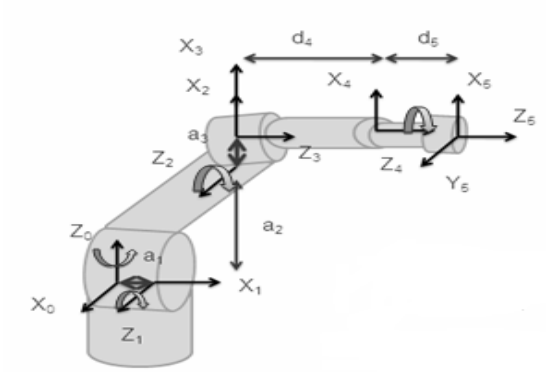

Figure 2. Shows the Kinematics of manipulator system

Positions of all of the joints and the values of all of the geometric link parameters. In manipulator system, five Degree of freedom jointed arm configuration Revolute-Revolute-Revolute-Prismatic-Revolute (RRRPR) is designed to carry a mine detection sensor and marking unit at the end effectors as shown in Fig.2.

The Denavit - Hartenberg parameters have been worked out for this configuration as shown in Table 1. It represents the link parameters like link offset d_i, link length a_i, link twist α_i and link rotation θ_i.

TABLE I. D-H PARAMETERS OF MANIPULATOR

Joint	θ_i	α_i	a_i	d_i
1	θ_1	90	0	0
2	θ_2	0	a_2	0
3	θ_3	90	0	0
4	0	0	0	d_4
5	θ_5	0	a_5	0

a_i = the distance from z_i to z_{i+1} measure along x_i

α_I = the angle between z_i and z_{i+1} measured about x_i

d_i = the distance from x_{i-1} to x_i measured along z_i

θ_i = The angle between x_{i-1} and x_i measured about z_i

By multiplying sequentially the transformation matrices from the initial frame to the end-effectors frame. The transform matrix for the four joint as arrived in equation (1).

$$T_5^0 = T_1^0 \; T_2^1 \; T_3^2 \; T_4^3 \; T_5^4 \qquad (1)$$

$$\begin{bmatrix} \cos\theta_1 & 0 & \sin\theta_1 & a_1\cos\theta_1 \\ \sin\theta_1 & 0 & -\cos\theta_1 & a_1\sin\theta_1 \\ 0 & 1 & 0 & d_1 \\ 0 & 0 & 0 & 1 \end{bmatrix}.$$

$$\begin{bmatrix} \cos\theta_2 & 0 & -\sin\theta_2 & a_2\cos\theta_2 \\ \sin\theta_2 & 0 & -\cos\theta_2 & a_2\sin\theta_2 \\ 0 & 0 & 1 & d_2 \\ 0 & 0 & 0 & 1 \end{bmatrix}.$$

$$\begin{bmatrix} \cos\theta_3 & 0 & \sin\theta_3 & a_3\cos\theta_3 \\ \sin\theta_3 & 0 & -\cos\theta_3 & a_3\sin\theta_3 \\ 0 & 1 & 0 & d_3 \\ 0 & 0 & 0 & 1 \end{bmatrix}.\begin{bmatrix} 1 & 0 & 0 & a_4 \\ 0 & 0 & 1 & 0 \\ 0 & -1 & 0 & d_4 \\ 0 & 0 & 0 & 1 \end{bmatrix}.$$

$$\begin{bmatrix} \boldsymbol{\cos\theta_5} & \boldsymbol{0} & \boldsymbol{\sin\theta_5} & \boldsymbol{a_5\cos\theta_5} \\ \boldsymbol{\sin\theta_5} & \boldsymbol{0} & \boldsymbol{-\cos\theta_5} & \boldsymbol{a_5\sin\theta_5} \\ \boldsymbol{0} & \boldsymbol{1} & \boldsymbol{0} & \boldsymbol{d_5} \\ \boldsymbol{0} & \boldsymbol{0} & \boldsymbol{0} & \boldsymbol{1} \end{bmatrix}$$

(2)

$$X = d_5 \sin(\theta_1) + \cos(\theta_1)\,(a_2\cos(\theta_2) + d_4\sin(\theta_2+\theta_3)) \qquad (3)$$

$$Y = -d_5\cos(\theta_1) + \sin(\theta_1)\,(a_2\cos(\theta_2) + a_5\cos(\theta_2+\theta_3+\theta_5) + d_4.\sin(\theta_2+\theta_3))$$

(4)

$$Z = -d_4\cos(\theta_2+\theta_3) + a_5\sin(\theta_2+\theta_3+\theta_5)$$

(5)

The kinematics identifying the end effectors coordinate are given in equation (3, 4 and 5). The velocities and acceleration equations of the end effectors can also be determined by differentiating from equations (3, 4 and 5) with respect to time.

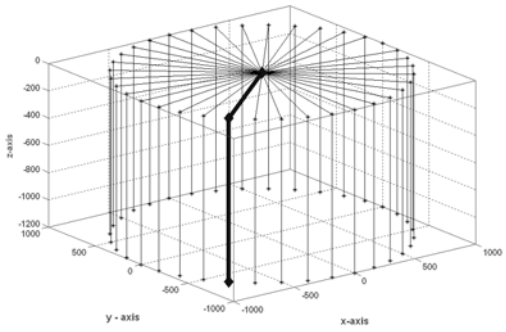

Figure 3. Shows the Kinematics of base rotation alone

Fig. 3 shows the kinematic works envelop of the single manipulator arm when the base of the arm rotates 360 angle. Similarly Fig.4 represents the different position of the manipulator links when the deployment of the mine detection sensor and again folding back the home position

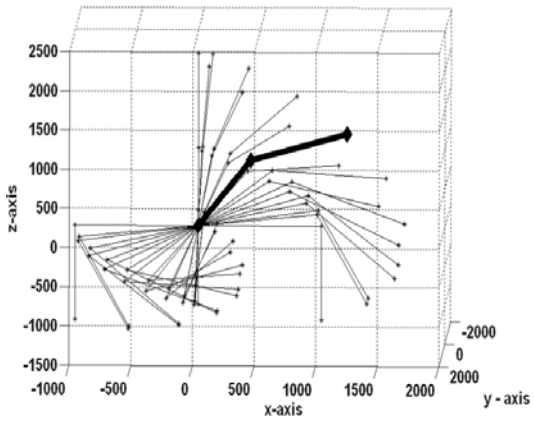

Figure 4. Shows the work envelope of manipulator during deployment condition

IV. INVERSE KINEMATICS

It is essential to move the mine detection sensor in the straight line like moving the sensor only in x direction alone and similarly, move the sensor only in z direction. It can be achieved by means of the inverse kinematics that the angle of the manipulators will be arriving. It is possible to dictate the manipulator movement in a straight line by specifying the x, y and z distance. Once the final target is known, further work out the angle of rotation for rotary joints and displacement for linear joints are arriving by means of the inverse kinematics.

$$d_4 = \sqrt{\left(p_x^2 + p_y^2 + p_z^2\right)} \qquad (6)$$

$$\theta_{3} = cos^{-1}\left(\frac{p_z}{d_4}\right) \qquad (7)$$

$$\sin\theta_1 = (p_y - d_4 \sin\theta_3 \qquad (8)$$

$$\cos\theta_1 = (p_x - d_4 \sin\theta_3 \qquad (9)$$

$$\theta_1 = A\tan^{-1}(\sin\theta_1 / \cos\theta_1) \qquad (10)$$

The above mentioned equations (7 to 10) are utilized to derive the joint angle for the given x, y and z position of the sensor. Fig.5 shows the position of the different links in the manipulator arm while moving the sensor in the side sweep condition in straight line requirement.

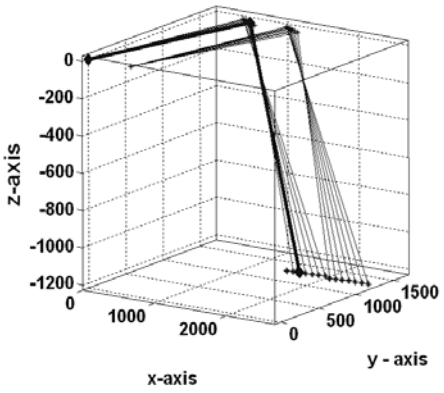

Figure 5. Shows the position of manipulator to move the sensor in horizontal straight line requirement

V. TRAJECTORY CONTROL

The paths planning of the mine detection sensor for the straight line motion are achieved by means of suitable trajectory calculation. This algorithm calculates the absolute angle of each link as a function of time. The absolute angle of each link is estimated using absolute encoder fitted on the manipulator arm. The algorithm uses the inverse kinematics of the 5-DOF manipulator discussed in to generate the joint space trajectory. The GUI has the provision to define the starting and ending of the sensor with the desired pose of the manipulator in the undulated surface. In this case the path planning algorithm calculates the number of steps and the size of each step. Then the low level trajectories will be generated and transferred to the actuators. The trajectory for each servo motor is simulated using MATLAB/SIMULINK.

VI. CONTROL ARCHITECTURE

Five brushless DC motors are used in each manipulator. The BLDC DC motor is controlled by servo drives. To control the multi axis manipulator, the position is provided to the system through the graphical user interface. The position received by the controller in turn control the motors in position, velocity.

The analog and digital output values received and transmitted to the controller. The controller used is PXI system. Graphical user interface and an upper level software in the controller developed in LABVIEW. The upper level control software generates trajectories in joint space for all motors for the end effectors positioning and generates control commands for the servo drives. It also checks the data from absolute encoder. The basic block diagram of controller architecture is shown in Fig. 6.

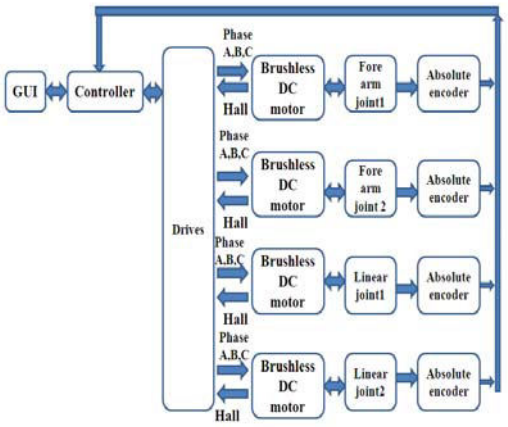

Figure 6. Shows manipulator controller architecture

The architecture of position control scheme is shown in Fig 7. This particular architecture is suitable only for controlling two joints simultaneously, considering one as master and other as slave and following the error with respect to master. The each joint of the manipulator is controlled by a position servo loop. The joint trajectory control algorithm accepts a new joint set point and trajectory parameters, based on system parameters and system constraints computes a position profile for each joint of the manipulator. In the simultaneous two axis control the two joints are controlled in such a way that both the joints starts moving at the same time with respect to the set point, Always one joint correct itself to the error of the other joint. One joint will be like master, other joint follows the error of the master and correct the error in order to protect the sensor which is mounted on the end effectors. Feedback from the two arms is provided as an input to the error estimator, the error calculated between the two joints is provided to the decision logic where it provides the feed back to the controller of the slave joint considering the current position of the slave joint and the error between the two joints. In this paper, two serial manipulator are joined together by the end effectors , hence to maintain the synchronization, each joint like fore arm of left with fore arm of right, back arm right with back arm left is paired as master and slave .The main critical point in this kind of manipulator is, if the errors between the two joints are exceeding the limits, it may cause damage to the sensors. Hence the error needs to be controlled critically for each trajectory points.

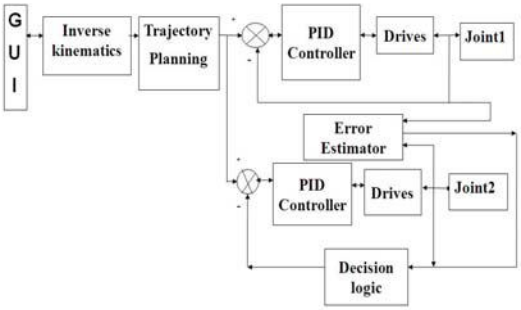

Figure7. Shows two axis joint position control

The Simulated control program for controlling the one joint of the manipulator arm is shown in Fig 8 . The trajectory path is provided as the input to the control algorithm and tuned the PID parameters for the following path, the output follows the input. Figure 9 shows the output of fore arm joint when the trajectory path starts from theta 15 and ends in theta 75.

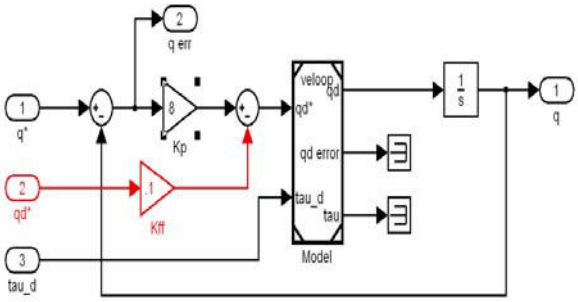

Figure 8. Simulation of position and velocity loop of one joint

Figure 10 shows the output of fore arm joint when the trajectory path starts from theta 30 and ends in theta -60.The Simulated inputs are given as the inputs to the trajectory planning of real time controller. The parameters used in simulation are used as a basis for controlling and further tuning the manipulator during real time operation. The properties of the brushless DC servomotor is given in Table II.

TABLE II Properties of Brushless DC servomotor

S.No	parameters	value
1	J	230gcm^2
2	*KT*	0.063 Nm/A
3	*R*	0.35Ω
4	*L*	1mH

The minimal requirement for a manipulator is the capability to move from an initial position to a final assigned position with stability and with minimal error in attaining positions. Software Control design of robot manipulator involves tuning of a PID at the each level of motor , driving for the manipulator joints.

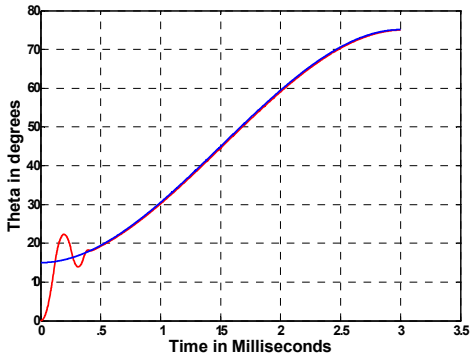

Figure 9. Shows the simulated output control after PID tuning for path moving from angle 15 to 75

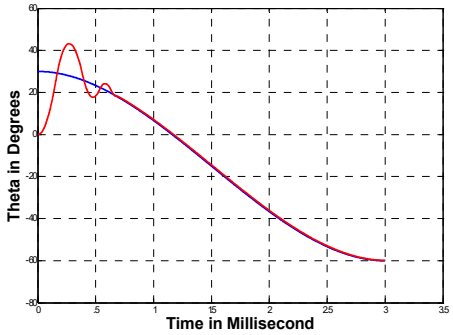

Figure 10. Shows the simulated output control after PID tuning for path moving from angle 30 to -60

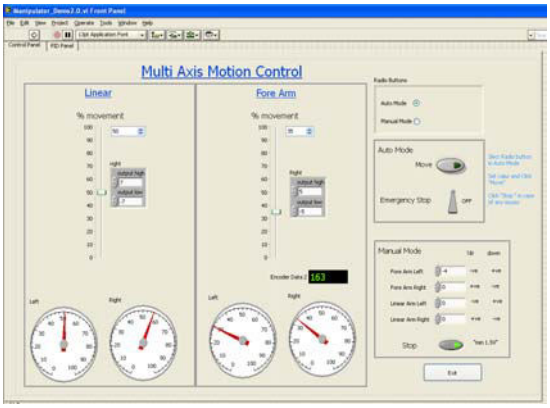

Figure 11. Graphical user interface developed for the Real time controller.

The graphical user interface is shown in Fig. 10 to control the multi-axis of the manipulator. This user interface facilitates to operate the single manipulator with specific joints in the manipulator. Also have a provision to control the two similar joints of the left and right manipulator simultaneously. The scheme of simultaneous control of manipulator joints with PID loop and feedback control of encoder is shown in Figure 12.

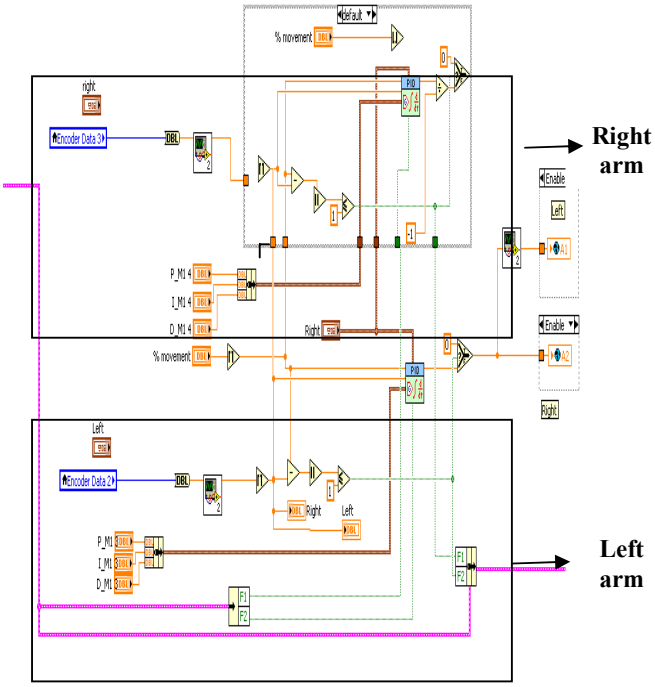

Figure 12. Scheme for simultaneous control of the manipulator joints

VII. EXPERIMENTS

The manipulator has been developed and fitted on the Unmanned tracked vehicle with the 3.5 m ground penetrating radar mine detection sensor as shown in Fig.13. The movement of the sensor to rise up vertically and swing the sensor to cover the required range of data acquisition is controlled through the GUI and PXI based controller. The error is minimized within the allowable limit while moving the joints in both the arms such as left and right serial manipulator. The real time control of the simultaneous multi axis control implemented and tested.

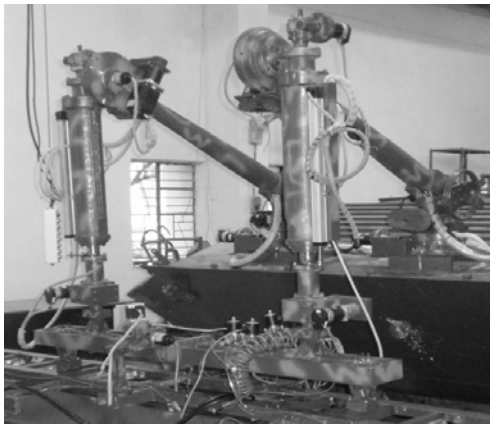

Figure 13. Hardware of manipulators fitted on the unmanned tracked vehicle

VII. CONCLUSION

This paper discussed the configuration of the manipulator suits for the specific requirements of carrying mine detection sensor on the unmanned tracked vehicle. Forward and inverse kinematics of the manipulator system has been arrived and then the work envelope of the manipulator during the mission without disturbing the other system has been finalized. The processes for optimal trajectory planning are developed for a five degree-of-freedom manipulator conducting point-to-point positioning and extended to include dual five degree-of-freedom manipulator with the end effectors employing synchronization. The control architecture is finalized to control the simultaneous movement of two serial arms for the single mission such as positioning and orientation of the mine detection sensor. Hardware of the manipulator arm are fabricated and integrated with the unmanned tracked vehicle and conducted experiments for the mission requirements with suitable PXI based controller and GUI.

REFERENCES

[1] GICHD (Geneva International Centre for Humanitarian Demining), Mine Action Equipment: Study of Global Operational Needs, 2002.

[2] Japan Science and Technology Agency (JST), Research area: "Research and Development for Supporting Humanitarian Demining of Anti-personnel Mines -Sensing Technology and Access and Control technology"

[3] Craig J. Introduction to robotics: mechanics and control. Boston (MA, USA): Addison-Wesley Longman Publishing Co., Inc.; 1989.

[4] O. Von Stryk and M. Schlemmerm "Optimal control of the industrial robot Manutec R3," *International Series of Numerical Mathematics*, 115 (Basel: Birhauser, 1994), pp. 367-382.

[5] R.P. Paul: Robot Manipulators: Mathematics, Programming,and Control (MIT Press, Cambridge 1981)

[6] Taylor R. Planning and execution of straight line manipulator trajectories. IBMJ Res Develop 1979;23(4):424–36.

[7] J.M. McCarthy: *An Introduction to Theoretical Kinematics* (MIT Press, Cambridge 1990)

[8] J.C. Latombe: *Robot Motion Planning* (Kluwer, Boston 1991)

[9] H. Choset, K.M. Lynch, S. Hutchinson, G. Kantor,W. Burgard, L.E. Kavraki, S. Thrun: *Principles of Robot Motion: Theory, Algorithms, and Implementations* (MIT Press, Cambridge 2005)

◈◈◈

Virtual Oscilloscope for Electronic Measurement Technology

[1]Sachin Shinde, [2]Deepak Bhoir & [3]Sapna Prabhu

(M.E) Electronics DEPT
Fr. Conceicao Rodrigues College of Engineering, Bandra (w.), Mumbai-50
Mumbai University

Abstract— This document gives LabVIEW is a graphical programming language that uses icons instead of lines of text to create applications. In LabVIEW, we build a user interface with a set of tools and objects. We can purchase several add-on software toolsets for developing specialized applications. All the toolsets integrate seamlessly in LabVIEW. Electronic measurement technology course is a public basic course which has relations with electronic measurement principles and methods. The proposed system **"Virtual Oscilloscope"** operates as like as original CRO. This is the software version of the CRO hard ware.and the common typical electronic measurement instruments' operating principles, performances and applications. It has such outstanding characteristics as theory has close relations with practices, outstanding practices and wide applications. By using LabVIEW developing software which based on computer visual virtual instrumentation to program the Virtual Instruments with traditional instruments' functions, we can demonstrate them in classroom by combing with PowerPoint conveniently. So, the aim of this project to develop the software kit in LABVIEW which shows all the operation of CRO in short replaces CRO hardware by CRO software. Using graphical programming language we design this system. The proposed system has all the functions which are in a CRO. This is the application of Electronics Measurement technology with virtual instrumentation, and helpful for class course teaching.

Keywords— *Electronic measurement technology; LabVIEW; Virtual Instrumentation; PowerPoint;*

1. INTRODUCTION

An OSCILLOSCOPE is a device for recording and visualizing the instantaneous value of alternating voltage and is used in many professions and academic institutions. Oscilloscopes are well documented, but to study the theory is not enough to learn how to use these measuring instruments. Therefore it is natural to create a hands-on training that can be used by anyone interested in self-study.

The following chapter explains the work the subject and illuminated background of learning theory. In another chapter of the history and functions of an oscilloscope are presented. It leads to the creation of a new virtual oscilloscope. The end result is a functioning new virtual oscilloscope, and be for teachers through its interfaces to document and the ability to import your own test signals easily into the system, a valuable tool can. But a real device can not replace it, and it should not.

*What is a **Oscilloscope***

Oscilloscope is a measuring device which can show various waveforms & voltages, Frequency, time period, wavelength can be measured using Oscilloscope.

*How does An **Oscilloscope** Work*

An oscilloscope works by measuring the voltage signal as it travels through the object. It is used to help we find breaks in the circuits or shorts.

*How to Use An **Oscilloscope***

The only way to use a oscilloscope is when dealing with electronics it will find and measure and find faulty electrical circuits on any electrical platform.

2. CATHODE-RAY OSCILLOSCOPE (CRO) OBJECTIVE

- To introduce the basic structure of a cathode-ray Oscilloscope.
- To get familiar with the use of different control switches of the device.
- To visualize an ac signal, measure the amplitude and the frequency.

The device consists mainly of a vacuum tube which contains a cathode, anode, grid, X&Y-plates, and a fluorescent screen (see Figure below). When the cathode is heated (by applying a small potential difference across its terminals), it emits electrons. Having a potential difference between the cathode and the anode (electrodes), accelerate the emitted electrons towards the anode, forming an electron beam, which passes to fall on the screen.

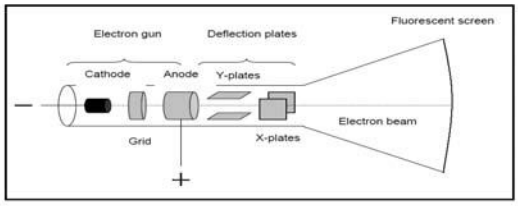

Fig 1. The basic structure of CRO

When the fast electron beam strikes the fluorescent screen, a bright visible spot is produced. The grid, which is situated between the electrodes, controls the amount of electrons passing through it thereby controlling the intensity of the electron beam. The X&Y-plates, are responsible for deflecting the electron beam horizontally and vertically.
A sweep generator is connected to the X-plates, which moves the bright spot horizontally across the screen and repeats that at a certain frequency as the source of the signal. The voltage to be studied is applied to the Y-plates. The combined sweep and Y voltages produce a graph showing the variation of voltage with time, as shown in Fig. 2. *Front panel* of the *CRO*

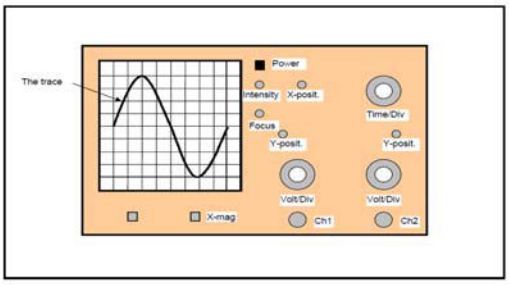

Fig 2. The Front Panel of CRO

An **oscilloscope** (also known as a **scope**, **CRO**, **DSO** or, an **O-scope**) is a type of electronic test instrument that allows observation of constantly varying signal voltages, usually as a two-dimensional graph of one or more electrical potential differences using the vertical or 'Y' axis, plotted as a function of time, (horizontal or 'x' axis). Although an oscilloscope displays voltage on its vertical axis, any other quantity that can be converted to a voltage can be displayed as well. In most instances, oscilloscopes show events that repeat with either no change, or change slowly [1]. Oscilloscopes are commonly used to observe the exact wave shape of an electrical signal. In addition to the amplitude of the signal, an oscilloscope can show distortion, the time between two events (such as pulse width, period, or rise time) and relative timing of two related signals.

3. INTRODUCTION TO THEORETICAL VIRTUAL LEARNING LABVIEW

An oscilloscope is a device for recording and visualizing the instantaneous value of AC voltages. It is a versatile instrument that is used by many professions and sciences. The need to know about the use and operation of the instrument to convey is understandable. But on the one hand, the manufacturer provides an instruction manual to an oscilloscope, on the other hand, stacking books in the libraries of books that explain everything there is to know about oscilloscopes. Why do we need then a teaching and learning software for virtual laboratories? This chapter interprets the theme of the work and discusses the benefits of educational software than printed educational materials have. It provides a typology of educational software and relates them to learning paradigms. Finally, the use of multimedia elements in the virtual teaching is illuminated. At the end of the chapter, the aim of this work is reformulated.

LabVIEW is a graphical programming language that uses icons instead of lines of text to create applications. In contrast to text-based programming languages, where instructions determine program execution, LabVIEW uses dataflow programming, where the flow of data determines execution. In LabVIEW, we build a user interface with a set of tools and objects. The user interface is known as the front panel. We then add code using graphical representations of functions to control the front panel objects. The block diagram contains this code. In some ways, the block diagram resembles a flowchart. We can purchase several add-on software toolsets for developing specialized applications. All the toolsets integrate seamlessly in LabVIEW. Refer to the National Instruments Web site at ni.com for more information about these toolsets.

4. INTERPRETATION OF THE THEME

Actual vs. workspaces.

virtual laboratories "... where reaching the more likely are the highest level, where it is because the real overthrow, it is called virtual. "Whether something is called a real or virtual depends on the stimulus density, with which it is detected by the nerves, perceptions, and then processed into ideas. The denser and more accurate perceptions are, the more real they seem, says Flusser Villem. Flusser cites the example of a chair, the only "is a bunch of swirling particles", but is perceived as real, because you can see and touch him and. The density of the point stimuli is gathered more than they could resolve the central nervous system. This is something really really Virtual.

Actually, virtual laboratories are therefore "real work spaces." This work is not concerned with creating teaching and learning software for a fictional, not real space, but a teaching and learning program that reflects a real system realistically possible in a perceived as a virtual system. The focus is on the realistic play, not on the system, in which they are playing, with the exception that the playback system may not have the required density to be considered as real. Otherwise, it would correspond to the real system, and when it does this is either the real system or a copy unnecessary. Currently there is no danger,

however, the reality can be confused with virtuality, because the playback systems of virtual worlds are not developed far enough to replace the reality.

Teaching and learning software thus makes sense only if it is not as good as the reality. Teaching and learning software can not replace the real teaching, but only support: The oscilloscope developed in this study is not a "real scope", but it is at exactly the point where it topples into the real, or at least prepares the way for this. This is the main novelty of this project compared to the "Existing virtual oscilloscope" featured teaching and learning software.

5. TEACHING, LEARNING AND THE COMMUNICATION CHAIN

Teaching and learning are two views of an action. The teacher sent messages to the learner through a medium based on common knowledge of teachers and learners. Knowledge is "a collection of facts (declarative knowledge) and rules (procedural knowledge)".To deliver a message that encodes both the teacher and transmitter of the message content in a character set that is also present in the learner, and the string transmitted over a medium. The medium can be varied - for example Sound, graphics, writing. The learner decodes the transmitted and decrypted string in the message sent by the teacher. The learner responds in turn by messages that are sent to the teacher. This particular form of action is communication, because the participants are the communication partners.

Communication leads to expansion of the knowledge base of the communication partners. Both communication partners are the sender and receiver of messages. The reaction of a communication partner on the message of the other communication partner is called feedback. Through feedback experiences a communication partner, whether and how his message has reached the intended target. Feedback is the indicator function of a communication chain. Only with the help of this reaction can be successful learning is the only way the teacher knows the student what he understood by his message and where he could expand his stock of knowledge.

LabVIEW is a graphical programming language that uses icons instead of lines of text to create applications. In contrast to text-based programming languages, where instructions determine program execution, LabVIEW uses dataflow programming, where the flow of data determines execution. In LabVIEW, we build a user interface with a set of tools and objects. The user interface is known as the front panel. We then add code using graphical representations of functions to control the front panel objects. The block diagram contains this code. In some ways, the block diagram resembles a flowchart.

We can purchase several add-on software toolsets for developing specialized applications. All the toolsets integrate seamlessly in LabVIEW. Refer to the National Instruments Web site at ni.com for more information about these toolsets.

6. CONCEPTS OF VI FOR OSCILLOSCOPE

LabVIEW is a software package from National Instruments that is used to write custom data acquisition programs called **VIs (virtual instruments)**. The user interface of a VI is called the "front panel". It provides we with an assortment of "controls", switches and dials that can be used to configure the VI, as well as "indicators", graphs and numeric displays that are used to display the measured data. Although VIs can be quite variable in their appearance and function, most of the ones we encounter in this course will be designed to mimic an oscilloscope and look somewhat like that of Figure 3.

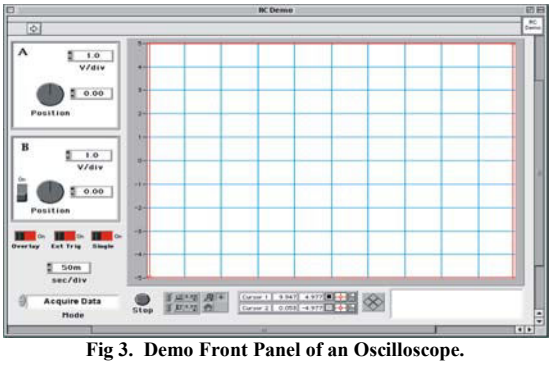

Fig 3. Demo Front Panel of an Oscilloscope.

In its most common configuration, an oscilloscope continuously measures voltage and provides a graphical record of voltage (y axis) versus time (x axis). Various dials and switches on the oscilloscope control the horizontal and vertical scaling and a multitude of other factors. Most modern oscilloscopes provide the ability to monitor more than one input signal simultaneously so that the relative timing of two signals can be compared.

The LabVIEW oscilloscope VIs that we will use in this course set up to mimic the appearance and functionality of a traditional oscilloscope while still providing the advantages of modern computer data acquisition.

6.1 Front Panel Controls

Proceeding from top to bottom, the controls on the front panel can be described as follows:

Run Arrow

Although a VI may be configured to automatically start as soon as we load it, in most cases we will need

to start by clicking on the "run arrow" near the top left corner of the front panel. With the oscilloscope VIs we will need to use this button often to restart the VI after stopping it to save data or make measurements. The run arrow darkens (i.e.) to signal when the VI is running.

V/div Control
This control changes the vertical sensitivity (i.e. gain) of the oscilloscope. The value indicated by the control is the voltage increment corresponding to one division in the vertical direction. Thus loour numeric values indicate higher sensitivity. Each input channel has its own independent V/div control. We change the value by clicking on the associated "up/down arrows" .

Position Control
This control is used to set the vertical position of the signal. The value indicated is the vertical position, in divisions, assigned to an input signal of 0.000 V. We can change the position quickly by dragging the position knob in a circular fashion with the mouse or by highlighting the old position value and typing in a replacement. Small adjustments can be made by clicking on the associated up/down arrows. Each input channel has its own independent Position control.

Channel B On/Off
Although input channel A is always recorded, channel B can be switched on or off. This is simply a matter of clicking on this switch.

Overlay
In its default configuration, the oscilloscope discards previous data before it plots a new trace. When the overlay switch is ON, the previous data is retained such that the most recent trace is co-plotted with previous traces. This feature is useful when we wish to generate a single graph that illustrates the effect of changing an external parameter (e.g. stimulus amplitude) on the appearance of the measured signal.

External Trigger
This switch allows for synchronization of the oscilloscope with an external device such as a stimulator. When it is ON, the oscilloscope waits for a voltage pulse (sync pulse) on its external trigger input before recording a measurement trace.
Note : When the oscilloscope is waiting for a sync pulse, the controls on the front panel are not read until either a sync pulse occurs or the wait for external trigger times out. When a VI is in this state, clicking on a control (e.g. Stop button) won't take effect until the trigger wait ends. Since we don't see an immediate response, a common mistake is to click buttons more than once. When the VI eventually does respond, all of the adjustments are performed and controls that our clicked more than once are adjusted more than once, usually without the desired result.

Single Sweep
When this switch is on, the oscilloscope will stop after recording 1 measurement trace. Single sweep is particularly useful when we wish to save the data or make measurements with the graph cursors after each trace.

Mode
When in **Acquire Data** mode, the VI acts as an oscilloscope. Other modes may be implemented to save data to files suitable for analysis by other programs.

Sweep Rate (sec/div)
This control sets the horizontal scale (i.e. the sweep rate) for the oscilloscope. Clicking on the up/down arrows changes the value.

Stop
Click on this button to stop the VI.

7. CONCLUSION & FUTURE WORK

In this simulation project, we can also generate a waveform by giving amplitude and frequency values. We can also select the type of waveform like,
- Sine wave
- Cosine wave
- Rectangular wave
- Triangular wave
- Saw tooth wave

Filter which is used to filter out the noise signal from the input signal. There are so many types of filters available which is of two forms either in analog form or digital form. We can use any type of filter for filtering the unwanted signal from the source.
In this project where we have used the filters for filtering out the noise signal from the input signal from the source. After filtering we can analyze the signal in the spectrum and moreover we can also calculate the total harmonic distortion which is present in the input signal.

Fig 4. Future View of Virtual CRO

8. REFERENCES

[1]. Kularatna, Nihal (2007), "Fundamentals of Oscilloscopes", *Digital and Analogue Instrumentation: Testing and Measurement*, Institution of Engineering and Technology, pp. 165–208, ISBN 978-0-85296-999-1

[2]. Spitzer, Frank; Howarth, Barry (2006), *Principles of modern Instrumentation*, New York: Holt, Rinehart and Winston, p. 119, ISBN 0-03-080208-3

[3]. Wedlock, Bruce D.; Roberge, James K. (2005), *Electronic Components and Measurements*, Prentice-Hall, pp. 150–152, ISBN 0-13-250464-2

[4]. "*Virtual Instrumentation Using LabVIEW*" authored by Prof. Sanjay Gupta.

[5]. "Application of Virtual Instrumentation which Based on Lab VIEW in Electronic Measurement Technology Course" 2011 International Conference on Electronics and Optoelectronics (ICEOE 2011) Yujun Bao School of Electronic Information & Electric Engineering, Changzhou Institute of Technology CZU Changzhou, China 978-1-61284-276-9111/$26.00 ©2011IEEE.

[6[. *LabVIEW TM* User Manual April 2009 Edition Part Number 320999E-01.

[7]. *LabVIEW TM* Measurements Manual April 2009 Edition Part Number 322661B-01.

[8]. QuickStart Guide February 2007 Edition Part Number 321527C-01.

[9]. Pei Liyun, The Application of LabVIEW to Multimedia Teaching of Electronic Measurements and Instruments[J], CHINA MODERN EDUCATIONAL EQUIPMENT,2008, (9).

[10]. BAO Yu-jun, Application of LabVIEW in the Electronic Measurement Techniques Course[J], JOURNAL OF CHANGZHOU INSTITUTE OF TECHNOLOGY, 2009. 22(6)

◈◈◈

An Intelligent Technique to Power Refrigerator & Air Conditioning System by Renewable Sources of Energy

[1]S.Bhuvaneswari, [2]Neeraj Kumar, [3]Yogesh Kumar, [4]Prashant Kumar, [5]Subhash Ranjan, [6]Ankit Raj, [7]Avishek Prasad, [8]Bhavesh Kumar

[1,2,3,4,5,6,7&8]Dr.MGR Educational & research institute university

Abstract— A state – of the art review is presented of different technologies that are available to deliver refrigeration from solar energy. The review covers solar electric, wind mill and some new emerging technologies. In this paper, a technique is used to run the refrigerator as well as air conditioner through the use of heat generated from refrigerator simultaneously. Thus the entire process is highly efficient as it minimize losses of the whole system. The use of relay in this technique of multi energy source refrigerator is that when the required power is not provided from solar, it will trip the circuit to wind energy and if both are inadequate the power will be supplied from electricity. In this system, refrigerator will operate with two panel and the panel movement is controlled by using PLC controller through the stepper motor and rotate the panel in the direction of maximum intensity of sun .In this paper a relay driver circuit(Logic switching) is used to trip the source which are generating maximum power at normal conditions. A Z- source inverter is connected to charge controller which converts DC into flexible and flexible AC to run the refrigerator. A variety of combined or hybrid system have also been investigated. Solar refrigeration can also inexpensive it would give the electric grid much relief mostly in summer days.

Keywords— *Refrigerator, solar panel, wind mill, heat exchanger, battery, charge controller, Z – source inverter.*

I. INTRODUCTION

A refrigerator (colloquially fridge) is a common household appliances that consist of a thermally insulated compartment and a heat pump(mechanical ,electronic or chemical) that transfer heat from inside of fridge to its external environment. So that inside of fridge is cooled to temperature below the ambient temperature of room. Lowest temperature means lower the reproduction rate of bacteria, so refrigerator reduce the rate of spoilage. A refrigerator maintains a temperature a few degree above the freezing point of water called a freezer.

There are two things that need to be known for refrigeration 1. A gas cools on expansion. 2. Second law of thermodynamics

As we know a solar powered refrigerator is a refrigerator which runs on electricity provided by solar energy. The use of solar energy to power refrigeration strives to minimize the negative impacts on refrigerator to the environment. Solar refrigeration is inexpensive and it would give the electric grid much relief. Electricity demand is at peak on hot summer days – 120 giga watts more in summer than winter. In this paper the key is the energy exchanged when liquid turns to vapour and vice- versa, the process that cools you when you sweat. By far the most common approach , the one used by the refrigeration in your house, uses an electric motor to compress a refrigerant – say – Freon – turn it into liquid. When the pressure created by compressor is released, the liquid evapourates , absorbing heat and lowering the temperature. Absorption chiller like solar refrigerators use a heat source rather than a compressor to change the refrigerant from vapour into liquid. The two most common combination are water mixed with either lithium bromide or ammonia. In each case the refrigerating gas is absorbed until heat is applied, which raise the temperature and pressure. At high pressure, the refrigerant condenses into liquid. Turning off the heat lower the pressure, causing the liquid to evaporate back into a gas , thereby creating the cooling effect. The solar refrigerator comprises of all traditional components like the compressor, condenser, expansion , valve and the evaporator or the freezer. The solar system of the solar refrigerator comprise of the solar panel which collects the solar energy. The solar panel are fitted with photovoltaic cells that convert the solar energy into electrical energy and store it in the battery. During the normal running of the solar refrigerator, the power is supplied directly by the solar panel, but when the output power of solar panel is less, the additional power is supplied by the battery. The battery is recharged when excess amount of power is produced by the solar panels.

The output supply of the batteries and the solar panel is DC with voltage of about 12V. A typical solar system produces 300 mw or 600mw of power depending upon the size of the desired refrigerator. The voltage regulator is connected to the battery to convert the low voltage dc supply to high voltage ac supply to run the compressor. It is advantage to use ac supply compressor since it can run on domestic electrical supply also. Some of the solar refrigerator use compressor that run directly on dc supply.

II. SYSTEM DESCRIPTION

Fig.1

A. Charge controller :- The charge controller regulator the flow of electricity to protect the batteries from overcharging and over discharging. In this system, a MPPT charge controllers are used which needed to extract maximum power point to draw maximum available power. It reduces complexity of system.

B. Z-source inverter:- It can reduce the Z-source capacitor voltage stress greatly and has an inherent limitation to inrush current. It reduces harmonics and increase the efficiency of the system.

C. Heat exchanger:-

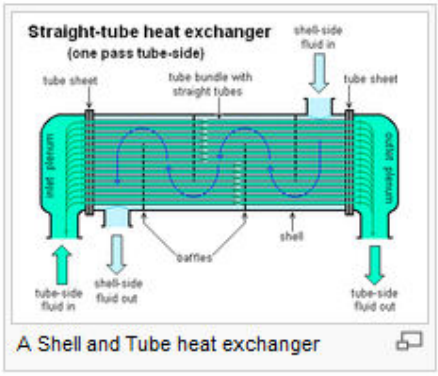

Fig.2

A heat exchanger is a piece of equipment built for efficient heat transfer from one medium to another. The medium may be separated by a solid wall, so that they never mix, or they may be indirect contact . In this system shell and tube heat exchanger are used which consist of a series of tubes one of tube contain the fluid that must be either heated or cooled. The second fluid runs over the tube that are being heated or cooled .

D. Dehumidifier:- A dehumidifier is a machine that takes moisture out of the air by condensing it onto a cold surface. It reduces the level of humidity in the air. Air conditioner inherently act as dehumidifier when they chill the air

E. Relay circuit:- A circuit that uses a small mechanical switch or a semiconductor device to energize a relay which will then close a contact to complete another circuit. In this system REED relay is used which is enclosed in a solenoid. The switch has a set of contacts inside an evacuated or insert gas filled g/an tube which protects the contacts against atmospheric corrosion. It is much faster than laser relays.

F. LDR sensor:-

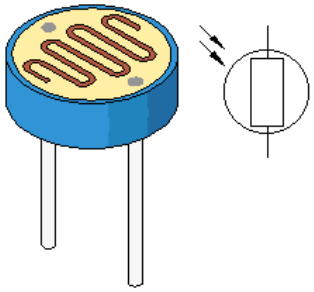

Fig.3

A light dependent resistor is a device which has a resistance which varies according to the amount of light fall on its surface

III. WORKING & PRINCIPLE

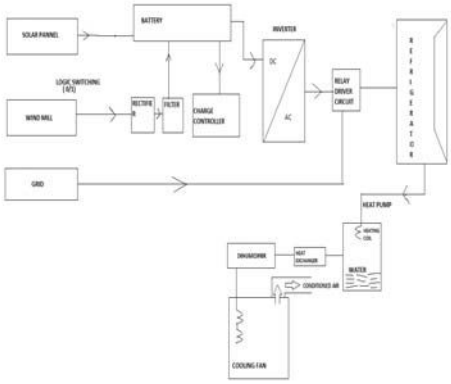

Fig.4

A. *Construction:-*

In this system , two renewable source of energy solar panel and wind mill is used which cut down the usage of electricity. Both are connected with the relay circuit and operates on basis of power productions. The power produced by the sources used to power the compressor of refrigerator through inverter. The heat

pump of refrigerator which is connected to the heating coil water basin. The heat exchanger and dehumidifier is connected to water basin which cool down the droplet of water and sent to condensed rod helps to produced conditioned air

A. Working:-

Solar panel converts sunlight directly into electricity to power the compressor of refrigerator because sunlight is not available at night time or during poor weather conditions a rechargeable batteries are used to store electric energy. A properly designed and maintained battery subsystem will allow the refrigerator to operate a week or more without sunlight. The use of relay in the this technique of multi energy source refrigerator is that when the required power is not provided from solar , it will trip the circuit to wind energy and if both are inadequate , the power will supply from electricity mains. The heat pump which is connected to refrigerator at its top is used to transfer heat from inside of fridge to its external environment. The heat pump which is connected to heating coil which put down in the water basin. So heat inside the water makes it evaporatorating. During this case, vapour gets collected and passes through the pipe through heat exchanger which transfer to dehumidifier. The air by condensing it onto

a cold surface. Thus it reduces the level of humidity in the air. The cold moisture running through the cooling chamber,makes the surrounding cooler wiyh the help of cooling fan. Thus, this technique is used to run the refrigerator as well as air conditioner with simple technique. Thus the entire process is highly efficient.

IV. FLOW CHART

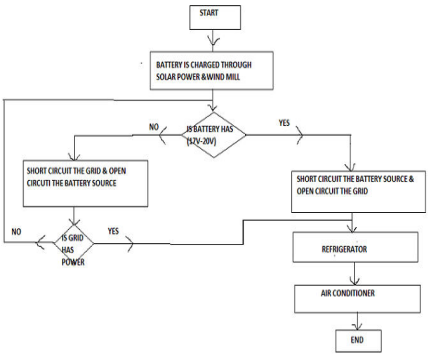

Fig 5

V. MATHEMATICAL MODEL

A. EFFICIENCY CALCULATION

- The efficiency of solar panel is defined by the ratio of power(W)kw to the product of solar panel surface area $A_s(M^2)$ and the direct irridation of solar beam $I_p(kw/m^2)$.I_p=1kw/m^2 is commonly used for calculation of nominal efficiency.

  $\eta_{sol\text{-}pow}=W/I_p*A_s=W/Q_s$

  where Q_s=cooling surface
- The work W is consumed by mechanical compressor to produce the cooling power Q_c. Refrigeration machine efficiency is defined as the cooling power Q_e divided by work input W

  $\eta_{pow\text{-}cool}=Q_e/W$
- The total efficiency of the system is

  $\eta_{sol\text{-}cool}=Q_e/Q_s$

B. RATING

Panel=12v
Mini refrigerator=200 Watts
5 hr=200*5=10000
5hr=1 kwhr

Now in 1 day=5 kwhr
For 1 unit=Rs 4
For one day cost =Rs 20
For 1 month=Rs 600

Therefor,for only refrigerator alone so much power and money is spent .But with the above system,no running cost will be there except the initital cost.It is totally economically free and one of the gift of nature.

V. PLC EXPERIMENTAL RESULTS

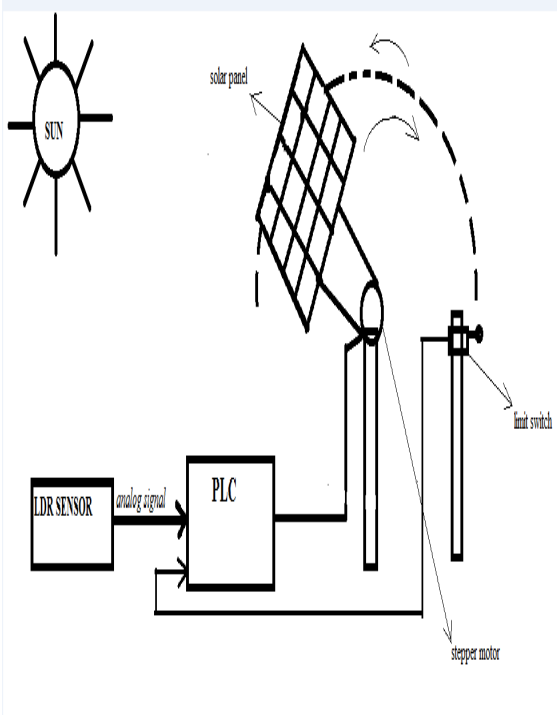

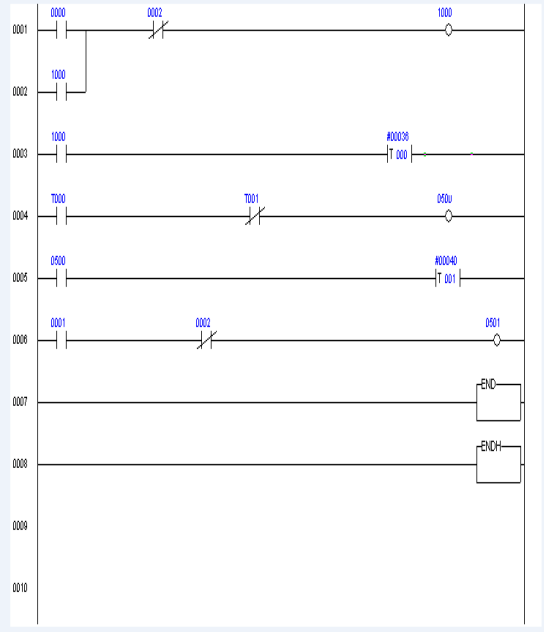

VI. CONCLUSION

The paper concludes that a variety of option are availab le to convert solar energy into refrigeration effects.Therefore we have conclude our system in which refrigerator and air conditioner is powered by renewable source which is more efficient for future.

VII. ACKNOWLEDGMENT

I would like to thank my respected co-ordinator S.bhuneswari mam for inspiring and guiding for this project.I would also like to thanks Mr.L.Ramesh ,HOD of EEE for implanting this idea.

REFRENCES

[1]. ..D.S kim and C.A infant Ferreira “Solar refrigeration options –a state of –of-the art review”

[2]. Alexis,G.k.,”A solar ejector cooling system using refrigerant.”

[3]. Wang, R.Z., Oliveira, R.G., 2005. Adsorption refrigeration – an efficient way to make good use of waste heat and solar energy. In: Proceedings of International Sorption Heat Pump Conference, Denver, USA.

[4]. Wang, R.Z., Jia, J.P., Zhu, Y.H., Teng, Y., Wu, J.Y., Cheng, J., 1997.

Direct Torque Control For Doubly Fed Induction Machine Under Voltage Dips

[1]Mandala Srikanth Goud & [2]Venu Madhav Gopala

Dept. of Electrical & Electronics Engineering
Padmasri Dr B.V. Raju Institute of Technology
Hyderabad, India

Abstract— This paper proposes a rotor flux amplitude reference generation strategy for Doubly Fed Induction Machine (DFIM) based Wind Turbine. It is specially designed to address perturbations, such as voltage dips, keeping controlled the torque of the wind turbine, and considerably reducing the stator and rotor over currents during faults. This is done by, a Direct Torque Control (DTC) strategy that provides fast dynamic response and accompanies the overall control of the wind turbine. Despite the fact that the proposed control does not totally eliminate the necessity of the typical crowbar protection for this kind of turbines, it eliminates the activation of this protection during low depth voltage dips. Comparison of the simulation results obtained without reference generation of flux and with reference generation strategy. The model is developed by using MATLAB/Simulink.

Keywords- *DFIM, CrowbarProtection, Direct Torque Control, Voltage Dips and Rotor Flux Generation Strategy.*

Abbreviations and Acronyms-

i - Current space vector.
- Magnetizing Inductance.
- Stator, Rotor self-inductance.
- Stator, Rotor leakage-inductance.
- Stator, Rotor resistance.
- Voltage space vector.
- Flux space vector.
- Synchronous and slip angular frequency.
- Rotor electrical speed.
- Subscripts denoting stator and rotor.
-Subscript denoting rotor reference frame.
- The machine torque base
- Number of pole pairs
. Frequency of the grid
- Voltage of the grid
- Estimated stator flux amplitude
- Estimated rotor flux amplitude
- Speed of stator
- Speed of rotor

I. INTRODUCTION

One of the major sources of Renewable Energy presently is the Wind energy. DFIM based wind turbine is in turn a critical and vital component of wind power generation which usually experiences and lot of variations in different parameters, such as speed, torque, voltages etc. Voltages dips are mostly inevitable in case of a DIFM based wind turbine.

The main objective of the control strategy proposed in this paper is to eliminate the necessity of the crowbar protection when a low-depth voltage dip occurs. Hence, by using direct torque control (DTC), with a proper rotor flux generation strategy, during the fault it will be possible to maintain the machine connected to the grid, generating power from the wind, reducing over currents, and eliminating the torque oscillations that normally produce such voltage dips [1].

II. DUAL FED INDUCTION MACHINE

A. Basics

Figure 1. shows the basic concept of the doubly-fed induction generator. It consists of rotor-side converter and grid-side converter. The DFIM is mostly popular in variable speed application than in case of fixed speed application and is best suited in wind power generation system. These DFIG's are sensitive and susceptible to voltage dips [2] and hence require protection on the rotor side converter.

B. Protection of DIFG

Thus crowbar protection (a resistive network) can be used at the rotor-side converter, but this method disconnects the system from the grid or disconnects the rotor-side converter from the rotor without disconnecting the wind turbine from the grid [3]. However, it would be preferred to avoid the activation of the crowbar in case of low voltage dips.

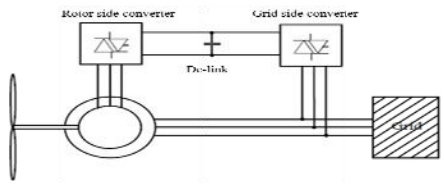

Figure 1. Basic diagram of Doubly Fed Induction Generator System

C. Concept

Figure 2. indicates the wind turbine generation system along with the proposed control block diagram. The DFIM is supplied by a back-to-back converter through the rotor and the stator is directly connected to the grid as shown. As the crowbar is present on the rotor side, here we discuss the control strategy corresponding to the rotor side converter only. The figure 2 consists of two different blocks used in the control of DFIG, A DTC that controls the machine's torque (T_{em}) and the rotor flux amplitude ($|\vec{\psi}_r|$) with high dynamic capacity and the second block that generates the rotor flux amplitude reference, in order to handle with the voltage dips.

When the wind turbine is affected by a voltage dip, it will need to address three main problems:

- from the control strategy point of view, the dip produces control difficulties, since it is a perturbation in the winding of the machine that is not being directly controlled (the stator);
- the dip generates a disturbance in the stator flux, making necessary higher rotor voltage to maintain control on the machine currents; and
- if not special improvements are adopted, the power delivered through the rotor by the back-to-back converter will be increased due to the increase of voltage and currents.[2]

Finally the rotor increases the DC bus voltage. Taking these effects into consideration and various other parameters like the speed, torque etc ,the use of crowbar protection is helpful during various fault conditions and sometimes ineluctable but avoiding the activation of crowbar is more desirous and makes the system more efficient. Thus the proposed control strategy aims to eliminate the activation of crowbar in case of low voltage dips.

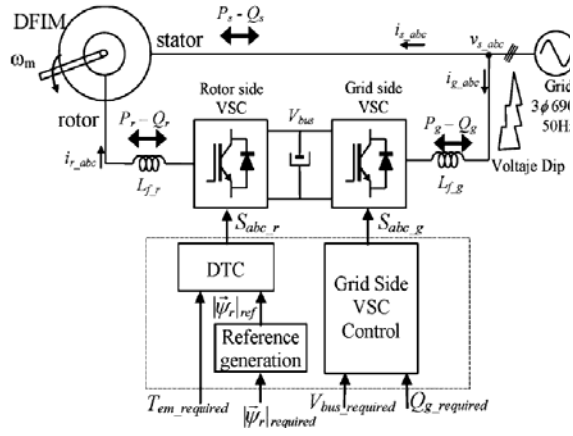

Figure 2. Wind Power generation based on DIFM

III. MATHEMATICAL ANALYSIS

Here when a voltage dip occurs, the stator flux evolution of the machine is imposed by the stator voltage equation

$$\vec{v}_s^s = R_s \vec{i}_s^s + \frac{d\vec{\Psi}_s^s}{dt}. \tag{1}$$

However, generally very high stator currents aren't allowed, thus the stator flux evolution can be approximately obtained by the sum of sinusoidal and an exponential term as shown in [3] and (neglectingR_s). Hence we obtain the equations

$$\begin{aligned} \Psi_{\alpha s} &= K_1 e^{-K_2 t} + K_3 \cos(\omega_s t + K_4), \\ \Psi_{\beta s} &= K_5 e^{-K_2 t} + K_3 \sin(\omega_s t + K_4). \end{aligned} \tag{2}$$

It is mostly preferred that there be sinusoidal current exchange between the system and the grid during the fault occurrence, for which the rotor and stator currents should be sinusoidal but by checking the equations that represent the rotor and stator currents as a function of fluxes, shown below

$$\vec{i}_s^s = \frac{L_h}{\sigma L_r L_s}\left(\frac{L_r}{L_h}\vec{\Psi}_s^s - \vec{\Psi}_r^s\right),$$

$$\vec{i}_r^s = \frac{L_h}{\sigma L_r L_s}\left(\frac{L_s}{L_h}\vec{\Psi}_r^s - \vec{\Psi}_s^s\right). \tag{3}$$

Here we employ DTC technique to control the rotor side flux only, as a consequence of which it is difficult to obtain sinusoidal exchange. The proposed solution cancels the exponential terms from equation (3), i.e. to generate equal oscillation in the rotor flux amplitude and in the stator flux amplitude. By using oscillatory rotor flux instead of constant value improves the quality of currents which can be confirmed through the simulation results obtained.

IV. ROTOR FLUX REFENCE GENERATION STRATEGY

Figure 3. Represents the proposed rotor flux reference generation strategy. Here for the block diagram and According to the proposed control strategy a small quantity ($\Delta|\vec{\psi}_r|$), is added to the required rotor flux according to the following expression

$$\Delta|\vec{\psi}_r| = |\vec{\psi}_s| - \frac{|\vec{v}_s|}{\omega_s}. \tag{4}$$

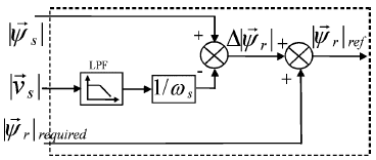

Figure 3. Rotor Flux Reference Generation Strategy

Here, the estimated stator flux ($|\vec{\psi}_s|$) and the grid voltage ($|\vec{v}_s|$), are not affected by the voltage dips. The proposed method uses a low pass filter to measure

this voltage ( ) as shown by the block diagram in figure 3, here it also must be noted that the constants – (2) are not needed in this proposed system as the exponential terms are canceled reducing the complexity involved.

In brief, the voltage drop in the stator resistance has been neglected, i.e. at steady state without the presence of the dips the term added to rotor flux ( ) will be zero. And in case of a dip occurrence the added term ( ) to the rotor flux reference will be approximately equal to the oscillations, resulted due to the dip, in the stator flux amplitude.

V. SIMULINK MODEL OF THE PROPOSED ROTOR FLUX REFERENCE GENERATION STRATEGY

Figure 4. Shows the considered MATLAB/Simulink model used to obtain the simulation results. The model contains a DFIG based wind generation system with a three phase fault, i.e. a low voltage dip. Here base wind speed has been considered to be 12 m/s and a pitch angle of 45 degrees has been considered. The Subsystem1 of the model represents our proposed rotor flux reference generation strategy block as shown in Figure 5.

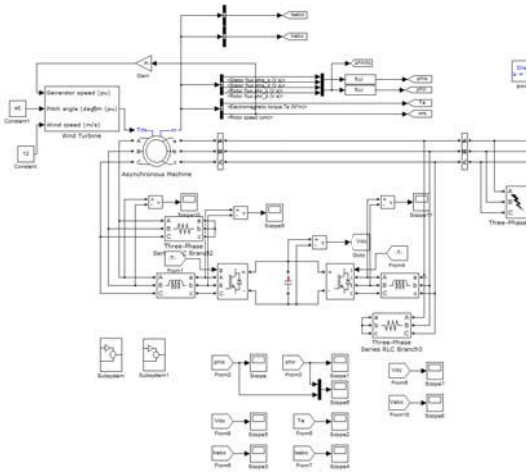

Figure 4. Main Simulink model of the DFIG based wind energy generation system with a three phase fault.

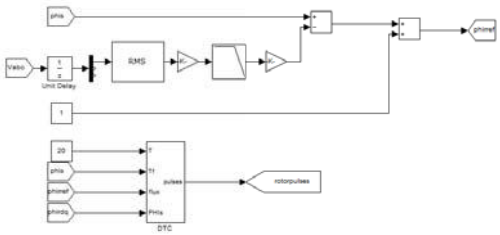

Figure 5. Simulink model of the proposed rotor flux reference generation strategy.

VI. SIMULATION RESULTS

The simulations are performed in MATLAB/Simulink. And the details of the simulated wind turbine are as follows

- Nominal Power = 2 VA
- Voltage(line-line) = 690 V_{rms}
- Frequency = 50 Hz
- Type = DIFG
- Stator Resistance = = $29x10^{-3}$ Ω
- Stator inductance = =$5.99x10^{-4}$ H
- Rotor Resistance = = $22x10^{-3}$ Ω
- Rotor inductance = = $5.99x10^{-4}$ H
- — = –
- No. of pairs of poles = 2

Using these values the simulation has been carried for a sample time of 1.The output waveforms for the Simulink model in the figure 6, with and without rotor flux reference generation strategy, when a voltage dip occurs are as shown below

A. Output Waveforms

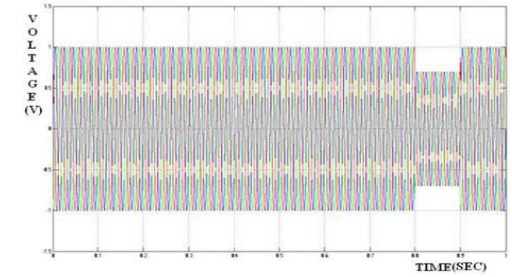

(a)

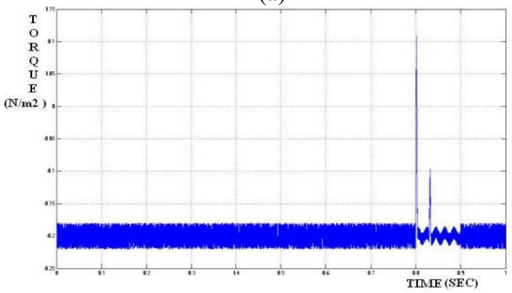

(b)

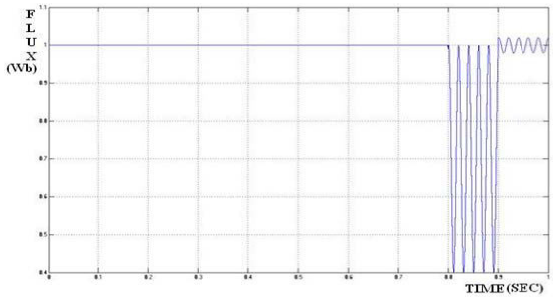

(c)

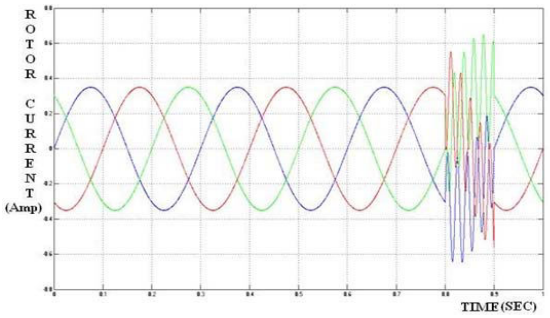

(d)

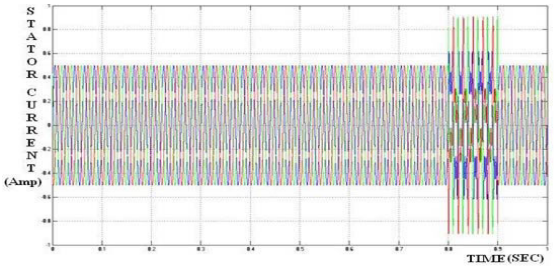

(e)

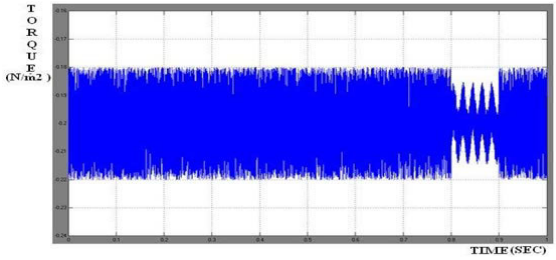

(f)

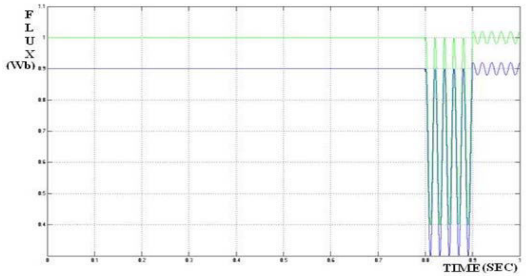

(g)

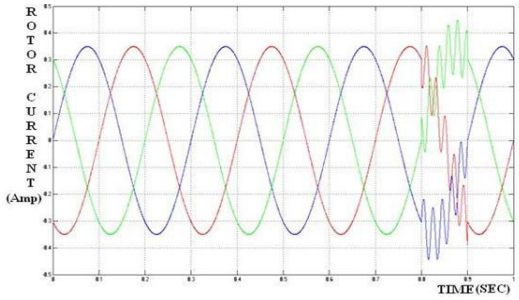

(h)

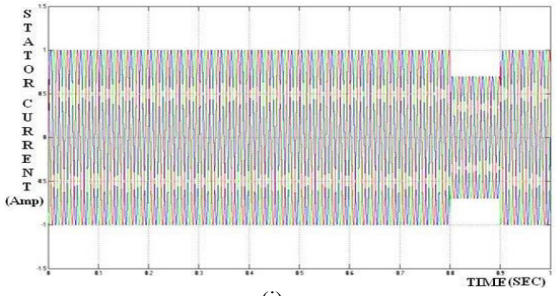

(i)

Figure 6. Simulation comparison of DFIM behavior, withoutand with proposed reference generation.,where the various results are as follows

(a) Stator voltage. (b) Torque without reference. (c) Flux without reference (d)Rotor current without reference (e) Stator current without reference (f) Torque with reference (g) Flux with reference (h) Rotor current with reference (i) Stator current with reference

The principal aim of the various results obtained during the simulation is to show how the considered DFIM responds to the proposed rotor flux reference generation strategy, i.e. how the DFIM handles the low depth symmetric voltage dip with and without the proposed control strategy. [Here the low depth, in this case 30 %, symmetric voltage dip is indicated by the figure 6.(a) and the speed is assumed to be approximately constant].

When the dip occurs it is desirable to maintain the torque controlled to the required value (20%), therefore allowing eliminating any mechanical stresses (if any) to the wind turbine. Clearly from the figure 6(b) and (f) we can evaluate that it can only be achieved if the generated rotor flux is oscillatory, this rotor flux is thus generated according to the proposed block diagram in figure 3 such that the rotor flux is generated in accordance with stator flux amplitude [see Figure 6(c) and (g)].Here the proposed control strategy also maintains the stator and rotor currents below or within the safety limits, avoiding high over currents, which can be inferred from figure 6 (h) and (i). Thus the DTC is suitable and well-suited control strategy to act in case of faults requiring quick flux dynamics and to eliminate torque perturbations and preventing mechanical stresses.

These results gives an insight about the behavior of the DFIM during low voltage dips, unlike predicted in theory, the deterioration of the quality of these currents is hard to avoid .Here if the rotor flux is not made oscillatory and kept constant then the currents will reach till their limit values as shown by the figure 6(d) and (e), which in a real scenario would disconnect the wind turbine from the grid or alternatively activate the crowbar protection.

Ultimately, it can be inferred that the proposed control works effectively and as desired at any operating point of the wind turbine, as well as at any type of fault (single phase, double phase, etc).The performance of the proposed control may be limited only when the rotor voltage required is greater than that available at a give DC bus voltage value.

VII. CONCLUSION

Clearly the Simulation results have confirmed during low depth voltage dips, the proposed control strategy obviates the necessity of the crowbar and also maintains the torque and current values within their limits. In fact, the dc bus voltage available in the back-to-back converter, determines the voltage dips depth that can be kept under control. Further explorations and analysis is being carried out to develop a modified rotor flux reference generation strategy so as to withstand deeper voltage dips without the activation of crowbar protection, which would not only eliminate the crowbar protection circuit making the system more economical but also would make the wind energy generation system more efficient by reducing potential losses in power generation due to disconnection of wind turbine from the grid.

REFERENCES

[1] G. Abad,M. A. Rodr´ıguez, J. Poza and J. M. Canales "Direct Torque Control for Doubly Fed Induction Machine-Based Wind Turbines Under Voltage Dips and Without Crowbar Protection," IEEE TRANSACTIONS ON ENERGY CONVERSION, VOL. 25, NO. 2,2010.

[2] J. Lopez, P. Sanchis, X. Roboam, and L. Marroyo, "Dynamic behavior of the doubly fed induction generator during three-phase voltage dips,"Energy Conversion, IEEE Transactions on, vol. 22, no. 3, pp. 709–717.

[3] Kadam D.P.and Dr. Kushare B.E "Converter Protection Scheme for Doubly-Fed InductionGenerators during Disturbances," International Journal of Computer Science and Network (IJCSN)Volume 1, Issue 2, April 2012.

[4] M. Ali Dami, K. Jemli, M. Jemli, M. Gossa," Doubly Fed Induction Generator, With Crow-Bar System, under Micro-Interruptions Fault," International Journal on Electrical Engineering and Informatics - Volume 2, Number 3, 2010

[5] B. Babypriya, R. Anita, "Modelling, simulationand analysis of doubly fed induction generator for wind turbines," Journal of Electrical Engineering,vol.60, no.2, 2009, pp 79-85.

[6] B.Chitti Babu and K.B.Mohanty ,"Doubly-Fed Induction Generator for Variable Speed Wind Energy Conversion Systems- Modeling & Simulation," International Journal of Computer and Electrical Engineering, Vol. 2, No. 1, February, 2010.

[7] Christian Wessels, Student member, IEEE and Friedrich W. Fuchs, Senior member, IEEE, "Fault Ride Through of DFIG Wind Turbines during symmetrical voltage dip with Crowbar or Stator Current Feedback Solution," Energy Conversion Congress and Exposition (ECCE), 2010 IEEE.

[8] A.S. Mäkinen and H. Tuusa," Effect of transient flux compensation control on fault ride through of doubly fed induction generator wind turbine," International Conference on Renewable Energies and Power Quality (ICREPQ'11) Las Palmas de Gran Canaria (Spain) April, 2010

[9] Gonzalo Abad,Jesu´s Lo´pez,Miguel A. Rodrı´guez,Luis Marroyo and Grzegorz Iwanski," DOUBLY FED INDUCTION MACHINE MODELING AND CONTROL FOR WIND ENERGY GENERATION," IEEE Press published by John Wiley & Sons, Inc,2011.

[10] M. Soliman, O.P. Malik and D.T. Westwick,"Ensuring Fault Ride Through for Wind Turbines with Doubly Fed Induction Generator: a Model Predictive Control Approach," 18th IFAC World Congress Milano (Italy) , 2011

[11] P.Kundur,"Power system stability and control," New York, US: McGraw-Hill, Inc., 1994.

[12] Krisztina Leban,"Doubly Fed Induction Generator Fault Simulation," Institute of Energy Technology,Aalborg 2009.

Security Strengthening With Deformation Decrease in Acoustic Steganography (SSDD)

[1]Prakash.R, [2]Karthika.G.R, [3]Sasikala.R, [4]Divya.R, [5]Anguraj.S, [6]Shatharajah.S.P

[1,2,3,4] B.Tech student, Department of IT, K.S.R college of Engineering, Tiruchengode, Namakkal.
[5] Assistant Professor, Department of IT, K.S.R College of Engineering, Tiruchengode, Namakkal.
[6] Professor, Department of MCA, Sona College of Technology, salem.

Abstract- Owing to the hurried expansion in the field of the isolated computing in recent years, there is need of ordered protection for the information that is send through a set of systems. To fulfill this need, steganography is used as the one of the planned method to guard the secret message against the eavesdroppers. The implemented method provides one of the techniques of embedding the secret message bits into the audio series. The concept of the proposed method is that synonyms and antonyms of a word, replaces each and every statement of the secret message for a number of iterations and thus provides the raise of complexity. The synonyms and antonyms are again converted to number sequence and are formed into matrix. The matrix is inversed to increase the security. The principle aim is to reduce the distortion that is caused while embedding the covert message into the LSB and MSB audio bits using the replacement technique. The concept of genetic algorithm is used to reduce the distortion caused in the cover audio series and also increases the robustness of the embedded audio sequence. The robustness is provided against the intentional attacks which try to know the embedded secret message and some accidental attacks which try to add some unwanted message into the audio sequence. The main advantage of the proposed technique is to increase the difficulty and robustness of the audio sequence in audio steganography.

Keywords*: Steganography, synonym, antonym genetic algorithm, distortion.*

I. INTRODUCTION

Steganography is a technique of covert announcement in which the sender and receiver only can realize the hidden message. Stego is a Greek word which means 'covered' and graphics is a word which means 'writing'. Steganography may also be defined as the study of techniques for hiding the existence of the secret message in the presence of the covered medium. Many methods are proposed to hide the data the protocol to hide the data in the stego medium like audio, video, image, text. The size of the secret message should be small when compared to cover medium. In steganography, secret message is hidden in another message in such a way no one can detect except the dispatcher and the recipient. Steganography is a best method which is based on modification of LSB and MSB bit (substitution technique). The secret message that is to be embedded in audio sequence is called stego object. The medium in which the secret message is embedded is called cover object. The protection of the covert message lies on the efficiency of implemented method of steganography. The efficiency of the steganography can be measured with various properties.

- **Capability:**
  The competence is measure of maximum capacity of the secret message that can be mbedded into the covered medium without introducing distortion above the certain level.
- **Impermeability:**
  The sequence that is obtained after encoding the secret message should have only considerable amount of changes from the original medium.
- **Confidentiality:**
  The embedded message in the cover medium must provide efficient security and sufficient complexity in such a way, that eavesdropper cannot decode the secret message.

II. CONCEPT OF PROPOSED METHOD

1. Effectiveness of language

In any language, each and every word has various same meanings words (synonym) that can be used appropriately in various places. In the similar way a word also have the opposite meaning (antonym). This synonym and antonym can be used to replace the secret word. The synonym can be substituted for the number of times based on the key value. Instead of the synonym, antonym can also be used. The combination of both synonym and antonym can also be used based on the key value.

Recognition of the synonym

Consider a word, for example "Xerox Machine" and the encoding key is 2, then the number of synonyms available in the same meaning as that of the word machine is given in the alphabetical order.

S.no	Synonym	Key
1	Apparatus	1

2	Appliance	2
3	Contraption	3
4	Device	4
5	Engine	5
6	Instrument	6
7	Mechanism	7
8	Piece of equipment	8

Since the key is 2, select the second word from the table i.e Appliance instead of the word machine. The word appliance is replaced by its synonym which is in the second position in the alphabetical order.

Recognition of the antonym

Antonym of a word can also be replaced by using the same technique as that of the replacement of a word by the synonym. Note a synonym and antonym can be replaced alternatively with varying key length to enhance the security of the covert message that is embedded.

2. UNBALANCED KEY EXTENT

The main principle of this layer is to implement the varying key concept and to convert the secret message into the cipher text. In this method, the key length is varied by addition of the constant number or multiplied by constant number or square of a number and is repeated till it reaches the maximum length.

Suppose the starting key is 0, constant key is 2 and maximum limit is 26, then after it reaches the maximum length of 26, it again returns to 0. This type of encryption, form the first layer of security.

EXAMPLE Xerox-appliance

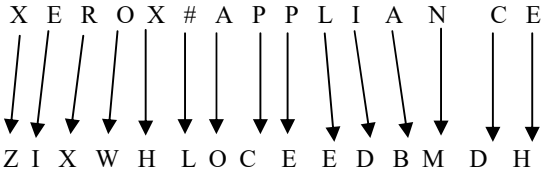

NOTE:

In the above example the Xerox does not have the synonym and thus the particular word is changed by varying key length and this enhances the security. Similarly the space is denoted as the symbol # and is denoted by the number 27 in this example.

PLAIN TEXT	KEY LENGTH	CIPHER TEXT
X	0+2=2	Z
E	2+2=4	I
R	4+2=6	X
0	6+2=8	W
X	8+2=10	H
#	10+2=12	L
A	12+2=14	O
P	14+2=16	C
P	16+2=18	E
L	18+2=20	E
I	20+2=22	D
E	22+2=24	B
N	24+2=26	M
C	26+2=1	D
E	1+2=3	H

3. CALCULATION OF THE EMBEDDING SEQUENCE:

The cipher text that is obtained by the above substitution is converted into numbers in order to embed it into the audio. By embedding the letters directly will contain the disadvantage of providing less security. For example, using the ASCII value all letters will posses 9, 10 and 11. Thus it is easy to decode for the hackers.

S.no	CIPHER TEXT	Key	value
1	Z	2	1
2	I	4	13
3	X	6	3
4	W	8	4
5	H	10	18
6	L	12	24
7	O	14	2
8	C	16	19
9	E	18	23
10	E	20	25
11	D	22	26
12	B	24	26
13	M	26	12
14	D	1	5
15	H	3	12

4. INCREASED SECURITY BY MATRIX MULTIPLICATION

The embedding sequence that is generated above is taken in the matrix format and is converted to encoding matrix by inversing it. The encoding matrix may be a inverse matrix that is generated above or a matrix that is given as the same. The numbers that are generated by the above layers are converted into a number matrix and the inverse matrix is embedded into the audio sequence in order to increase the security.

$$\begin{bmatrix} 1 & 13 & 3 & 4 \\ 18 & 24 & 2 & 19 \\ 23 & 25 & 26 & 26 \\ 12 & 5 & 12 & 0 \end{bmatrix}$$

The above matrix is partitioned and inversed and is embedded onto the audio sequence. This matrix is embedded into the audio sequence.

$$\begin{bmatrix} -0.07 & 0.05 & -0.03 & 0.06 \\ 0.09 & 0.01 & -0.02 & 0.02 \\ 0.03 & -0.05 & 0.03 & 0.01 \\ -0.06 & 0.00 & 0.05 & -0.09 \end{bmatrix}$$

5. EMBEDDING THE CIPHER TEXT IN AUDIO

The ciphered sequence that is generated by the above or the encrypted message is directly embedded into the audio sequence both in the LSB and in deeper layers of the LSB bits of audio sequence.

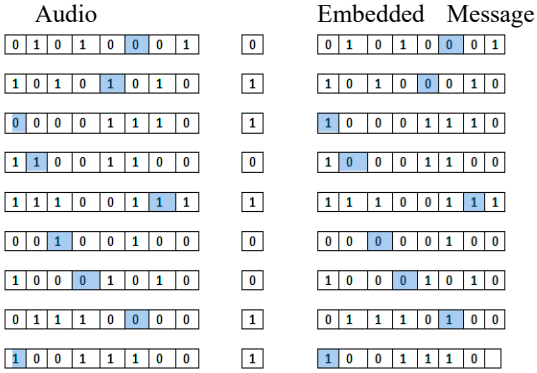

This provides increased robustness and high security. Encryption and decryption are used in this method for improved confidentiality, deniability and large capacity of the information can be embedded into the audio sequence.

6. ENHANCEMENT THROUGH GENETIC ALGORITHM

The audio sequence that is obtained above is taken to calculate the amount of distortion using the fitness value determined by genetic algorithm. The fitness value is fixed for original audio sequence and is compared with the embedded audio sequence in order to calculate the distortion value. The distortion amount can be reduced by selecting the particular key value. This helps to increase robustness and to reduce error that is caused by the encoding of the covert message into the audio sequence.

The entire process can be given by a flow chart as

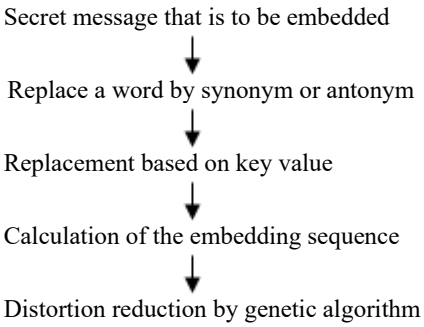

7. CONCLUSION

Thus steganography is a method of sending the covert message in a protected manner and deliver it the covert message to the recipient without any error. The proposed method uses the strength of synonym and antonym of the word to protect the secret message. The main advantage of this method is that its concept is simpler, but provides more security by using varying key length and it enhances the robustness. By using genetic algorithm the distortion is reduced. The result of the paper is that it provides maximum protection for the covert message and minimum distortion using genetic algorithm.

REFERENCES

[1]. Zamani, M., Manaf, A.A., Ahmad, R.B., Zeki, A.M., & Abdullah, S.(2009) A genetic-algorithm-based approach for audio steganography, world academy of science, engineering and technology 2009

[2]. Anguraj S., Kumerasan K., "A Structured system of embedded based on artificial intelligence by incorporating Genetic Algorithm" 978-1-4244-7770-8/10/$26.00 2010 IEEE

[3]. "Robust Audio steganography via genetic algorithm", information and communication technologies, 2009 ICICT apos 09. International Conference on Volume, Issue, 15-16 Aug 2009 Page(s):149-153 Digital Object Identifier 2009/ICICT.2009.5267197

[4]. Anguraj S., Dr.Shantharaj S.P., Arul Murugan R., Balaji.,Maneesh R.,Prasanth S." A Fusion of A-B map cipher and ASET Algorithms for the Enhanced Security and Robustness in Audio Steganography" IEEE-International Conference on Recent Trends in InformationTechnology,ICRTIT,2011,MIT,AnnaUniversity, Chennai, June 3-5,2011.

[5]. Mazdak Zamani, Hamed Taherdoost,Azizah A. Manaf, Rabiah B.Ahamed and Akaram M.Zeki, "ASecure Audio Steganography Approach" 2009 by the Institute of Electrical and Electronics Engineers

[6]. Shafakhatullah Khan Md., Vijaya Bhasker., and Shiva Nagaraju, " An Optimized Method for Concealing Data using Audio Steganography".

[7]. Pramatha Nath Basu, Tammay Bhowmik, "On Embedding of text in Audio- A case of Steganography", International Conference on Recent Trends in Information and Computing,2010.9

Assessment of deaf speech and normal speech using digital processing technique

[1]Siddharth Basu & [2]Nitin Ambatkar

Dept. of Electronics (Commuinication), Priyadarshini College of Engineering, Nagpur, India

Abstract- This proposed project will deal with analysis on acoustical characteristics of speeches of deaf people for the purpose of increasing speech recognition rate. The problem associated with deaf speech as compared to normal speech is that, there is high variability in deaf speech and by hearing once we could not understand it .Since the problem with deafness results in poor quality speech. This type of problem is marked in those born deaf, since their inability to hear their utterance prevents the acquisition of speech in normal way .The other problem with deaf speech is that not much study is done on how speech is acquired produced and perceived and this reason has hindered the progress in the development of speech processing aids for deaf. And because of this reason we will take samples of deaf and normal speech and their pitch frequency of vocal fold and resonant frequency of vocal tract or formant will be considered for analysis which is foremost characteristic of speech.

I. INTRODUCTION

Rarely is a person completely deaf, and a hearing loss could fall anywhere along the continuum from totally deaf to hearing. The amount of usable or residual hearing varies greatly from person to person. Depending upon the type of loss, the person may or may not benefit from the amplification that a hearing aid provides. Hearing aids only amplify sound; they do not make sound clearer. The severity of a person's hearing loss could be different at various frequencies. Therefore, ability to hear different voices will vary depending on a number of factors, including the pitch of the voice. Also, it is important to note that a person's ability to hear a voice is different than the ability to discriminate between sounds and to understand speech.

The life activity most affected by hearing loss is communication. Colleagues and friends must be versatile in finding an effective communication method. Pen and paper are handy communication devices in some situations. Although you want to avoid gross or exaggerated arm waving, pantomime is helpful. Be aware that if you point to an object or area during a conversation with a person who is deaf or hard of hearing, that person wills most likely turn to look at where you are pointing. Allow their gaze to return to you before continuing with what you are saying. Though not effective for all people who are hearing impaired, knowing some sign language and finger spelling is helpful. Learn some elementary or survival signs from colleagues, coworkers, or managers who are deaf or hard of hearing.

People who become hard of hearing or deafened later in life, through old age or illness, generally will continue to use spoken English. Depending on the degree of hearing loss, people in this group have several options: use additional amplification or learn to lip-read. In fact, lip reading (or speech) is extremely difficult skill which requires the deaf person to study the lip movements and facial expression of the speaker, together with numerous other factors (physical gestures) to determine what is being said. There are many potential obstacles to lip reading. Hearing aids and lip reading are most effective in face to face communication between a small numbers of people. Unfortunately there are many events such as public meetings and lectures where the speaker may be poorly lit or too far away to be seen or heard clearly, or where high levels of background noise prevent the successful use of hearing aid. With people whose hearing becomes severely impaired in later life, deterioration in speech quality may take place because of the loss of acoustic feedback even though they have well established skills in speech production. Various training methods are used for this problem of deaf speech. Most rely heavily on a trained teacher who basically demonstrates the correct production of an utterance that the pupil learns by feeling vibrations of teacher and then his own throat, nose etc. By hands and by observing positioning of lips, tongue etc. In addition, electronic aids, such as pitch indicators, are sometimes employed. There is now a growing interest in the use of computer based aids.

2. METHODOLOGY OF SPEECH ASSESMENT.

1. The input speech samples are collected from the deaf and normal speakers.
2. Calculate the pitch for alternate cycles of each speech samples by SHR(sub harmonic to harmonic ratio).
3. The variation of pitch formants of the different deaf speech signals is calculated. The variation of pitch formants of the different normal speech signal is calculated.

4. The Fo (pitch formant) for deaf speech using SHR is measured. The result of this study will be the classification of the speech based on a deaf subject and a normal hearing person.

3. BLOCK DIAGRAM OF DEAF SPEECH ASSESSMENT

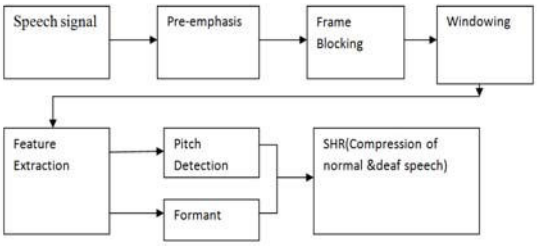

STEPS INVOLVED IN DEAF SPEECH ASSESMENT

1. **Pre-emphasis**

   Here the speech signal is filtered with the first order FIR filter to spectrally flatten the signal. We use one of the most widely used Pre-emphasis filter. Pre emphasis is a process of passing the signal through a filter which emphasizes on high frequency. In speech signal most part of energy is carried out by low frequency, when frequency increases pre emphasis also increases energy of signal.

2. **NORMALIZATION**

   After pre-emphasis, each word has its energy normalized. Based on the energy distribution along the temporal axis, it is computed the centre of gravity and this information is used as reference for temporal alignment of the words.

3. **FRAME BLOCKING**

   The Pre-emphasized speech signal is blocked into frame of N samples in frame blocking the speech wave form is cropped to remove silence or acoustical interference that may be present at the beginning or end of a sound file.

4. **WINDOWING**

   Windowing block minimizes the discontinuities of signal by tapering the beginning and ending of each frame to zero.

   Different windows available:

- **Hamming window**
- **Bartlett window**
- **Welch window**
- **Blackman and tukey window**
- **Hanning window**

We have used hamming window because a hamming window basically forces a signal to start and end at zero so as to copy a periodic signal. This is important because fft command makes the assumption that the input signal is periodic over –(∞) to +(∞).Without windowing there would be discontinuities in the repeated signal.Since most signal are not periodic to begin with , it is desired to use window to enforce periodicity.

5. **SHR**

Pitch perception is closely related to the sub harmonic to harmonic ratio(SHR) that is amplitude ratio between sub harmonic and harmonic. When the ratio is small, the perceived pitch remains the same. As the ratio increases above certain threshold, the sub harmonic become clearly visible on the spectrum, and the perceived pitch becomes one octave lower than the originl pitch. These findings suggest that pitch may be optimally determined by computing SHR and comparing it with pitch perception data.

6. **PITCH DETECTION**

Pitch i.e. fundamental frequency(F0) is an important features in speech research areas. Numerous pitch detection algorithms have been proposed.

Different PDA'S and their RAWBACKS:

- Auto correlation function based PDAS-it is more convenient for common usage. And it gives accurate results for pitch estimation of normal and low computation complexity.
- Normalized cross correlation function based PDAS-It gives best results in pitch detection accuracy and voiced/unvoiced classification. But it is computationally more complex.
- Average magnitude difference based PDAS-The AMDF has great advantage in very low computational complexity. It is possible to implement it in real time application. However this algorithm shows poor results in accuracy of pitch estimation and pattern recognition.
- Cepstral analysis based PDAS-It shows good pitch estimation accuracy. Fundamental frequency estimation in this algorithm is immune to error due to effect of vocal tract. But it is computationally complex. And it requires additional parameters for voiced/unvoiced decision.

We have used SHR for pitch detection and formant extraction because the above drawbacks are removed in SHR algorithm and above all it gives good results for pitch detection by comparing the amplitude ratio of sub-harmonic and harmonic with pitch perception results. So the pitch of normal speech and speech with variation (i.e. of deaf person) can be easily determined. And that is why this algorithms is one of the most reliable PDAS and superior to other PDAS .

7. FORMANT EXTRACTION

Formant is the distinguishing or meaningful frequency components of human speech and of singing. The formant with lowest frequency is called F1, the second F2, the third F3. Most often the first two formants are useful enough to disambiguate the vowel. These two formants determine the quality of vowels in terms of open/close and front /back dimensions

4. PITCH DETECTION PROCESS

Normal vowel production results from a quasi-periodic vibration of the vocal folds acting upon the air-stream escaping from the lungs. All sounds produced with vocal fold vibration are known as voiced sounds and the mechanism of speech production. While great progress has been made in understanding the physiological and psychological aspects of speech processing, much work remains to be done. An important contribution that auditory science can make to speech processing is to identify what features of the speech stimuli are relevant, and what underlying time frequency analysis strategies should be undertaken in order to extract them. Such features would then form the front end of a speech recognition system, or determine the structure of a speech coder. The fundamental frequency (Fo) of voiced sounds is determined physiologically by the vocal fold vibration rate. Control of Fo is used to communicate prosodic features of speech such as stressing and intonation. Production of prosodic features is an essential part of the normal human communication process. Previous reports on speech indicate that deaf individuals have a significantly higher Fothan normal hearing individuals therefore; an accurate and valid measurement of Fo is a critical element in the assessment and treatment of deaf speech. There are at least two methods for determining the Fo of speech The deaf subject 8 years old had a deaf, deafened, hard of hearing loss. The normal hearing subject was 7-12 years old. Each subject was instructed to prolong the isolated digits ten times. Before recording, the subjects were asked to practice for some time to familiarize them with the glottograph.

PITCH EXTRACTION USING SHR

The pitch extraction from a speech file is difficult because the glottis excitation is correlated with the vocal conduct. The PDA are based on three main methods : -

1.Frequency methods such as FFT, Cepstrum, STFT.

2. Temporal methods: based on the autocorrelation function such as, LPC, Parallel, PPA.

3. Time-frequency methods: spectrogram, wavelet.

Since the above methods exhibits some disadvantages, SHR is used in which pitch of alternate pulse cycles in speech is taken. This algorithm employs a logarithmic frequency scale and a spectrum shifting technique to obtain the amplitude summation of harmonics and sub harmonics, respectively. Through comparing the amplitude ratio of sub harmonics and harmonics with the pitch perception results, the pitch of normal speech as well as speech with alternate pulse cycles (APC) can be determined.

Furthermore, superior to most other algorithms, it handles sub harmonics reasonably well.

(a) Amplitude alternation.

(b) Period alternation.

Sub harmonic-to-Harmonic Ratio (SHR) is amplitude ratio between sub harmonics and harmonics. When the ratio is small, the perceived pitch remains the same. As the ratio increases above certain threshold, the sub harmonics become clearly visible on the spectrum, and the perceived pitch becomes one octave lower than the original pitch. These findings suggest that pitch may be optimally determined by computing SHR and comparing it with the pitch perception data.

5. ABOUT FORMANTS

Formants are defined as 'the spectral peaks of the sound spectrum |P(f)|' of the voice. Formant is also used to mean an acoustic resonance and in speech science, phonetics is a
resonance of the human vocal tract. It is often measured as an amplitude peak in the frequency spectrum of the sound, using a spectrogram. Formant values can vary widely from person to person, and all voiced phonemes have Formants even if they are not as easy to recognize. Voiceless sounds are not usually have formants instead, the plosives should be visualized as a great burst.

Formant trackers typically have two steps:
1) Computation of formant candidates for every frame
2) Determination of the formant track, generally

using continuity constraints. One way of obtaining formant candidates at a frame level is to compute the roots of a pth order LPC polynomial. There are standard algorithms to compute the complex roots of a polynomial with real coefficients. Each complex root zi can be represented as

$$z = \exp -\pi b + j2\pi f$$

where fi and bii are the formant frequency and bandwidth respectively of the ith root. Real roots are discarded and complex roots are sorted by increasing f, discarding negative values. The remaining pairs (fi ,bi) are the formant candidates. In our experiments we have used p=12.We computed these LPC coefficients from 30-millisecond Hamming windows, with 20 milliseconds overlapping, using the autocorrelation method. Here we have calculated first six formants and only four formants are plotted for clarity.

6. EXPERIMENTAL RESULTS

PITCH CONTOUR PLOT FOR DEAF PERSON FOR WORD (BEANS)

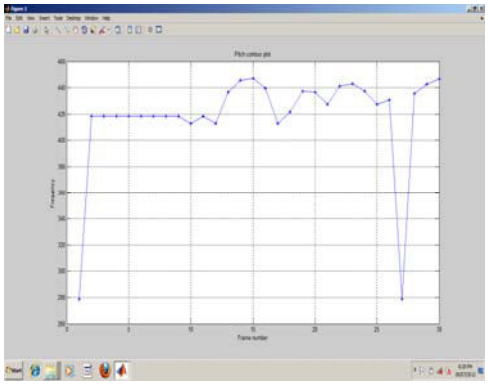

FIGURE:1

PITCH CONTOUR PLOT FOR NORMAL PERSON FOR WORD (BEANS)

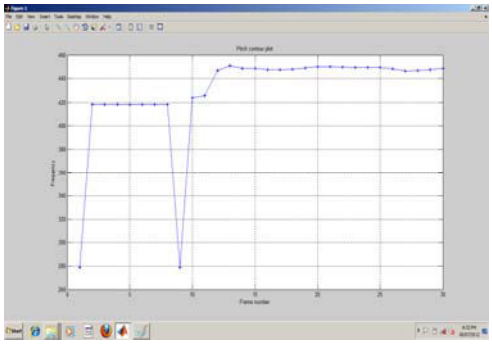

FIGURE:2

SPECTOGRAM PLOT FOR NORMAL PERSON FOR WORD (BEANS)

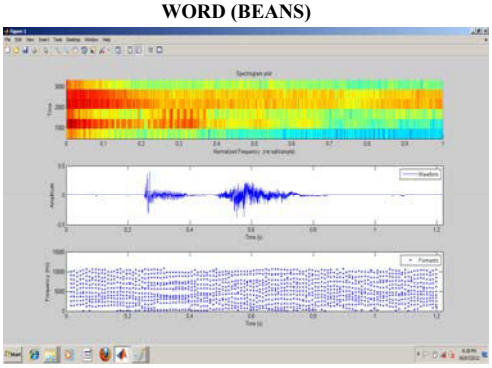

FIGURE:3

SPECTOGRAM PLOT FOR DEAF PERSON FOR WORD (BEANS)

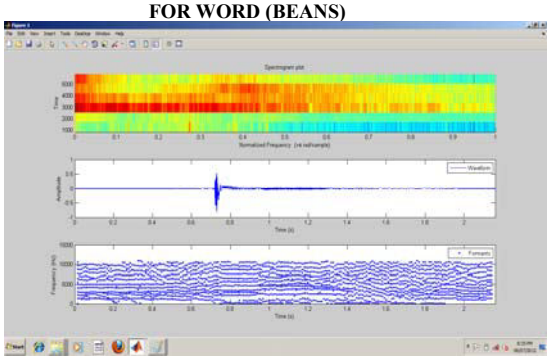

FIGURE:4

SHR PLOT FOR NORMAL PERSON FOR WORD (BEANS)

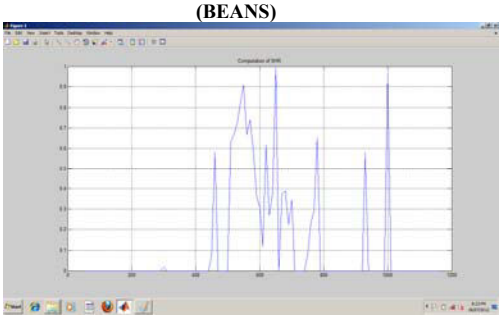

FIGURE:5

SHR PLOT FOR DEAF PERSON FOR WORD (BEANS)

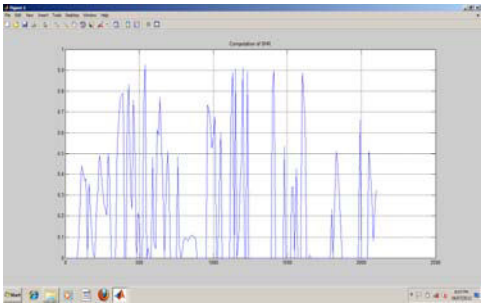

FIGURE:6

7. RESULT AND CONCLUSION

Two databases are used for evaluation. The first is the isolated words uttered by the normal speaker. The speech signal is sampled at 16KHz with 16-bit resolution. Here the bound of the frequencies that are used for estimating pitch is taken as 1250Hz. with SHRP threshold is taken as 0.4.Then pitch values are estimated using SHR algorithm. Another database is the isolated words from deaf and hard of hearing person Similarly pitch extraction is done using SHR. From pitch contour we have seen there is more variation in deaf speech as compared to normal speech and from spectrogram plot we have seen that amplitude of deaf is more as compared to normal.

The results of this study are based on one deaf and one normal hearing. However, the differences observed in the two measurements are expected to occur in other deaf and normal individuals. The results of this study indicate that the differences in measurement of Fo in deaf speakers may be investigated further with a larger sample size. The measure of Fo provided by the SHR includes the fundamental frequency of the vibration of the vocal folds plus any other acoustical energy that is produced in the glottal area. The pitch is sufficient for the identification of the deaf or normal speaker but has to be assisted by the first four (Fl,F2,F3,F4) formants necessary for speech classification. Here we have seen that there is more variation in deaf speech as compared to normal and amplitude of deaf speech is more as compared to normal.

REFERENCES

[1]. Dr.Colin Brooks,(2000).“Speech to text system for deaf, deafened and hard of hearing people”, The Institution of Electrical Engineers IEE, Savoy Place, London WC2R OBL, UK.

[2]. R.G .Crichton, M.A., and F. Fallside, B.Sc, M.A., Ph.D., C.Eng., M.I.E.E.(1974). “Linear prediction model of speech production with applications to deaf speech training” Proceedings IEE, Vol. 121, No. 8.

[3]. Harry Levitt, (1973) “Speech Processing Aids for the Deaf: an overview”.IEEE, Transactions on audio and Electroacoustics, Vol.Au-1,No.3.

[4]. Harry Levitt, Member, IEEE,(1971), “Acoustic Analysis of Deaf Speech Using Digital Processing Techniques” IEEE Fall Electronics Conference, Chicago, Ill.

[5]. J. M. Picjlett, (1969),“Some Applications of Speech Analysis to Communication Aids for the Deaf”, IEEE Transactions on Audio Electroacoustics, AU-17, NO. 4.

[6]. Prashant S. Dikshit', Edward L. Goshom2, and Ronald L. Seaman'.(1993), “Differences in fundamental frequency of deaf speech using FFT and Electroglottograph”, Biomedical Engineering Conference, Proceedings of the Twelfth Southern IEEE, Page(s): 111 – 113.

[7]. Thomas R. Willemine Francis F. Lee,(1972),Fellow IEEE,“Tactile Pitch Displays for the Deaf”, IEEE Transaction on Audio and ElectroacousticsVolL. AU-20, No.1.

[8]. Chris J. Clement, Florien J. Koopmans-van Beinum and Louis C. W. Pols,(1996),“Acoustical characteristics of sound production of deaf and normally hearing infants” Fourth international conference on spoken language, vol.3, 1549-1552.

[9]. Rabiner et al., (1976), “A Comparative Performance-Study of Several Pitch Detection Algorithms,” IEEE Transactions on ASSP, Vol. ASSP-24, No.5.

[10]. Xuejing Sun,(2002), “Pitch determination and voice quality analysis using subharmonic-toharmonic ratio”, International conference on Acoustics, Speech and Signal Processing, IEEE.

[11]. Proceedings. (ICASSP '02). Page(s): I-333 - I-336 vol.1 Signal & Image Processing : An International Journal(SIPIJ) Vol.1, No.1, September 2010 25

[12]. James W. Pitton, kusnwang, and Bing-Hwang Juang, ,(1996), Fellow IEEE, “Time frequency analysis and auditory modeling for automatic Recognition of speech”, Proceedings of the IEEE, Vol.84, no.9.

[13]. CherifAdnene,(2000),“Pitch and formants extraction algorithm for speech processing” The 7th IEEE International Conference on Electronics, Circuits and Systems, Volume: 1 Digital Object Identifier: Page(s): 595 - 598 vol.1 .

[14]. Alex Acero,(1999), “Formant analysis and synthesis using hidden markovmodels”.Relatedwebsite is http://citeseerx.ist.psu.edu/viewdoc/summary?doi=10.1.1.137 .9825.

◈◈◈

E-Stamp Authentication Using K-N Sercet Sharing Color Image Visual Cryptography

[1]Lavanya.R, & [2]Y.S. Nijagunarya

Department of CSE, Siddaganga Institute of Technology, Tumkur, INDIA

Abstract- Stamp paper scam was a big blow in Indian history, Government losses several crores of rupees in this scam. The tentacles of the fake stamp and stamp paper, better known as the Telgi scam. Government is taking many steps to stop these types of scams. In this paper, we are providing a solution to identify the stamp paper is released by Government or it is duplicated one using *k-n* secret sharing color image Visual Cryptography concept. To develop a web based application, which will generate the "e-stamp papers" with authentication, so that we can able to find whether the stamp paper is original or duplicate.

I. INTRODUCTION

Visual Cryptography is a special encryption technique to hide information in images in such a way that it can be decrypted by the human visual system. The benefit of the visual secret sharing scheme is in its decryption process. Where without any complex cryptographic computation encrypted data is decrypted using Human Visual System (HVS). But the encryption technique needs cryptographic computation to divide the image into a number of parts let n.

The concept of secret sharing was developed many years back, when Adi Shamir has shown the idea in the paper Adi Shamir, how to share a secret, published in ACM, laboratory for computer Science, Massachusetts Institute of Technology, 1979[1]. He shows that "How to divide data D into n pieces in such a way that D is easily reconstruct able from any *k* pieces, but even complete knowledge of *k-1* pieces reveals absolutely no information about D". He utilized this idea to save the key for using the encryption.

In 1994, Naor & Shamir shows a new concept using images in their paper "Visual Cryptography"[2]. They extend the new scheme to secret sharing problem. In the paper, abstract it said "It can be extended into a visual variant of the *k* out of *n* secret sharing problem in which a dealer provides a transparency to each one of the *n* users any *k* of them can see the image by stacking their transparencies, but any *k-1* of them gain no information about it". After the basic concept, many researcher find out different schemes for the Visual Cryptography C.N. Yang, Visual Cryptography: An introduction to visual secret sharing schemes, department of computer science and information engineering national dong hwa university shoufeng , Hualien 974, TAIWAN, access on June - 07- 2007[3]. The improvement goes to gray scale image to color images and different ways and techniques were developed with amazing ideas. However, the field is still communication channel. Using the properties of the HVS to force the recognition of a secret message from overlapping shares, the secret image is decrypted without additional computations and any knowledge of cryptography.

The model for Visual Cryptography is given by Naor & Shamir as follows: A printed page of cipher text and a printed transparency (which serve as a secret key). The original clear text is revealed by placing the transparency with the key over the page with the cipher, even though each one of them is indistinguishable from random noise. The model for visual secret sharing is as follows: What are Visual Secret Sharing Schemes? [4]. There is a secret picture to be shared among n participants. The picture is divided into n transparencies (shares) such that if any m transparencies are placed together, the picture becomes visible. If fewer than m transparencies are placed together, nothing can be seen. Such a scheme is constructed by viewing the secret picture as a set of black and white pixels and handling each pixel separately.

The term multimedia essentially means of communication through multiple media. From the earlier times, man has attempted to communicate his ideas through various means like gestures, sounds, paintings, writings, etc.

The multiple sense organs of man enable him to comprehend and support such kind of multi –model communications. In the real world, the non-textual form of communication, like cave paintings, was used much before the written form originated. In the computing world, however, the trend has been just the reverse; text was the predominant form of communication over most of the earlier part of computing history. The book on principles of

multimedia [5] gives an insight into these solutions and highlights the landmarks achieved.

II. EXISTING SYSTEM

In existing systems, the stamp papers have been counterfeited which caused the huge loss to the government. Government lost several crores of rupees because of these scam. The tentacles of the fake stamp paper, better known as the Telgi scam. To prevent the counterfeit of stamp papers, some of the states of India are implementing the electronic form of stamp papers. Since, they are using the grey scale technology. The visual impairments and the pixel expansion are the major drawbacks. The size of the generated image is twice the size of the original stamp image.

III. PROPOSED SYSTEM

To prevent counterfeit of stamp papers, E-stamp authentication method uses *k-n* secret sharing color image Visual Cryptography concept. Admin is a super user, and he can able to create n -number of users. Similarly, admin can able to create verification officer and do all the operation like (edit, delete, and view).

Admin user has to create the stamp paper according to specification given by the Government. While creating the stamp paper admin has to specify the value of the stamp paper, the stamp paper certificate number will be generated automatically by the system and the certificate number is unique. Admin has to provide an authentication image for each stamp paper. Once the authentication image is specified, the image is divided into *n* shares using *k -n* secret sharing color image Visual Cryptography. Among the divided shares one share will be stored in database and another one will be printed on the stamp paper, remaining shares will be sending to verification officers through web mail.

Member users are bank employees who sell the stamp paper to the end users. Member user has the option to print the E-stamp paper and give it to the end users or customers. Member user has to select the stamp paper which is in stock status and has to fill the customer details and stamp paper purpose details in relevant field, then only he can able to print the stamp paper. This system uses the portable Document Format (PDF) files interface to print the stamp paper, which means the stamp paper is generated in the PDF format. It will open automatically in the PDF file, so that member user can able to print it easily. While stamp paper is printing one share of the authentication image of particular stamp paper will be retrieved from the database and printed along with the stamp paper. Once stamp paper is sold then the status of stamp paper is changed from stock to sold. Which means member user is not able to sell the same stamp paper again.

Once the customer purchased the E-stamp paper from the member user and utilized for land purchase or rental deed or any other purpose. At any time if its required to check the originality of E-stamp paper, verification officer role is important.

A person who wants to know the originality of stamp paper has to approach the verification officer with the E-stamp paper; verification officer will enter the certificate number and send a request to the web server to retrieve the authentication image of the stamp paper and share of the authentication image. The authentication image is displayed on the download share. The download shares overlapped on the stamp paper. If the authentication image on the screen and Visual Cryptography retrieval image from the E-stamp paper are same then the stamp paper is original, if the Visual Cryptography image differ then it is not original. Minimum *k* or more than *k* number of shared images required to reveal the authentication image.

Step 1: Read input Color image I, read number of Shares N

Step 2: Let W = Width and H = Height of the Image

Step 3: Create a numeric matrix R of size [W,H]

Step 4: Fill the matrix with random number

```
For s = 1 to W
    For q = 1 to H
        R[s, q]= Generate random number
            between 1 to N
```

Step 5: Let c = 1

Step 6: Create a new share image SI

Step 7: For s = 1 to w

```
    For q = 1 to H
        V = R[ s , q]
If V = c or V=c+1
    then SI[s , q] = I[s , q]
```

Step 8: Write all the content of SI in new share

Step 9: if c< N

```
    then c = c+1
    Go to step 6
```

Step 10: Stop

Fig.1. Algorithm for the Visual Cryptography:

IV. RESULT

The administrator uploads the stamp image and splits the stamp image into *n* shares. Among the divided shares one share will be stored in database and another one will be printed on the stamp paper, remaining shares will be sending to verification officers through web mail.

Fig2. Source Image

Image1.png **Image2.png** **Image3.png**

Image4.png **Image5.png** **Image6.png**

Fig 3: Shared Images

Fig 4: Reconstructed Image by considering all the shared images

Fig 5: Reconstructed Image with less than *k* number of shared images

Fig 6: The E-stamp paper which is finally issued to end user.

V. CONCLUSION AND FUTURE WORK

By using Visual Cryptography algorithm E-stamp authentication mechanism is developed. This E-stamp authentication system can be used to prevent the counterfeiting of stamp papers. The original and duplicate E-stamps can be detected easily and it prevents from the heavy financial loss to the government. It is practical, efficient and fast to the needs of the clients.

In E-stamp authentication system, there is chance of forgetting the user name and password by the administrator, verification officer and bank user. If the user name and password is got by some other person there is threat of misusing the stamp papers. It might result in heavy financial loss to the government. The verification process is time consuming. If the number of end users is more and there are limited verification officers, the work load will be more to the verification officer. The administrator, verification officer and the bank users should be able to keep their user name and password secret so that no other third person has access to their user name and password.

REFERENCES

[1] Adi Shamir, How to Share a Secret, published in ACM, Laboratory for Computer Science, Massachusetts Institute of Technology, 1979.

[2] Naor, M. and Shamir, A., Visual Cryptography, In Proc. Eurocrypt *94,* Perugia, Italy, LNCS 950, Springer Verlag., 1994, 1–12.

[3] C.N. Yang, Visual Cryptography: An introduction to visual secret sharing schemes, Department of Computer Science and Information Engineering National Dong Hwa University Shoufeng , Hualien 974, TAIWAN, access on June 07, 2007,

[4] What are Visual Secret Sharing Schemes?

[5] Ranjan Parekh, “Principles of Multimedia”, Tata McGraw Hill, 2006

◈◈◈